Landscape Configuration and Composition Trends of Indigenous Forest Using Multi- and Hyperspectral Imagery

A thesis presented in partial fulfilment of the requirements for the degree of

Master of Science

In

Geography

At Massey University, Manawatu, New Zealand.

Stefan Rex Carter

2023

Abstract

Historical land use in New Zealand led to the widespread destruction of indigenous forests, creating a complex landscape matrix within which forest fragments now survive. Legislative changes have effectively halted large-scale deforestation, yet small-scale fragmentation continues to occur. This negatively effects numerous ecological processes vital in maintaining healthy forest structure and function. To monitor fragmentation, state of the environment reports often quantify area and percentage of landscape change. While these metrics are important, they are poorly suited to quantifying the spatial configuration and distribution of forest fragments.

To quantify the spatial arrangement of indigenous forest remnants, two case studies were undertaken at different spatial and temporal scales. The first employed low-resolution (246 m^2), multispectral derived imagery from the Climate Change Initiative - Land Cover (CCI-LC) dataset to quantify regional fragmentation over a 28-year period. Landscape analysis was performed with FRAGSTATS and revealed both spatial and temporal variability in the arrangement of forest patches. This was evidenced by periods of fragmented growth and decline, along with periods of infilling in some regions. Despite several regions recording a net increase in forest area, the overall trend was towards greater disaggregation and fragmentation. However, it is essential to exercise caution when interpreting these findings as the coarse resolution of the CCI-LC dataset may not adequately describe fragmentation at the regional level.

The second case study employed high-resolution (1 m^2), hyperspectral imagery to quantify forest fragmentation on a rural property. Imagery was captured with the AISA FENIX hyperspectral camera and atmospherically corrected using a pixel-wise radiative transfer model. Land cover was classified with a one-dimensional convolutional neural network and landscape configuration was assessed with FRAGSTATS. The results were compared to the medium-resolution (1 ha nominal mapping unit) Landcover Database (LCDB) and the low-resolution CCI-LC. Greater accuracy in both land cover classification and definition were achieved with the hyperspectral imagery. Edge-perimeter and connectivity metrics were also substantially improved. Management strategies seeking to reduce fragmentation should consider the use of high-resolution, hyperspectral imagery in conjunction with landscape metrics to improve classification accuracy and precision.

Acknowledgements

I would like to dedicate this thesis to my wife, Jo, and my daughters, Ava, and Vienna. When I needed encouragement, patience, or support along the journey you were there.

To my geography supervisors, Professor Ian Fuller and Dr. Sam McColl, I would like to say thank you for all your amazing lectures, field trips, and guidance throughout my undergraduate and post-graduate years. Your positivity, approachability, and genuine enjoyment in teaching geomorphology have had a profound impact on many students, including myself, and I hope you both continue to thrive in your chosen fields.

To my remote-sensing supervisor, Dr. Nitin Bhatia, thank you for providing the main scripts used in the analysis, answering many tedious questions, and always reminding me when its coffee time. As my manager, I would also like to say thank you for enabling me to complete this thesis during work hours by tactfully spreading the load, mostly to Eduardo Sandoval. I greatly appreciate your mentorship and friendship through the writing of this thesis.

Finally, I would like to thank those who have financially supported m throughout this course of study, Chris Allen, James Allen, and MAF Digital Lab/Massey University. I would not have been able to progress through each stage of the program without your generosity and support. Thank you for helping me to achieve my dream and pursue my passion, it has changed the course of my life.

Contents

List of Figures

List of Tables

List of Abbreviations

1D CNN:	One-dimensional convolutional neural network
CA:	Class Area
CCI-LC:	Climate Change Initiative – Land Cover
CI:	Clumpiness Index
ED:	Edge Density
ENN:	Euclidean Nearest Neighbour Distance
LCCS:	Land Cover Classification System
LCDB:	Landcover Database
MFDI:	Mean Fractal Dimension Index
MPI:	Ministry of Primary Industries
RMA:	Resource Management Act 1991
PLAND:	Percentage Land Cover
TE:	Total Edge
UN FAO:	United Nations Food and Agriculture Organisation

1. Introduction

Indigenous forests around the world are highly regarded for their unique biodiversity, provision of ecosystem services, and natural beauty, but are often threatened or vulnerable to various forms of degradation associated with human activities. New Zealand is no exception to the rule, as indigenous forests have been severely affected by historical land use and continued pressure from external processes. The large-scale clearance of indigenous forests following the arrival of humans along with the growth of urban areas, agriculture, forestry, transport networks, and other infrastructural developments has resulted in a highly fragmented mosaic of land cover types that have drastically reduced the area and connectivity of forested environments. Whilst legislation has been successful in halting large-scale deforestation, fragmentation of the forest edge, particularly in the fragmented lowlands, continues to occur, altering forest dynamics through increased penetration of edge effects into the forest core. Despite the continued degradation and fragmentation of indigenous forests remnants, state of the environment reports at all levels of government lack information on the spatial configuration and distribution of fragments throughout the landscape which could be used to improve the management and allocation of resources to the most at risk areas.

Quantifying fragmentation into meaningful statistics can be achieved with remote sensing technology, land cover classifiers, and landscape analysis software. Multispectral and hyperspectral sensors can be used to derive land cover classes from the spectral profile of indigenous vegetation. Spectral samples can then be collected and used to train land cover classifiers which model land cover over the entire landscape based on features detected in the sampled spectra. This presents a more efficient and cost-effective methodology than traditional orthophotography captured with airborne and spaceborne cameras. Multi- and hyperspectral sensors can also capture data at a range of spatial and temporal scales, allowing for the development of time-series datasets for localised remnant monitoring to national and global scale forest inventories. These classified land cover datasets can then be analysed with landscape configuration software to derive fragmentation statistics related to underlying ecological processes. In doing so, indigenous forest fragmentation can be monitored and more appropriately managed to prevent further degradation of these highly valuable natural environments.

1.1 Objectives

This thesis aims to assess indigenous forest fragmentation at varying scales through two complementary case-studies. The first involves quantifying fragmentation at national and regional level using a low-resolution (246 m^2), multispectral derived, time-series dataset. The purpose of this approach is to perform an initial broad-scale assessment of forest fragmentation and identify

potentially vulnerable areas. The spatial configuration and connectivity of forest fragments will be quantified with the landscape analysis software FRAGSTATS and analysed from a regional perspective. Fragmentation patterns occurring over the 28-year period covered by the dataset will then be identified and described.

The second case study will examine farm-scale fragmentation patterns while comparing the spectral and spatial resolution differences of three classified datasets. The aim of this study is to establish the need for high-resolution (1 m^2), hyperspectral imagery in classification of land cover at local scale. This will first involve the classification of forest and non-forest vegetation on a rural property using imagery acquired with the high-resolution, AISA FENIX hyperspectral camera. Land cover classification will utilise a one-dimensional convolutional neural network (1D CNN) and landscape analysis will be performed with FRAGSTATS. The corresponding area from the low-resolution CCI-LC and medium-resolution (1 ha nominal accuracy) Landcover Database v5 (LCDB) will be extracted in ArcGIS and analysed with FRAGSTATS as well. The results will then be compared and the benefits of utilising high-resolution, hyperspectral imagery for localised land cover classification will be described.

2. Literature Review

2.1 Introduction

New Zealand's indigenous forests are comprised of unique floral and faunal assemblages spread across a diverse range of environments. With high levels of endemism, these environments have global significance as many species are found nowhere else in the world (Brockerhoff et al., 2006; Dowding & Murphy, 2001; McGlone, 1985; Taylor-Smith et al., 2020). Since the arrival of humans, deforestation for agriculture, settlements, and infrastructure has drastically reduced the extent of indigenous forests, declining from a pre-human forest cover of 82 % to 23 % of the land surface – a loss of some 14,000,000 ha of forest in a period of 750 years (Allen et al., 2013; Ewers et al., 2006; Forbes et al., 2020). The largest remaining forests are now predominantly located in hill country areas situated along the axial ranges of the two main islands. Lowland forests were largely destroyed but many small, isolated remnants are still found scattered throughout the country, mostly in the North Island (Dodd et al., 2011; Ewers et al., 2006; Stevenson, 2004).

The drastic loss of indigenous forest has resulted in various legislative and socio-economic changes that prioritise conservation and protection, yet forest degradation continues to occur (Brockerhoff et al., 2006; Hawes & Memon, 1998). In 2006, Ewers et al. (2006) found that of the 73 political districts in New Zealand, 55 had indigenous forest cover below the 30 % 'extinction threshold' level outlined by Andren (1994). Around 80 % of indigenous forests are owned and managed by the Department of Conservation who are required to protect and conserve them under the Conservation Act 1987 (Allen et al., 2013). However, the remaining 20 % (c. 1,500,000 ha) is in private ownership and is regulated by the Forests Act 1949 (Amended 1993) and Resource Management Act 1991 (RMA) which are administered by the Ministry for Primary Industries (MPI), regional councils, and other territorial authorities (Walker et al., 2021). Monks et al. (2019) argue that the continued decline in indigenous forests indicates the protection offered by the RMA has been inadequate in preventing further loss of indigenous vegetation, habitats, and biodiversity, while advances in technology have increased agricultural capabilities on marginal lands typically occupied by indigenous vegetation. Additionally, under the Forests Act, landowners can apply to MPI for a Sustainable Forest Management plan or permit that enables provisional logging of indigenous timbers on privately owned land.

2.2 Defining Forest Health

The continued degradation of indigenous forest remnants on privately owned land threatens forest health in a variety of ways (Cocklin & Doorman, 1994; Dymond et al., 2013; Hawes & Memon, 1998). Defining the general term 'forest health' as an assessment of the condition and function of a forest over a range of spatial scales provides two key avenues from which forest degradation can be

assessed: condition and function (Cieraad et al., 2015; McGarigal & Marks, 1995; Noss, 1999; Trumbore et al., 2015; Young & Mitchell, 1994). Function is primarily associated with biological complexity and provision of ecological services (Cieraad et al., 2015). Functional degradation therefore describes a forest afflicted by pests and disease, heavily altered by the presence of exotics, or lacking associated plant and animal species typically found within the biosphere (Dodd et al., 2011; Eikaas, 2004; Forbes et al., 2020; Hutchison, 2009; Monks et al., 2019). It may also describe changes in ecological systems due to soil and water contamination from anthropogenic activities, microclimatic changes associated with greater penetration of edge effects, loss of carbon sequestration capacity due to selective logging of mature trees, and many others (Davis et al., 2003; Eikaas, 2004; Stevenson, 2004; Young & Mitchell, 1994).

Conditional degradation refers to changes in structural attributes within a forest patch, as well as the configuration of patches throughout the landscape (Forbes et al., 2020; Noss, 1999). Within a forest patch, structural attributes refer to biomass, density of canopy cover, presence and complexity of structural layers (see Figure 1), as well as patch shape, degree of edge fragmentation, and patch size (Forbes et al., 2020; Pan et al., 2013). At landscape level, forest structure is primarily associated with areal extent but the degree of fragmentation, patch aggregation, spatial distribution, edge density, core area, number of patches, and other quantifiable metrics used to describe the spatial configuration and connectivity of patches within the landscape are also important (Ewers & Didham, 2007; Golubiewski et al., 2020; Hutchison, 2009; LaGro, 1991; McGarigal & Marks, 1995; Neel et al., 2004).

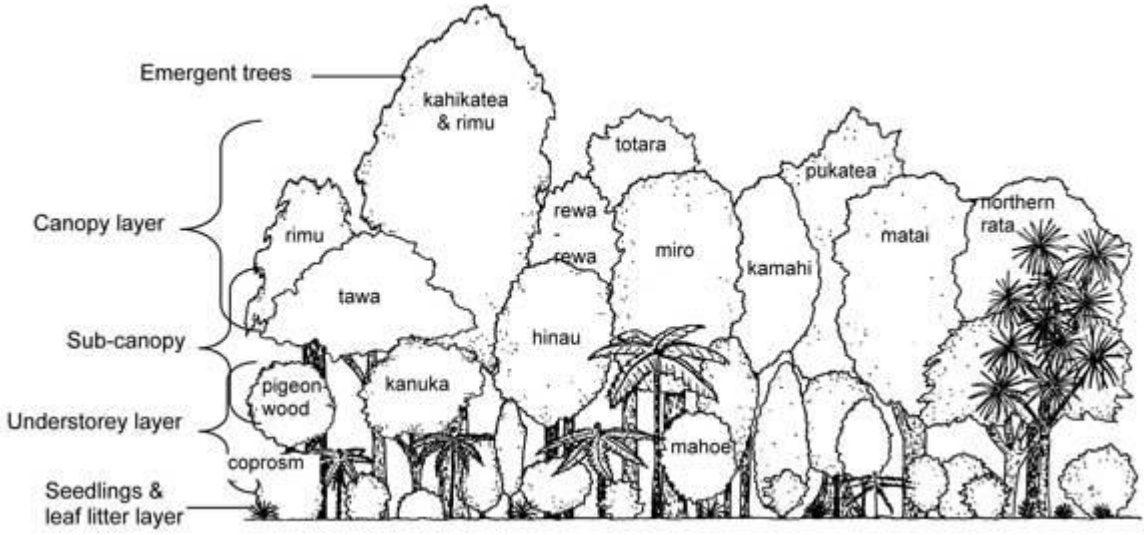

Figure 1. Example of Healthy Forest Structure in a New Zealand Forest. *Note:* A healthy indigenous forest remnant in New Zealand will contain multiple vegetative layers including an emergent, canopy, sub-canopy, understorey, and seedling/ground cover layers (Department of Conservation, n.d.).

2.3 Quantifying Forest Health

The myriad ways in which habitat function and condition can be altered make broad scale analyses challenging, but landscape indices can be a useful tool in quantifying the spatial aspects of fragmentation that affect biological and ecological functions vital to forest health (McGarigal & Marks, 1995; Noss, 1999; Walker et al., 2021). The selection of landscape indices should be carefully considered with regards to the intended structural or functional component of forest health being examined (Rutledge, 2003). For example, Rutledge (2003) notes that in landscape ecology, pattern is often given priority over process, when the underlying ecological process should dictate metric selection and image scale. This is because results produced from landscape indices can vary widely depending on image resolution, classification, and spatial extent, making correlations between landscapes of different scales difficult and interpretation of ecological functions ambiguous (Richard & Armstrong, 2010; Rutledge, 2003). However, the ecological processes associated with fragmentation are now well represented in the literature at patch level but there is a surprising lack of fragmentation data available to extrapolate these findings to landscape level (Dymond et al., 2017; Kozak et al., 2018; Riutta et al., 2014; van den Belt & Blake, 2014). This presents an opportunity to contribute to the growing body of work focussed on understanding and improving indigenous forest health.

2.4 The Research Gap

In New Zealand, landscape level analyses of forest fragmentation are generally reduced to percentage of land cover and change in area (Ewers et al., 2006; Lafortezza et al., 2010). For example, New Zealand's national state of the environment report, Environment Aotearoa 2022, describes forest fragmentation and overall health only in terms of area and percentage of land cover (Ministry for the Environment & Stats NZ, 2022). Area is a key landscape statistic employed in analyses of forest health, but it is not well suited to describing the degree of fragmentation occurring within a landscape (Didham & Ewers, 2012; Ewers & Didham, 2007). This is because fragmentation can increase while total forest area remains static or rises (Kozak et al., 2018; McGarigal & Marks, 1995; Monks et al., 2019).

The lack of fragmentation data extends to other land cover types in New Zealand as well. Curran-Cournane et al. (2023), discussing agricultural land fragmentation, note there is no nationally established system to monitor landscape fragmentation and data consistency varies across regions. In a similar vein, a 2020 report prepared by Manaaki Whenua - Landcare Research (2020) suggests quantifying the effects of fragmentation to support state of the environment reporting is a key area in which consistency can be improved across all levels of government (local, regional, and national). While these studies both come from an urban and agricultural perspective, they serve to highlight the growing awareness and demand for land cover fragmentation data in New Zealand that is also missing from assessments of indigenous forest health.

To improve the present fragmentation dataset, additional landscape metrics that quantify other spatial aspects associated with patch configuration and arrangement could be employed. For example, Bhatia and Cumming (2020) analysed meso-scale deforestation patterns on 23 oceanic islands using classified global land cover data and the landscape analysis software FRAGSTATS (McGarigal & Marks, 1995). Their analysis included landscape metrics designed to quantify the spatial configuration and composition of forest cover, such as aggregation and clumpiness indices, shape complexity, edge density, and patch-to-patch distance. Bhatia and Cumming (2020) conclude that landscape metrics applied at meso-scale were suitable for detecting subtle differences in forest configuration and could be used to link local and global deforestation processes.

In another study, Lafortezza et al. (2010) examined the relationship between fragmentation and species composition in New Zealand podocarp-broadleaved forests. Landscape metrics were derived from a heavily fragmented hill country forest and an unfragmented lowland forest. The authors, who also employed FRAGSTATS in their analysis, quantified various landscape metrics, including fractal dimension indices, distance to nearest forest edge, number of patches, edge density nearest

neighbour distance, and total edge length. From their results, Lafortezza et al. (2010) found fragmentation patterns could be correlated to species composition in New Zealand forests.

2.5 Edge Effects

These studies demonstrate the application of fragmentation indices in quantifying different aspects of forest health. As the ongoing structural degradation of forest remnants is a considerable threat to forest health in New Zealand, fragmentation indices provide a means by which to assess forest configuration patterns. In particular, they provide the opportunity to assess the degree of fragmentation with regards to the extent and prevalence of edge effects in forest fragments. This is because edge effects, which alter forest function and structure, can be associated with the area-perimeter ratio of forest patches (Didham & Ewers, 2012; Ewers & Didham, 2007; Hutchison, 2009; Lafortezza et al., 2010; Norton, 2002; Richard & Armstrong, 2010; Walker et al., 2021; Young & Mitchell, 1994).

Based on numerous global studies, Laurance (2000) explains how edge effects alter forest function and structure up to a distance of 150 m from the forest edge. Within this edge zone, changing light levels and microclimatic conditions alter environmental and ecological processes that maintain air and soil temperature, affecting species interactions, composition, and abundance (Norton, 2002). Similarly, Laurance and Yensen (1991) describe changes in seed germination rates, loss of shade tolerant plants, increased turbulence and treefall, altered predation dynamics, and proliferation of invasives. In a New Zealand study, Young and Mitchell (1994) found evidence of edge effects occurring up to 50 m from the forest edge in fragmented podocarp-broadleaf forests. This included differences in species composition, biomass, microclimate, tree mortality, and population dynamics within the edge zone.

Of concern, is that as forest margins are further fragmented, the edge zone extends deeper into the interior until the entire patch is dominated by edge dynamics (Young & Mitchell, 1994). When a forest patch is dominated by edge effects, indigenous species dependent on interior forest conditions can no longer survive in that environment (Barbaro et al., 2012; Harris & Burns, 2000; Lövei & Cartellieri, 2000). This has been quantified in New Zealand podocarp-broadleaved forests by Young and Mitchell (1994) who describe forest patches <1 ha in size as incapable of supporting interior forest conditions and fragments up to 9 ha as dominated by edge effects. These findings led the authors to conclude that edge effects were likely now a significant feature of forest dynamics in fragmented indigenous remnants.

2.6 Application of Landscape Metrics

To quantify edge effects with landscape metrics, the perimeter length and patch area are compared to determine the degree of edge fragmentation. The area-perimeter relationship can be described

from a number of metrics, including total edge (TE), edge density (ED), and the mean fractal dimension index (MFDI). Total edge represents the combined perimeter length of each patch in the landscape and is used in conjunction with class area to derive ED, measured in units per hectare (McGarigal et al., 2002). Total edge can also be used to determine shape complexity which relates to penetration depth of edge effects, particularly if the forest margin is highly convoluted (Ewers & Didham, 2007). Shape complexity can be computed using a fractal dimension index (Imre & Bogaert, 2004). The advantage in using a fractal dimension index, as with ED, is that it facilitates comparisons between landscapes of varying size and scale (McGarigal & Marks, 1995; Zeide, 1991).

Edge fragmentation studies demonstrate the application of landscape metrics in forested environments. For example, Riutta et al. (2014) quantified edge fragmentation in England and found 75 % of surveyed forest area was within 100 m of the nearest edge. This led the authors to conclude that a large proportion of forested habitats in England are likely affected by edge dynamics. In a similar study conducted in the United States, Riitters et al. (2002) examined forest fragmentation at a range of spatial scales. Their findings indicated 62 % of forests were within 150 m of the forest edge, noting that edge effects likely influenced ecological processes in most forested areas.

Along with edge fragmentation, the distribution of forest fragments throughout the landscape is also vital to forest health. The spatial pattern and distance between patches can be used to describe the degree of connectivity between habitats (Lafortezza et al., 2010; Noss, 1999). As mentioned above, small, isolated forest fragments have limited core area in which certain plant and animal species can survive, making them especially vulnerable to edge effects (Laurance & Yensen, 1991; Norton, 2002; Ohlemüller et al., 2006). In such landscapes, the degree of connectivity between patches becomes increasingly important in sustaining metapopulations through the provision of genetic diversity, resources, migratory pathways, and resource supply (Ehlers Smith et al., 2019; Keyghobadi, 2007). Quantifying the spatial arrangement and connectivity of forest patches can provide the information required to identify and monitor at risk areas and plan for improvements in habitat connectivity.

As with quantification of edge effects, there are numerous landscape metrics that can be employed to measure connectivity and spatial distribution. Connectivity, for example, can be described from the Euclidean nearest-Neighbour (ENN) distance, a metric that quantifies the mean distance to the nearest neighbouring patch (McGarigal et al., 2002). This can be a useful indicator in time-series analysis as a declining ENN distance is typically associated with increasing fragmentation (McGarigal & Marks, 1995). Another indicator of connectivity is the spatial distribution of patches within the landscape which can be described from aggregation indices, such as the Clumpiness Index (CI). The CI

is a measure of patch aggregation, or contagion, in a normal distribution which allow for comparisons between landscapes of varying size (McGarigal et al., 2002).

The assessment of forest habitat connectivity with these landscape metrics is well represented in the literature. For example, Galicia et al. (2008) used patch density, number of patches, and patch size to assess connectivity of dry tropical forest remnants in the lower Papagayo River basin, Mexico. In the Montérégie region in Canada, Ziter et al. (2013) employed similar metrics along with the ENN distance in their analysis of forest fragmentation and carbon storage. Bhatia and Cumming (2020) used aggregation and clumpiness indices in their meso-scale analysis of deforestation and economic growth on 23 oceanic islands. In the northern Rocky Mountains, USA, Crist et al. (2005) used aggregation indices, ENN distance, patch size, and number of patches to investigate how road networks impacted forest connectivity. These are just a few examples that demonstrate the application of landscape metrics in a range of different scales and ecological regions.

2.7 Classified Multispectral and Hyperspectral Imagery

To apply fragmentation indices and quantify the spatial configuration of indigenous forest, a classified land cover map is required for the landscape analysis (McGarigal et al., 2002). Classified land cover maps are often created from remotely sensed imagery which provides a more cost-effective data acquisition solution through utilisation of airborne and spaceborne platforms than ground surveying (Bourgoin et al., 2021; Liang & Wang, 2020; Roughgarden et al., 1991). As Toth and Jóźków (2016) explain, this involves passive multispectral or hyperspectral sensors capable of detecting emitted radiation over a range of spectral bands (see Figure 1). The greater spectral resolution provides more data for feature detection than other remote sensing methods and is therefore better suited to land cover classification (Liang & Wang, 2020; Toth & Jóźków, 2016).

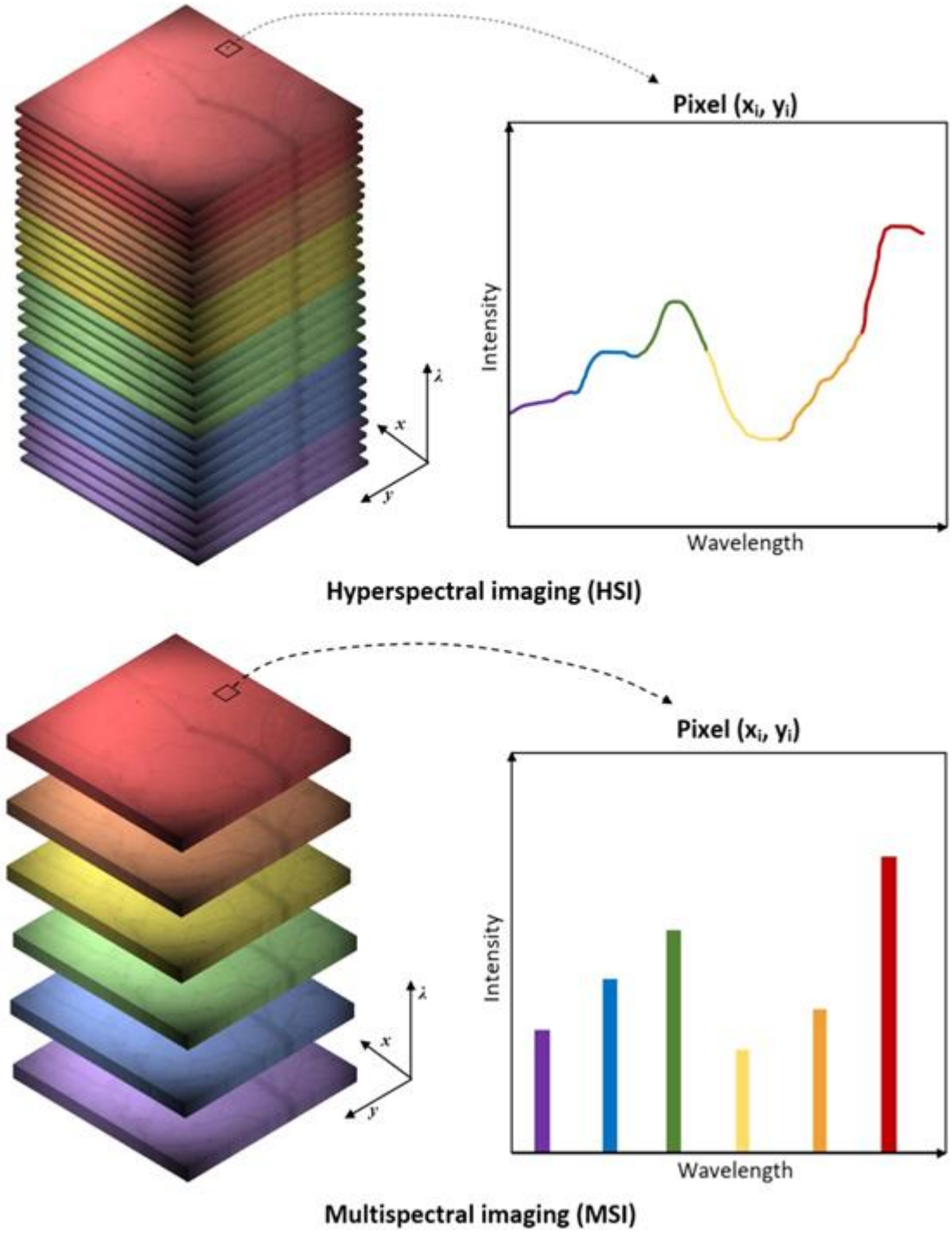

Figure 2. Hyperspectral and Multispectral Differences. *Note:* Hyperspectral (top) and multispectral (bottom) imagery capture a greater range of the electro-magnetic spectrum than traditional 3-band cameras. The bands in hyperspectral images are contiguous, capturing more of the spectral profile than the discrete wavelength bands captured with multispectral sensors (Giannoni et a., 2018, p. 3).

Classification of land cover is generally supervised or unsupervised, referring to the process by which pixels are classified (Enderle & Weih Jr, 2005; Liu, 2005). In an unsupervised land cover classification, spectral features are detected through clustering and dimension reduction algorithms that allocate pixels into a user defined number of land cover classes (Duda & Canty, 2002; Olaode et al., 2014). Unsupervised classification is an efficient way to classify large land cover datasets as it removes user bias in the selection of training data required for supervised classification (El Abbassi et al., 2021; Olaode et al., 2014). However, supervised classification generally achieves greater accuracy and model performance due to the inclusion of training data collected by the user (Bahadur KC, 2009; Zhang et al., 2016).

A training dataset is comprised of spectral samples carefully selected for each class and may involve the use of ground-truth data or high-resolution imagery to confirm sample selection (Richards & Richards, 2022). The sampled spectral data is then used to train a classifier which may take multiple iterations to achieve a satisfactory level of model performance (Zhang et al., 2016). Once trained, the model can be used to classify an entire image, allocating each pixel to a class within the parameters defined during the training process (Richards & Richards, 2022).

Numerous studies have compared the accuracy of supervised and unsupervised approaches in classifying land cover from multispectral data. For example, Hasmadi et al. (2009) compared the accuracy of supervised and unsupervised land cover classification with SPOT 5 imagery. They found the supervised classification had an accuracy of 90 % while the unsupervised classification was 81 % accurate. Similarly, Bahadur KC (2009) used Landsat data to classify land cover, producing a maximum classification accuracy of 83 % when supervised and 68 % when unsupervised. In another Landsat study, Ahmad and Quegan (2013) reported a supervised accuracy of 97 % and an unsupervised accuracy of 93 %.

Other research has focussed on the benefits of hyperspectral classification over multispectral. Boori et al. (2018) performed supervised and unsupervised classification on multispectral Landsat 8 data and hyperspectral Hyperion data. They found that the hyperspectral Hyperion data produced more accurate results than the multispectral Landsat 8 data, particularly when the classification was supervised, though all datasets demonstrated a high degree of accuracy. In another comparative study, Govender et al. (2008) found that the classification of multispectral satellite data resulted in genus level detection whereas hyperspectral data could be used to detect vegetation at genus and species level. The authors attribute the finer spectral resolution of the hyperspectral imagery to the observed improvements in vegetation detection.

These examples demonstrate how different image classification techniques combined with multispectral and hyperspectral imagery can be used to accurately quantify land cover. Using supervised classification techniques with hyperspectral imagery provides the best outcomes in terms of vegetation detection. However, unsupervised classification with multispectral imagery can still provide excellent results.

2.8 Conclusion

Improving assessments of forest fragmentation and habitat connectivity is of utmost importance to the future health of New Zealand's indigenous forests. To effectively manage and preserve these critical ecosystems, it is necessary to utilize advanced technologies such as multispectral and hyperspectral imagery from which the spatial configuration of forest remnants can be quantified. By mapping fragmentation patterns that affect connectivity and edge dynamics, targeted management strategies can be developed that improve forest health and mitigate the negative impacts of fragmentation. Prioritizing the implementation of landscape metrics that are associated with ecological processes related to forest structure and function will ensure the long-term viability of these vital ecosystems and the species that depend on them.

3. Case Study 1: National Scale Landscape Fragmentation Analysis

3.1 Abstract

Indigenous forests are highly fragmented and disproportionately allocated across New Zealand's 16 regional councils. To quantify regional fragmentation characteristics and trends, the classified Climate Change Initiative - Land Cover (CCI-LC) dataset was analysed with FRAGSTATS. The analysis revealed spatial and temporal variability in configuration of forest patches and their distribution over a 28-year period. Configuration-based metrics employed to quantify the area-perimeter ratio indicated increasing fragmentation was occurring in most regions. This occurred during periods of both growth and decline, though some infilling of convoluted forest fragments was observed. Composition-based metrics revealed similar spatial and temporal variability in patch distribution throughout the landscape. A common trend was increasing disaggregation towards the end of the study period as evidenced by a sharp decline in the Clumpiness Index and Euclidean Nearest-Neighbour distance. The increasing fragmentation and spatial disaggregation of indigenous forest patches suggests landscape metrics are well suited to monitoring forest health and should be included in state of the environment reporting. However, these results should be interpreted with caution as the coarse resolution (246 m^2) of the CCI-LC may not provide sufficient accuracy to quantify fragmentation at regional level.

3.2 Introduction

New Zealand's indigenous forests are highly valued for their cultural significance, habitat provision, ecosystem services, and aesthetic beauty yet they remain threatened due to human activities that continue to alter forest range, dynamics, and composition. To manage these vulnerable areas, landscape managers are increasingly turning to high resolution, remotely sensed, classified imagery obtained by earth observing satellites to quantify land cover change (Fynn & Campbell, 2018; Hall et al., 2009; Lafortezza et al., 2010). Landscape analysis is then employed to quantify forest loss and gain with results frequently presented in state of the environment reports in terms of area, or percentage of landscape, change (Ministry for the Environment & Stats NZ, 2022). While important in quantifying forest area, these metrics do not describe the spatial arrangement of forest fragments within the landscape. Utilising additional metrics that provide valuable spatial information could help improve environmental assessments through the inclusion of indices linked directly to ecological processes that maintain forest health (Didham & Ewers, 2012; Ewers & Didham, 2007).

3.2.1 Background

The present configuration of New Zealand's indigenous forests, like many around the world, is due to historical processes that led to the clearance of forests for agriculture, settlements, and access. The first humans to arrive in New Zealand were the Polynesians who reached the North Island in ca. 1250

AD. In the following 600 years, large tracts of indigenous forest were cleared, reducing the total extent from 82 % to around 53-68 % by 1840 (Ewers et al., 2006; Roche, 2017). In 1840, New Zealand became a colony of the British empire and mass European migration began, initiating a second phase of forest clearance. The new colonists were encouraged to continue clearing native forests and develop farms to increase the productivity of the land. By the mid-1940s, indigenous forest cover had been reduced to 23-25 % of land area and most of the remaining forest was located on steep hill country or along the axial ranges where agriculture was much more difficult (see Figure 3) (Ewers et al., 2006; Roche, 2017).

Growing concern at the rate of forest being cleared eventually led to the Forests Act 1949 which legislated against the removal of existing indigenous forest without a sustainable harvesting plan, helping dramatically slow the rate of deforestation in New Zealand (Ewers et al., 2006; Tilling, 1992). With initial legislation in place, the indigenous forest remnants were protected but fragmented, spatially constrained, and disproportionately located on steep hill country (Gillman, 2008; Norton, 2002; Ogden, 1995). Subsequent legislation (such as the Resource Management Act 1991) afforded additional protection yet forest loss is still occurring, further altering the spatial configuration and connectivity of forest patches which affects species composition, vegetative structure, landscape morphology, and ecosystem services (Barbaro et al., 2012; Ewers & Didham, 2007; Hall et al., 2009; Jedraszak et al.; Scarsbrook & Halliday, 1999; Smale et al., 2005; Staples et al., 2012).

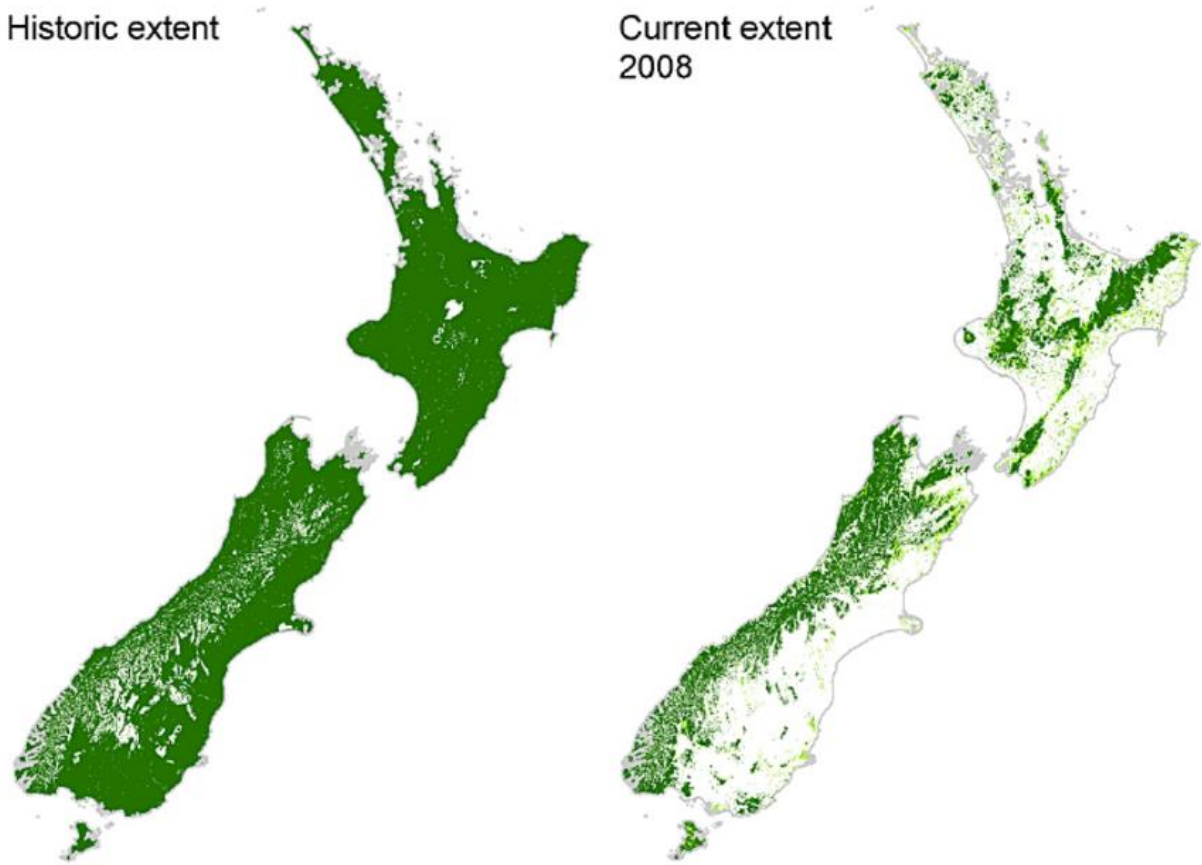

Figure 3. Historical Extent of Indigenous Forest Cover Compared to Extent in 2008. *Note:* The extent of pre-human indigenous forest cover around 1000 AD (left) compared to the 2008 extent (right). The images show the widespread loss and fragmentation of indigenous forests since the arrival of humans in 1250 AD (Ausseil et al., 2011, p. 205).

The continued decline of indigenous forests has not gone unnoticed with numerous state of the environment reports highlighting the loss of forest, often in terms of percentage of landscape (PLAND) change (Ewers et al., 2006; Riitters et al., 2000). Percentage of landscape is a valuable statistic for quantifying forest gain and loss, but it can be misinterpreted to infer that as area increases forest health improves (Trumbore et al., 2015). For example, Fynn and Campbell (2018) explain how forest fragmentation occurs during periods of both gain and loss such that PLAND figures can remain static while fragmentation is invariably occurring. Trumbore et al. (2015) argue that area alone does not adequately describe temporal changes in shape complexity or spatial configuration and should be supported by other metrics to holistically describe forest health. Utilising landscape metrics that quantify the spatial configuration and composition of indigenous forest remnants could provide

greater insight into regional forest fragmentation dynamics, improving management and future planning strategies (Bhatia & Cumming, 2020).

3.3 Data sources

3.3.1 Climate Change Initiative Land Cover

To assess indigenous forest fragmentation in New Zealand, an annually produced, globally classified dataset was required with sufficient resolution to detect regional-scale change. This would ensure the methodology could be employed globally while providing a long enough time span from which to observe and identify changes in forest fragmentation. The selected land cover dataset was developed by the European Union's Earth observation programme, Copernicus, under their Climate Change Initiative (CCI). The CCI-LC dataset is provided annually from 1992, has a spatial resolution of 300 m, and features 23 parent land cover classes that describe a wide range of environments (see Appendix A). The classes are based upon the United Nation's Food and Agriculture Organisation's (UN FAO) Land Cover Classification System (LCCS), a flexible, *a-priori* classification system with a hierarchical structure (UCL-Geomatics, 2017). Class allocation of vegetated areas occurs initially through definition of physiognomic and vegetative structure. Additional attributes, such as landform, lithology, climate, altitude, and aspect are then considered as the class allocation process proceeds down the hierarchy. The advantage to this approach is that land cover classification is objective and generalises well while maintaining applicability at varying scales (Herold & Di Gregorio, 2012).

According to the CCI-LC Product User Guide (UCL-Geomatics, 2017), the dataset is created from multispectral images that are classified within an automated processing chain. Multispectral imagery acquired by earth-observing satellites (see Table 1) are processed against a baseline land cover map generated from the MERIS Full Resolution and Reduced Resolution archives (2003-2012). Land cover changes are detected independently from the baseline land cover map at a resolution of 1 km using the AVHRR (1992-1999), SPOT-VGT (1999-2013), PROBA-V (2013-2019), and Sentinel-3 (2020) datasets. Changes detected for at least two consecutive years are recorded and the baseline land cover map is both backdated and updated, including the adjacent area up to 5 km from the detected pixel change. Images collected post-2004 are further remapped at 300 m when higher resolution imagery is available from the MERIS FR or PROBA-V archives. The process of back- and updating the baseline map ensures the classification remains consistent over time. Numerous studies (Bhatia & Cumming, 2020; Guidigan et al., 2019; Liu et al., 2018; Mousivand & Arsanjani, 2019; Wang et al., 2021) have employed the CCI-LC dataset at regional to global scale and demonstrated the consistency and inherent value in the dataset for landscape analysis.

Table 1. Satellites and Sensors That Provided Imagery for the CCI-LC Dataset.

Sensor	Satellite	Resolution at Nadir	Years Active
Advanced Very High-Resolution Radiometer (AVHRR)	National Oceanic Atmospheric Administration (NOAA)	1000 m	1992-1999
Medium Resolution Imaging Spectrometer (MERIS)	Environmental Satellite (ENVISAT)	300 m Full Resolution 1200 m Reduced Resolution	2003-2012
Vegetation (VGT)	Project for Onboard Autonomy – Vegetation (PROBA-V)	100 m VNIR 200 m SWIR	2014-Present
Vegetation (VGT)	Satellite Pour l'Observation de la Terre Vegetation (SPOT-VGT)	1150 m	1999-2013
Ocean & Land Cover Instrument (OLCI)	Sentinel-3	300 m Full Resolution 1200 m Reduced Resolution	2016-Present

Note: (UCL-Geomatics, 2017, p.23-24).

3.3.2 Landcare Database

Prior to performing the landscape analysis, a CCI-LC class was selected to represent NZ's indigenous forest. Class selection was verified with the medium resolution, vector-based Land Cover Database (LCDB v5.0) developed by Manaaki Whenua -Landcare Research. The LCDB features 33 land cover classes specifically created to describe local land cover. It was designed for use with NZ's 1:50,000 topographic maps and maintains the same scale and accuracy with a minimum nominal mapping unit of 1 ha (Manaaki Whenua - Landcare Research, 2020).

Imagery used in the LCDB was captured over five summer periods during 1996-97, 2001-02, 2008-09, 2012-13, and 2018-19 and was initially developed from classified SPOT imagery with land cover polygons manually adjusted and refined (Dymond et al., 2017). The present version, LCDB v5.0, is derived predominantly from Sentinel-2 imagery and has a higher classification accuracy than earlier versions while retaining backwards compatibility (Schindler et al., 2021). As the LCDB is widely used across both regional and national government agencies for planning, land management, and state of the environment reporting, it provides a high-quality, well-documented option for validating CCI-LC class selection.

3.4 Methods

3.4.1 Pre-processing

To perform class selection, the CCI-LC dataset of 28 classified global land cover maps was retrieved from Copernicus' *Climate Data Store* (ESA Climate Change Initiative - Land Cover, n.d.) and pre-

processed in ArcGIS. Pre-processing was performed to reduce file size and improve file handling in ArcGIS while also improving processing speed during computation of landscape configuration statistics (see Figure 4). Each CCI-land cover map was first converted from NetCDF to GeoTIFF format then clipped to the NZ coastline using the *NZ Coastlines and Islands Polygons* from LINZ (Land Information New Zealand, 2022). File compression was applied to each raster using lossless LZW (Lempel-Ziv-Welch) compression to preserve the original raster cell values. Finally, regional information was extracted for each of New Zealand's regional councils (see), resulting in 16 regional datasets each containing 28 CCI-LC maps correlating to the years covered (see Appendix B for more detail).

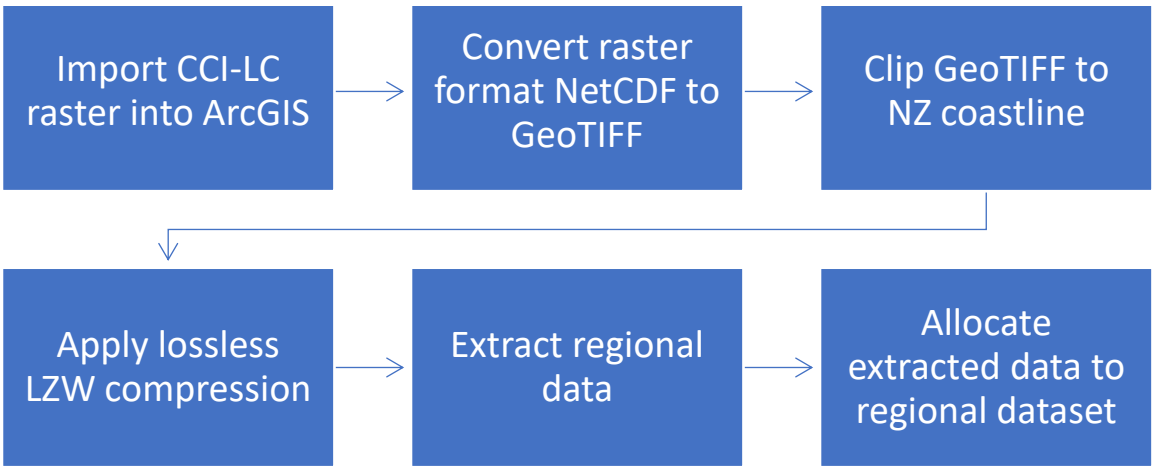

Figure 4. Schematic Representation of Pre-processing Workflow. *Note*: For more information see Appendix B.

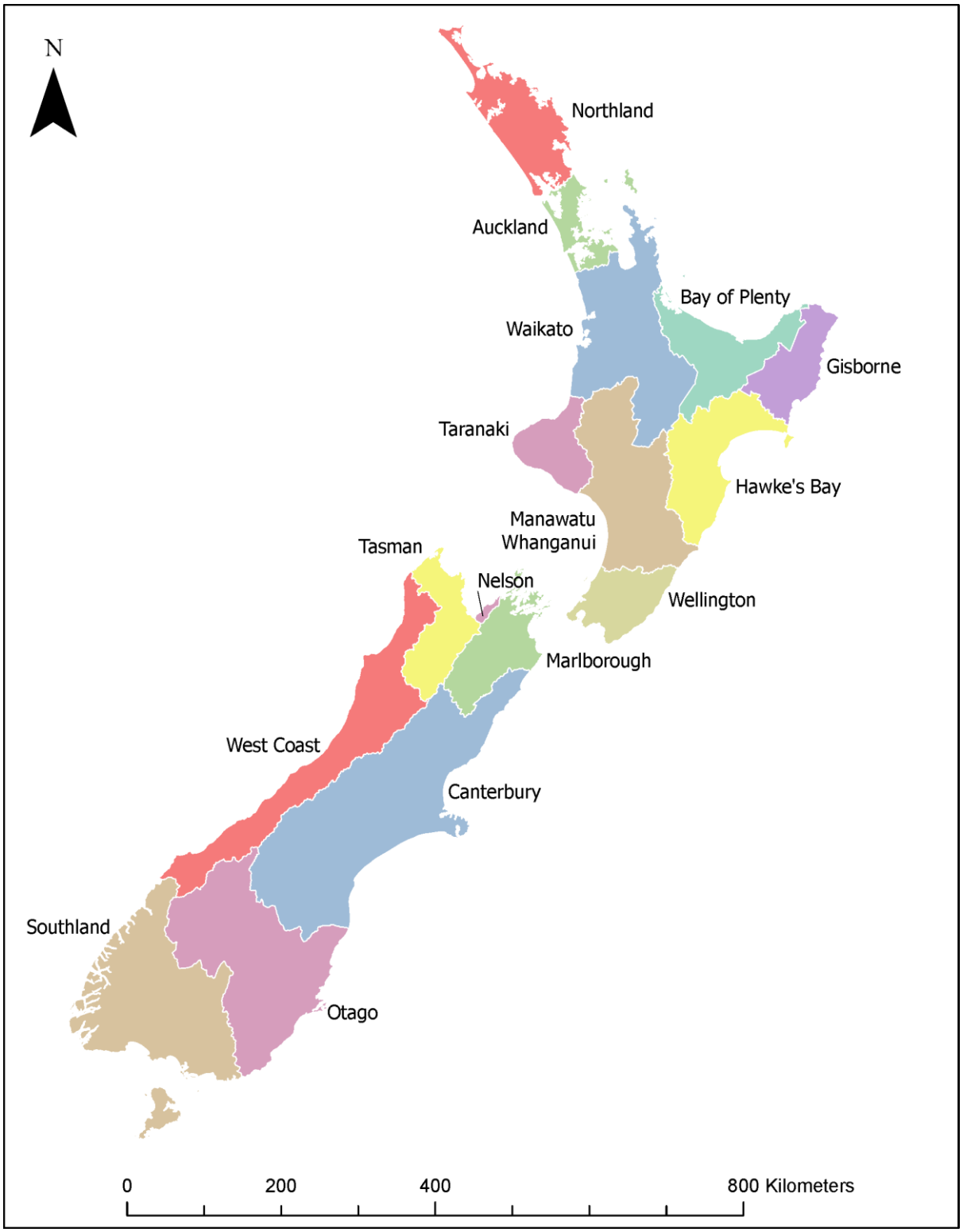

Figure 5. New Zealand's Regional Council Boundaries*. Note:* Regional boundary shapefiles were used to extract the corresponding CCI-LC data in preparation for landscape analysis.

3.4.2 Class Selection

Following pre-processing, the LCDB was employed to assist in correlating a CCI-LC class to indigenous forest. The LCDB describes a range of indigenous environments that could collectively be described as forest, including shrubland, mangroves, matagouri, and manuka/kanuka. There is also provision in the LCDB for successional forest types and mixed native/exotic land cover classes. However, for the purposes of this work, the *indigenous forest* class, defined as areas covered in mature indigenous beech, podocarps, and/or mixed broadleaved species, was selected (Manaaki Whenua - Landcare Research, 2019). The indigenous forest class accounted for 23.5 %, or >63, 000 km^2, of New Zealand's total land surface area in the 2018-19 LCDB survey (Manaaki Whenua - Landcare Research, 2019).

Identification of a CCI-LC class that spatially correlated with the LCDB's indigenous forest class was performed in ArcGIS. The LCDB v5.0 vector layer was retrieved from the Land Resource Information Systems Portal (Manaaki Whenua - Landcare Research, 2019) and clipped to the *NZ Coastlines and Islands Polygons* available through the LINZ Data Service (Land Information New Zealand, 2022). The indigenous forest class layer was then extracted for each of the five available time periods (1996-97, 2001-02, 2008-09, 2012-13, and 2018-19). The resulting raster layers were then used to clip the corresponding years from the CCI-LC dataset. The five clipped CCI-LC raster layers were then processed through the landscape configuration and composition software, FRAGSTATS, to quantify the total land area of each class within the LCDB indigenous forest polygons. The CCI-LC class occupying the greatest area within the LCDB indigenous forest polygons was then selected as the representative indigenous forest class.

3.4.3 Class Analysis

Following selection of an indigenous forest class from the CCI-LC dataset, the class was then extracted from each regional dataset using ArcGIS and landscape statistics were calculated in RStudio. Landscape analysis was performed with the FRAGSTATS derived *landscapemetrics* package (v1.5.4) by Hesselbarth et al. (2019). Six class-based metrics were employed for the analysis: class area (CA), percentage of landscape (PLAND), edge density (ED), mean fractal dimension index (MFDI), Euclidean nearest-neighbour distance (ENN), and the clumpiness index (CI) (see Table 2). Metrics were calculated for each regional CCI-LC dataset and the aggregated results output in table format.

Table 2. FRAGSTATS Metrics, Units, and Description.

Metric	Units	Description
Class Area (CA)	Hectares (ha)	Area encompassed by a class within a given landscape
Percentage of Landscape (PLAND)	Percent (%)	Percentage of landscape covered by a class
Edge Density (ED)	Metres per hectare (m ha^{-1})	A standardised value describing perimeter to area relationship of a class. Higher ED indicates a more fragmented forest margin
Mean Fractal Dimension Index (MFDI)	None	A measure of increasing shape complexity from simple Euclidean geometry. Ranging from 1-2, higher MFDI indicates greater shape complexity
Mean Euclidean Nearest-Neighbour Distance (ENN)	Metres (m)	Mean Euclidean distance to nearest patch of same class. A measure of patch connectivity
Clumpiness Index (CI)	Percent (%)	A measure of patch aggregation. Range is from -1 (maximum disaggregation) to 1 (maximally clumped) with values above zero

3.5 Results

3.5.1 Class Selection

The CCI-LC class selection results in Figure 6 reveal 23 of the 28 CCI-LC classes had pixels present within the LCDB's indigenous forest polygons. The class with the greatest representation in the LCDB polygons over all five correlating time periods was class 50, described as "Tree cover, broadleaved, evergreen, closed to open (>15%)" (UCL-Geomatics, 2017, p.26). Over 80 % of class 50 pixels were found within the LCDB indigenous forest polygons, accounting for over 78% of polygon area. The 22 remaining classes had significantly fewer classified pixels spatially constrained within the LCDB indigenous forest polygons. Classes of note included class 100 ('Mosaic tree and shrub (>50%)/herbaceous cover (<50%)), class 110 (Mosaic herbaceous cover), and class 120 (Shrubland). Over the five survey periods, these classes had averages of 29 % (class 100), 13 % (class 110), and 27 % (class 120). In terms of percentage of LCDB polygon area occupied, class 120 occupied the greatest percentage of polygon area at 7.0 %, while class 100 and 110 occupied 5.8 % and 2.9 % respectively. The remaining 19 CCI-LC classes had 12 % or less of their classified pixels contained within the polygons. When combined, these 19 classes accounted for 5.7 % of total LCDB polygon area.

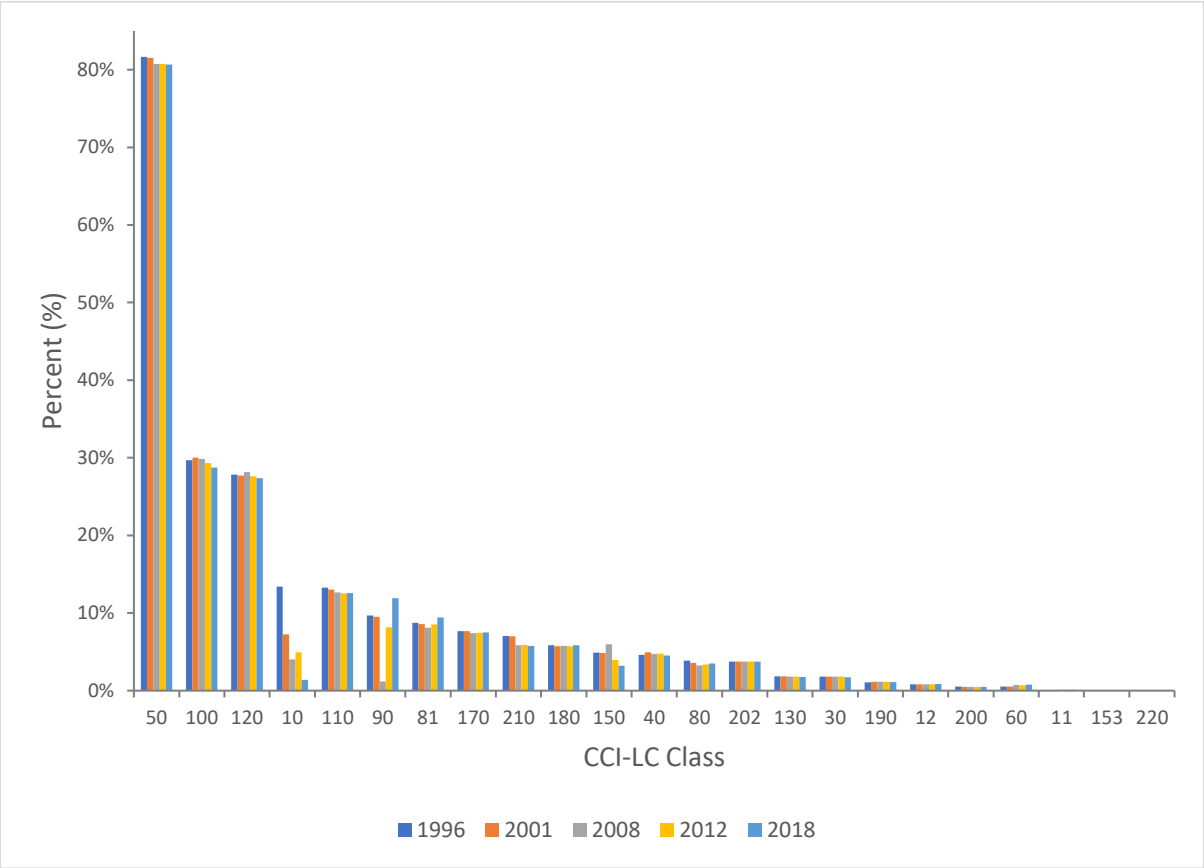

Figure 6. CCI-LC Classes Within LCDB Indigenous Forest Polygons. *Note:* For each of the five available LCDB data periods, over 80 % of CCI-LC pixels classified as class 50 could be found within the LCDB's Indigenous Forest class polygons. Class 50 is described as "Tree cover, broadleaved, evergreen, closed to open (>15%)" (UCL-Geomatics, 2017, p.26).

3.5.2 Class Area (CA)

The CA results were normalised and hierarchically clustered into four groups to assist in the identification of regional trends and group regions based on trend similarities (see Figure 7). To cluster the regions, the normalised CA results were analysed in R Studio using the dendextend package (v1.16.0). The largest cluster (blue) shown in Figure 7 contains 12 regions characterised by a general increase in CA, with all regions remaining within 0.2 of their maximum normalized value. This includes the two regions with the greatest net increase in CA, Canterbury (bold dashed grey line) and Waikato (bold dashed orange line). As shown in Table 3, Canterbury increased by 25,527.3 ha and Waikato by 26,948.6 ha over the study period. Manawatu-Whanganui had the third largest gain in CA with a net increase of 24,847.1 ha. The smallest net gain within the cluster occurred in Auckland, which added 6498.7 ha of indigenous forest.

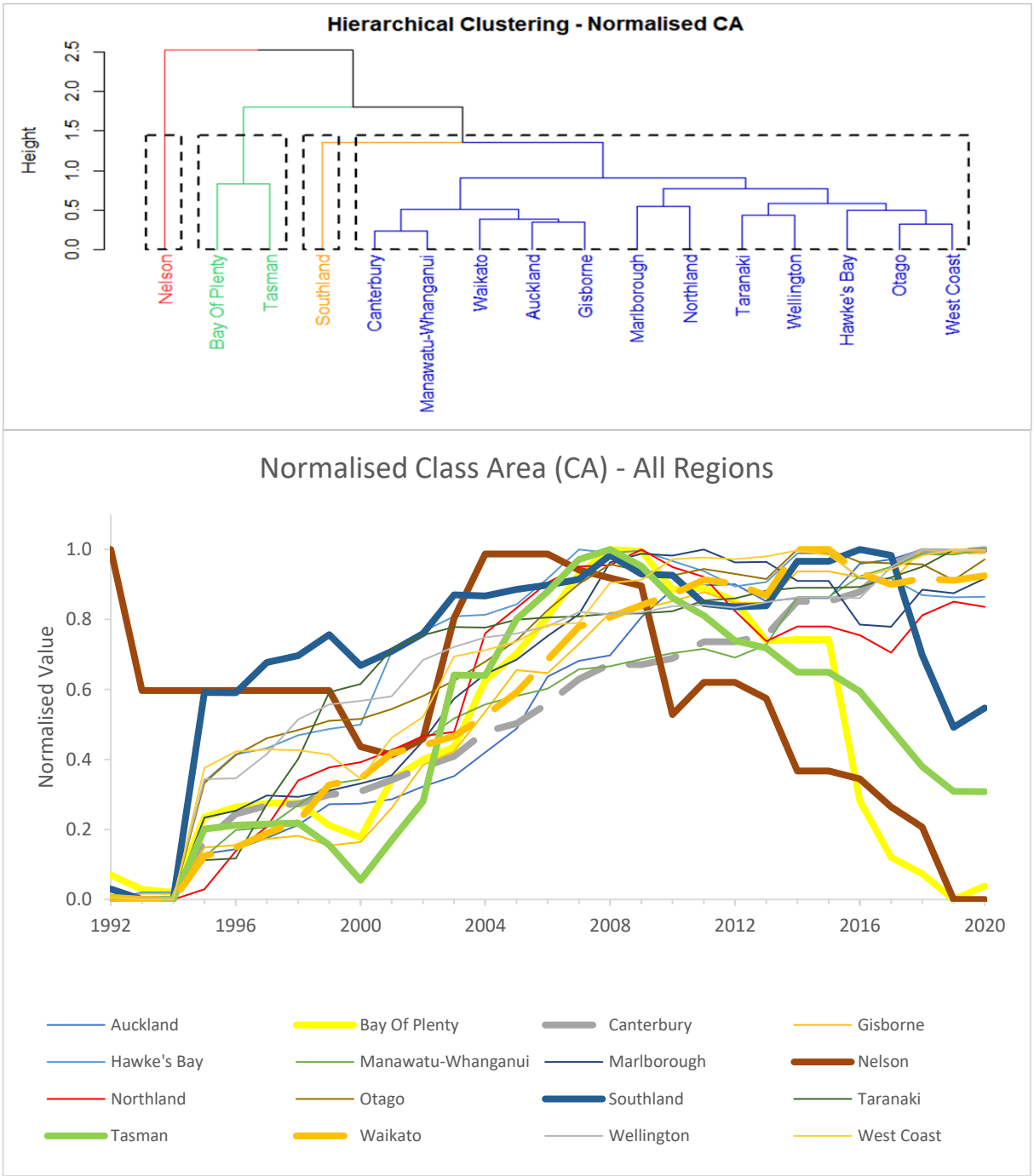

Figure 7. Class Area Results Hierarchically Clustered (top) and Normalised (bottom). *Note:* The dendrogram (top) shows the allocation of regions into one of four clusters based on hierarchical analysis of CA results. The blue cluster was the largest containing 12 regions. The line plot (bottom) shows the change in CA over the course of the study period. The four solid, bold lines indicate regions not found in the largest (blue) cluster. The bold, dashed lines indicate regions with the greatest net increase in CA: Canterbury and Waikato.

The green cluster in the dendrogram in Figure 7 contains the Bay of Plenty and Tasman which are distinguished in the normalised results at the bottom of the figure by bold yellow (Bay of Plenty) and green (Tasman) lines. These regions may be characterised by the rise and fall of their profiles, whereby both regions rose to a peak in 2008 before descending below 0.4 of their maximum normalized value. In Table 3, it can be observed that Bay of Plenty was one of only two regions to record a net loss in indigenous forest area, declining by 236.9 ha. This figure is much greater when examining the decline in CA from the 2008 peak through to 2020, where the region lost 9,086.1 ha over 12 years. This was the largest decline in forest area of all regions. Unlike Bay of Plenty, Tasman had a net gain in indigenous forest of 2,393.0 ha. However, Tasman also had a large decline in CA from its 2008 peak, losing some 5,417.6 ha of indigenous forest by 2020.

The red (Nelson) and yellow (Southland) clusters at the top of Figure 7 are the remaining two regions and have contrasting profiles. The normalised class results at the bottom of Figure 7 show Nelson's (bold brown line) indigenous forest area declined from 1992 but returned to a similar extent in 2004-06. From 2006-2020, CA steadily declined, reaching its lowest observed value in 2019-20. Table 3, however, shows Nelson had the greatest net loss in indigenous forest area, losing 242.9 ha. In contrast, the normalized results in Figure 7 show Southland (bold blue line) increased from 1992, reaching peak coverage in 2016 with 1,110,678.8 ha. However, Table 3 reveals that from 2016-2020 Southland experienced the second largest post-peak coverage decline in CA, losing 6,681.0 ha of indigenous forest.

Table 3. Net Area Change (1992-2020) and Change in Area from Year of Maximum Coverage to 2020.

Region	Total Regional Area (ha)	CA 1992 (ha)	CA 2020 (ha)	Net Change 1992-2020 (ha)	CA Max. (Year)	CA Max. (ha)	Area Change From CA Max to 2020 (ha)
Auckland	491179.1	44604.5	51103.2	6498.7	2018	51133.6	-30.4
Bay Of Plenty	1225600.3	570626.6	570389.8	-236.9	2008	579475.9	-9086.1
Canterbury	4523298.5	219433.0	244960.3	25527.3	2020	244960.3	0.0
Gisborne	835850.5	165104.7	175909.6	10804.9	2018	176025.0	-115.4
Hawke's Bay	1417034.5	301299.0	310142.2	8843.2	2007	311533.0	-1390.9
Manawatu-Whanganui	2221788.1	337424.8	362271.9	24847.1	2020	362271.9	0.0
Marlborough	1049684.2	242451.9	252825.6	10373.7	2011	253767.0	-941.4
Nelson	42363.4	21409.4	21166.5	-242.9	2006	21427.7	-261.2
Northland	1252968.0	155308.0	164436.6	9128.6	2009	166234.4	-1797.8
Otago	3187328.5	188445.5	201977.5	13532.0	2015	202372.3	-394.8
Southland	3183344.2	1096430.1	1103997.8	7567.7	2016	1110678.8	-6681.0
Taranaki	725663.1	162620.6	175891.4	13270.8	2020	175891.4	0.0
Tasman	965090.9	552679.1	555072.1	2393.0	2008	560489.8	-5417.6
Waikato	2458434.3	426609.5	453558.0	26948.6	2015	455768.8	-2210.8
Wellington	811331.4	190595.6	202044.3	11448.7	2018	202105.0	-60.7
West Coast	2335109.6	1305434.7	1317946.3	12511.6	2019	1317964.6	-18.2

Note: The net change in CA shows indigenous forest area increased in all regions except Bay of Plenty and Nelson from 1992-2020. In contrast, the change in CA from year of maximum coverage until 2020 shows most regions were experiencing a decline in indigenous forest area at the end of the study period.

3.5.3 Percentage Landscape (PLAND)

From the CA results PLAND figures were calculated, revealing wide regional differences in the amount of indigenous forest within each landscape (see Figure 8). The region with the highest percentage of indigenous forest area was Tasman with 57.65 %. This was followed by West Coast with 56.27 %, and Nelson with 50.33 %. Canterbury had the lowest mean PLAND value at 5.16 %, followed by Otago (6.21 %), and Auckland (9.82 %). The range of PLAND values also varied, with Otago recording the smallest range of 0.43 % and Taranaki the largest at 1.83 %. Taranaki also had the largest net increase in PLAND, increasing 1.83 % over the 28-year study period. Wellington (1.42 %), Auckland (1.33 %), Gisborne (1.29 %), Manawatu-Whanganui (1.12%), and Waikato (1.10 %) all recorded >1 % net increases in the percentage of landscape occupied by indigenous forest. In the Bay of Plenty and Nelson where a net loss in CA was observed, PLAND figures declined by -0.02 % and -0.62 % respectively.

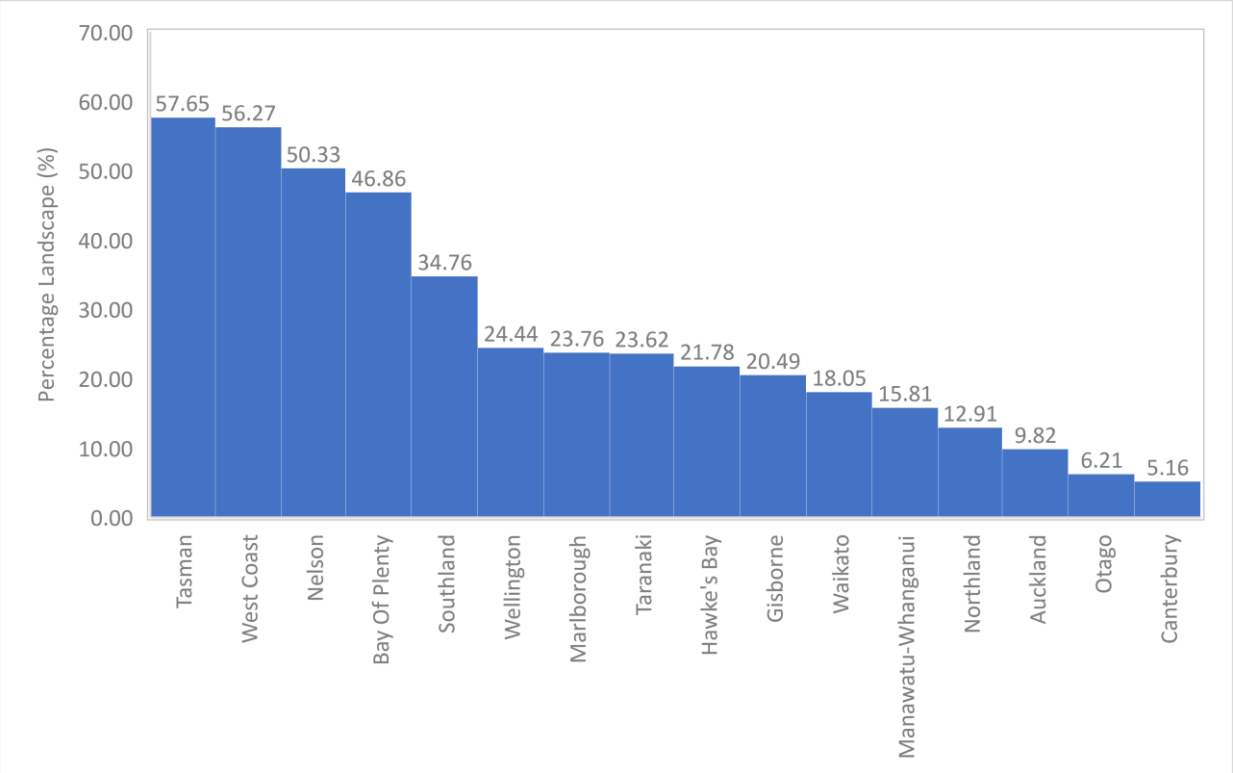

Figure 8. Mean Percentage Landscape Results. *Note:* The mean PLAND results, ordered from highest to lowest, reveal wide regional variability in the distribution of indigenous forest.

3.5.4 Edge Density (ED)

Figure 9 contains the ED results which were again highly variable. Nelson had the highest recorded ED value of 10.92 m ha^{-1} and the highest mean ED value with 10.81 m ha^{-1}. The second (Tasman) and third (West Coast) highest mean values were also South Island regions, Tasman recording a mean ED figure of 8.17 m ha^{-1} and West Coast recording 7.99 m ha^{-1}. Bay of Plenty had the highest mean ED in the North Island at 6.77 m ha^{-1}. Of all regions, Canterbury had the lowest ED value with 1.77 m ha^{-1} and the lowest mean value with 1.83 m ha^{-1}. The range in ED values was highest in Auckland at 0.6 m ha^{-1}, while the smallest range was 0.1 m ha^{-1} recorded in Hawke's Bay.

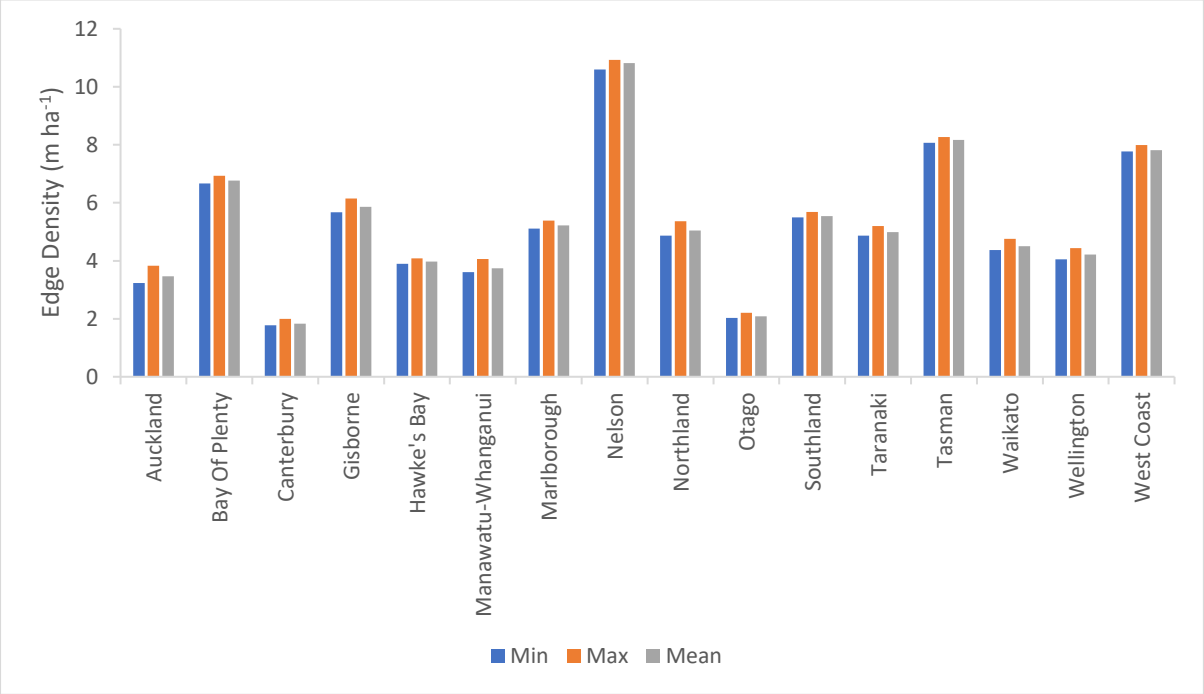

Figure 9. Minimum, Maximum, and Mean Edge Density Results. *Note:* There was a wide variation in ED results, ranging from a low of 1.7 m ha^{-1} in Canterbury to a high 10.9 m ha^{-1} in Nelson.

Figure 10 contains the results from hierarchical clustering along with the normalised ED results. Three broad trends from Figure 10 can be identified: increasing, a delayed increase, and declining. Regions in the blue dendrogram cluster (Auckland, Bay of Plenty, Canterbury, Gisborne, Hawke's Bay, Manawatu-Whanganui, Marlborough, Northland, Otago, Taranaki, Waikato, and Wellington) have a profile characterized by a general increase in the density of forest edge per hectare between 1992-2020. Regions in the red cluster (Southland and Westland) had a delayed increase, rising above a normalised value of 0.2 much later than those in the blue cluster. In Southland (bold dashed red line), the ED profile did not exceed 0.2 until 2014 and in West Coast (bold dashed yellow line) ED rose above 0.2 in 2017. Both regions reached their highest observed ED result in 2020. The remaining green dendrogram cluster, containing Nelson and Tasman, have profiles that declined. Both Nelson and Tasman had their highest normalised values at the start of the study period, with Tasman (bold blue line) declining from 1994 and Nelson (bold brown line) from 1999. Edge density in both regions declined till 2017 before rising from 2017-2020.

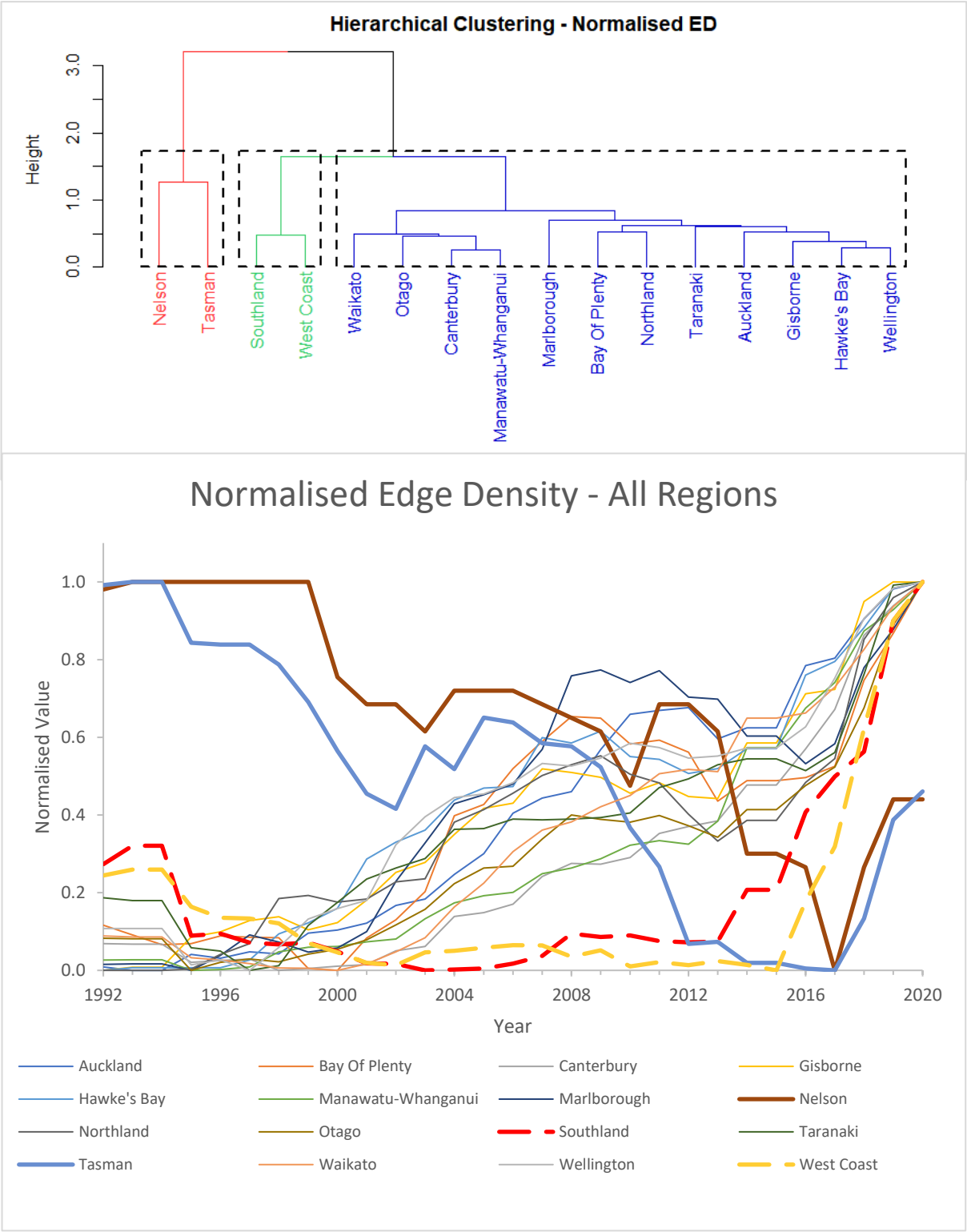

Figure 10. Edge Density Results Hierarchically Clustered (top) and Normalised (bottom). *Note:* The dendrogram (top) shows the three clusters identifiable in the line plot below. Edge density in the red cluster generally declined before an increasing from 2017. Regions in the blue cluster experienced a more consistent increase in ED while those in the green cluster experienced a delayed increase.

3.5.5 Mean Fractal Dimension Index (MFDI)

The MFDI results in Figure 11 show the shape complexity of indigenous forest patches declined over the study period, with many regions experiencing a faster rate of decline from 2015-2020. Bay of Plenty (bold orange line) had the highest MFDI values of all regions with a maximum of 1.0574 in 2013. However, from 2015-2020 the MFDI fell faster than previously observed, reaching the lowest observed value in the region of 1.0523 in 2020. In contrast, Nelson (bold brown line) had the lowest observed MFDI values with a minimum of 1.0310 (2017) and a maximum of 1.0399 (1993-1999). Nelson also experienced a post-2015 drop, reaching an MFDI minimum in 2017 before increasing to 1.0344 from 2018-2020. West Coast (bold green line) had the largest range with 0.0115, while the smallest observed range was 0.0031 in Waikato (bold blue line).

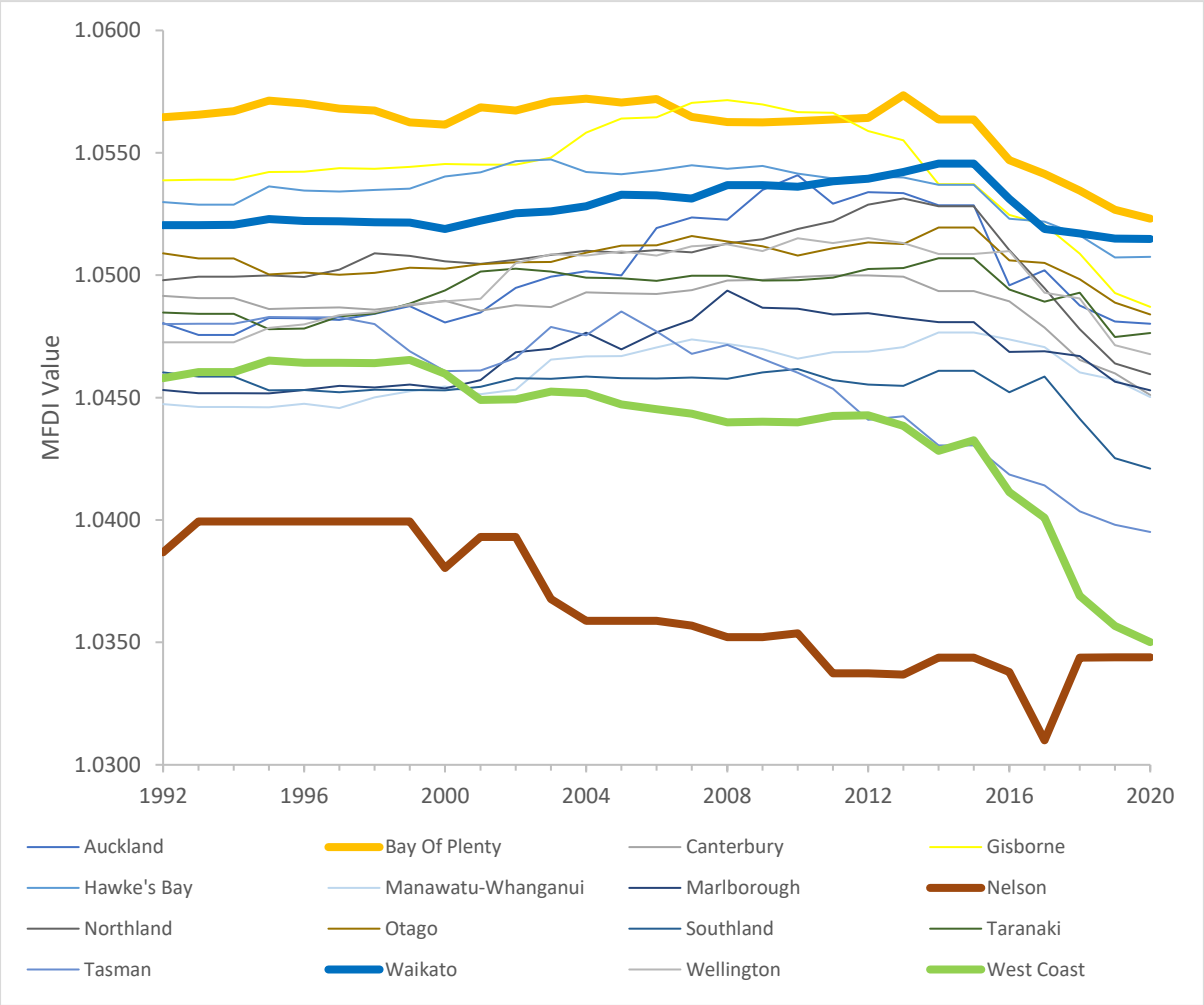

Figure 11. Mean Fractal Dimension Index Results. *Note:* The MFDI results show shape complexity in all regions was low - a potential limitation of the CCI-LC datasets resolution.

To investigate the post-2015 decline in MFDI values, hierarchical clustering was performed on the normalized MFDI results (Figure 12). The dendrogram in Figure 12 shows the three main clusters identified by the analysis and an associated line plot of the normalised MFDI results. The blue cluster contains nine regions (Tasman, Bay of Plenty, West Coast, Canterbury, Southland, Gisborne, Hawke's Bay, Northland, and Otago) and may be characterized by a higher shape complexity in the 1990s followed by a period of accelerated shape simplification, particularly from 2015 onwards. Tasman (bold blue line) is an outlier in the cluster, having steadily declined from a 2005 high through to 2020. Regions in the green cluster (Taranaki, Wellington, Manawatu-Whanganui, Waikato, Auckland, and Marlborough) have a lower shape complexity in the 1990s than regions in the blue cluster with normalized MFDI values below 0.5 in all regions until 1999. However, all green clustered regions steadily climb from the mid-1990s to the observed maximum which occurred between 2008-2015. Accelerated post-2015 shape simplification is then observed until 2020 like the blue cluster regions. The orange cluster is a true outlier, containing only Nelson. Nelson had a high MFDI in the early 1990s before falling steadily from 2002-2017. From 2017-2019, the normalised MFDI increased from 0 to near 0.4, remaining unchanged from 2019-2020.

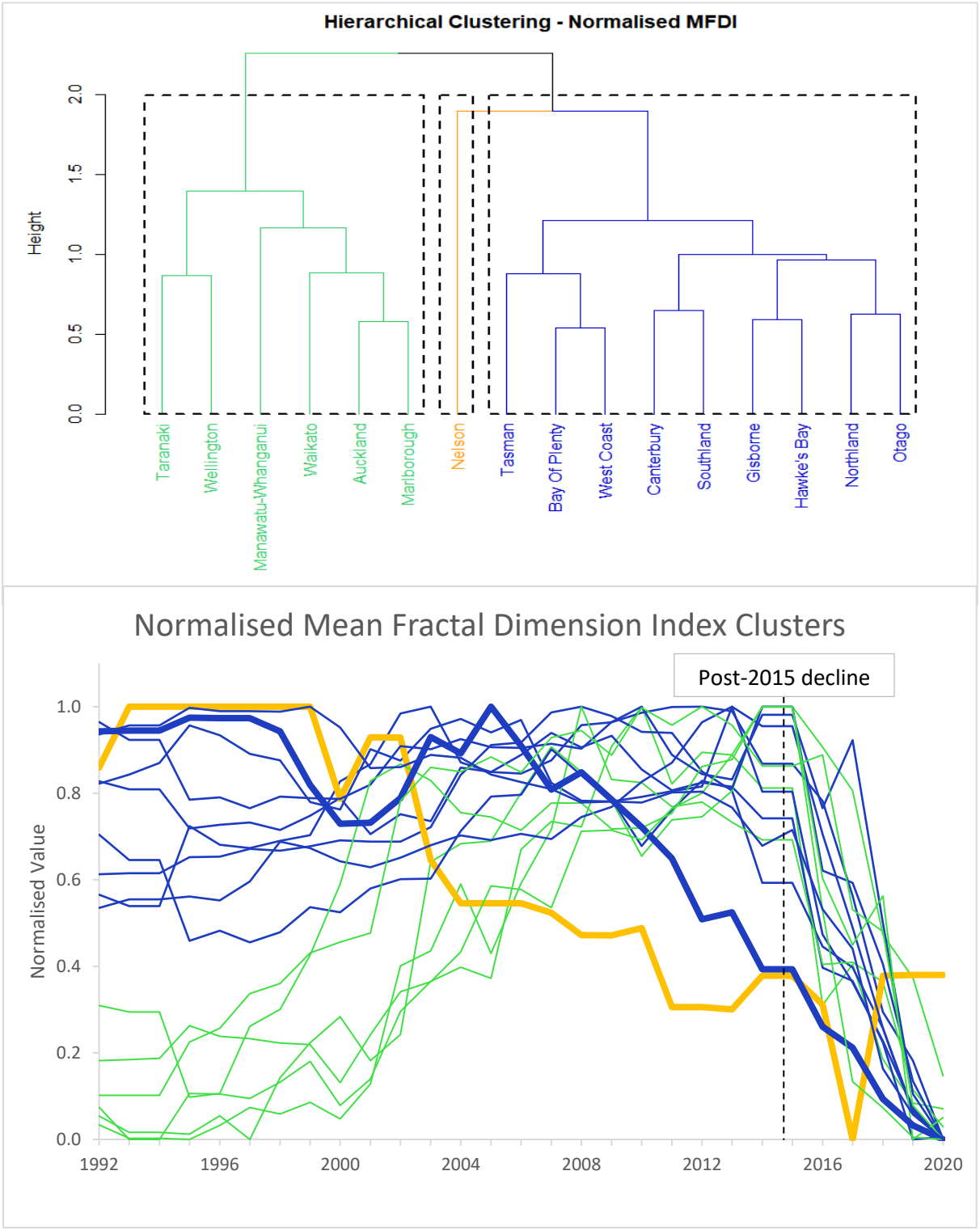

Figure 12. Mean Fractal Dimension Index Results Hierarchically Clustered (top) and Normalised (bottom). *Note:* Three clusters are shown in the dendrogram at top and are plotted by cluster colour in the line plot below for comparison. The sudden decline in shape complexity post-2015 is also indicated on the line plot.

3.5.6 Euclidean Nearest-Neighbour Distance (ENN)

Summary statistics of the ENN results in Figure 13 reveal New Zealand's largest region, Canterbury, had the greatest mean patch-to-patch distance, while the smallest region, Nelson, had the shortest. Canterbury's shortest ENN distance was 1267 m observed in 2020 and a maximum of 1411 m was observed in 2010. Nelson had the lowest patch-to-patch distance in all three categories with a minimum ENN distance of 632 m, maximum of 650 m, and an average of 640 m. This was followed by Tasman and West Coast, with average ENN distances of 663 m and 731 m respectively. Auckland, New Zealand's second smallest region, had the second highest ENN values behind Canterbury with a mean distance of 1205 m.

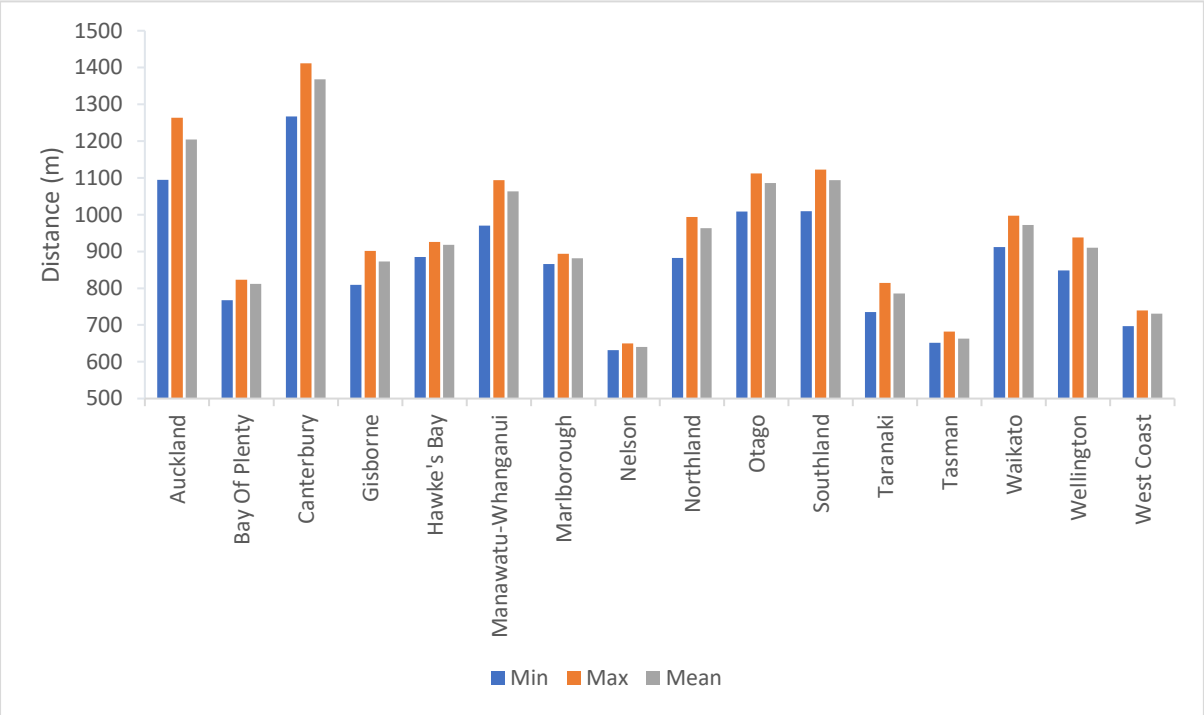

Figure 13 Minimum, Maximum, and Mean Euclidean Nearest Neighbour Distance.

The normalized ENN results in Figure 14 reveal that between 1992-2020 a net decline in ENN distance occurred in 14 of the 16 regions. Like the MFDI results, an accelerated period of decline is observable within most regions from 2015. The remaining two regions, Nelson (bold green line) and Tasman (bold blue line), are the only areas where a net increase in ENN distance was observed. However, the mean patch to patch distance in Tasman was in decline from a 2017 peak through to 2020, while Nelson's ENN distance had increased over the same period.

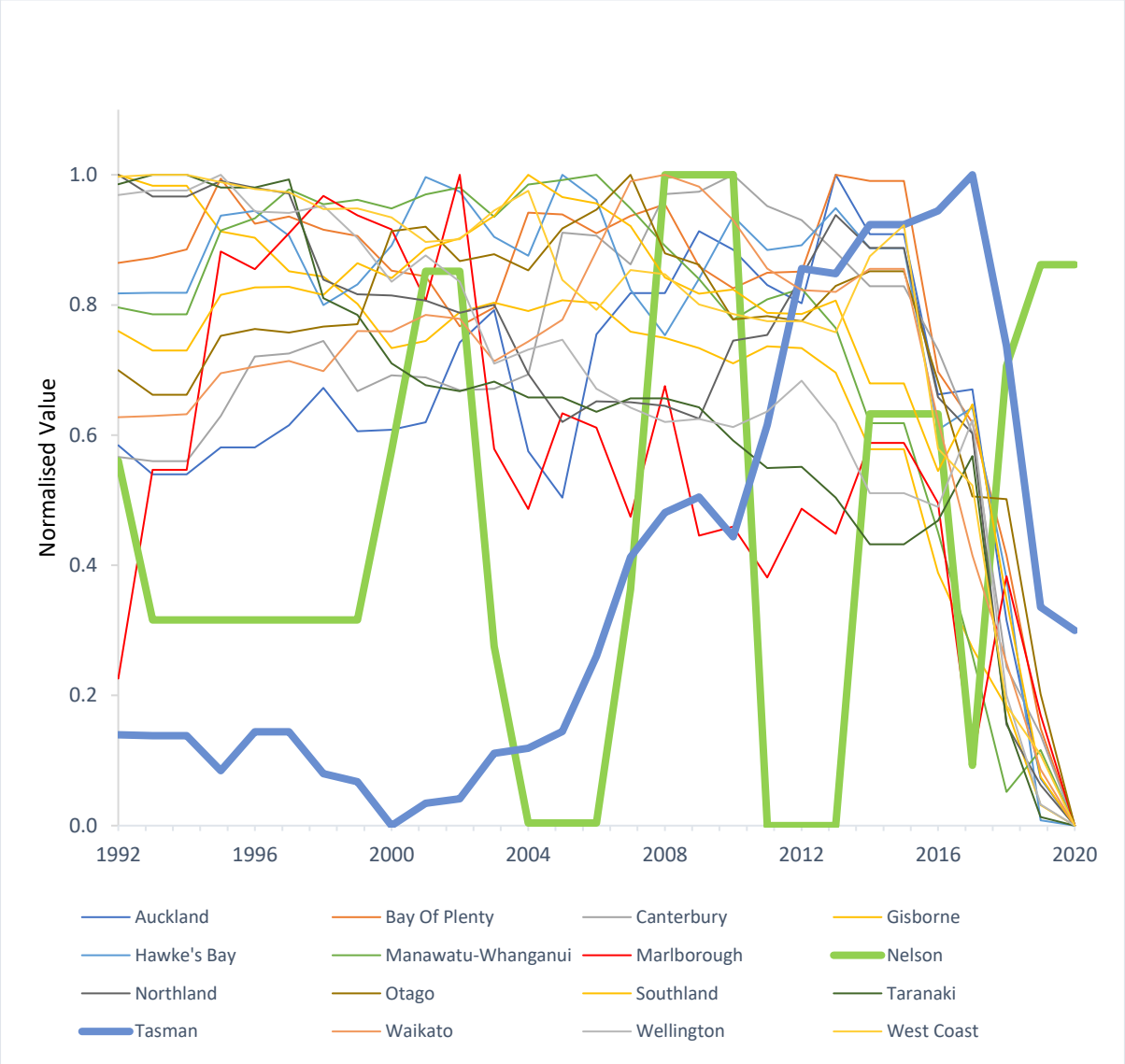

Figure 14. Normalised Euclidean Nearest Neighbour Distance. *Note:* Normalised ENN profiles with bold lines indicating Nelson and Tasman. The sudden shifts in Nelson's profile may be related to data resolution.

3.5.7 Clumpiness Index (CI)

The CI results shown in Figure 15 indicate Wellington (bold green line) had the greatest regional aggregation of mature indigenous forest patches and Northland (bold black line) had the lowest. Wellington's CI value ranged from a 1997 peak of 0.870 to a low in 2020 of 0.860. Northland fluctuated around 0.729 $\pm$ 0.001 until 2015 when the CI value began to decline. Northland's 2020 CI value was the lowest recorded CI value of all regions at 0.714. Like Northland, all other regions display a post-2015/16 decline, reaching a minimum, or near minimum, observed CI value by 2020. The only regions not to follow this trend were Nelson (bold brown line) and Tasman (bold blue line), though both

regions were declining from maximum CI values observed in 2017. Despite this fall, a net increase in CI was observed in both regions. Tasman made a net gain of 0.003 and Nelson increased by 0.005. In contrast, Northland had the greatest net loss with -0.014 followed by Auckland with -0.012.

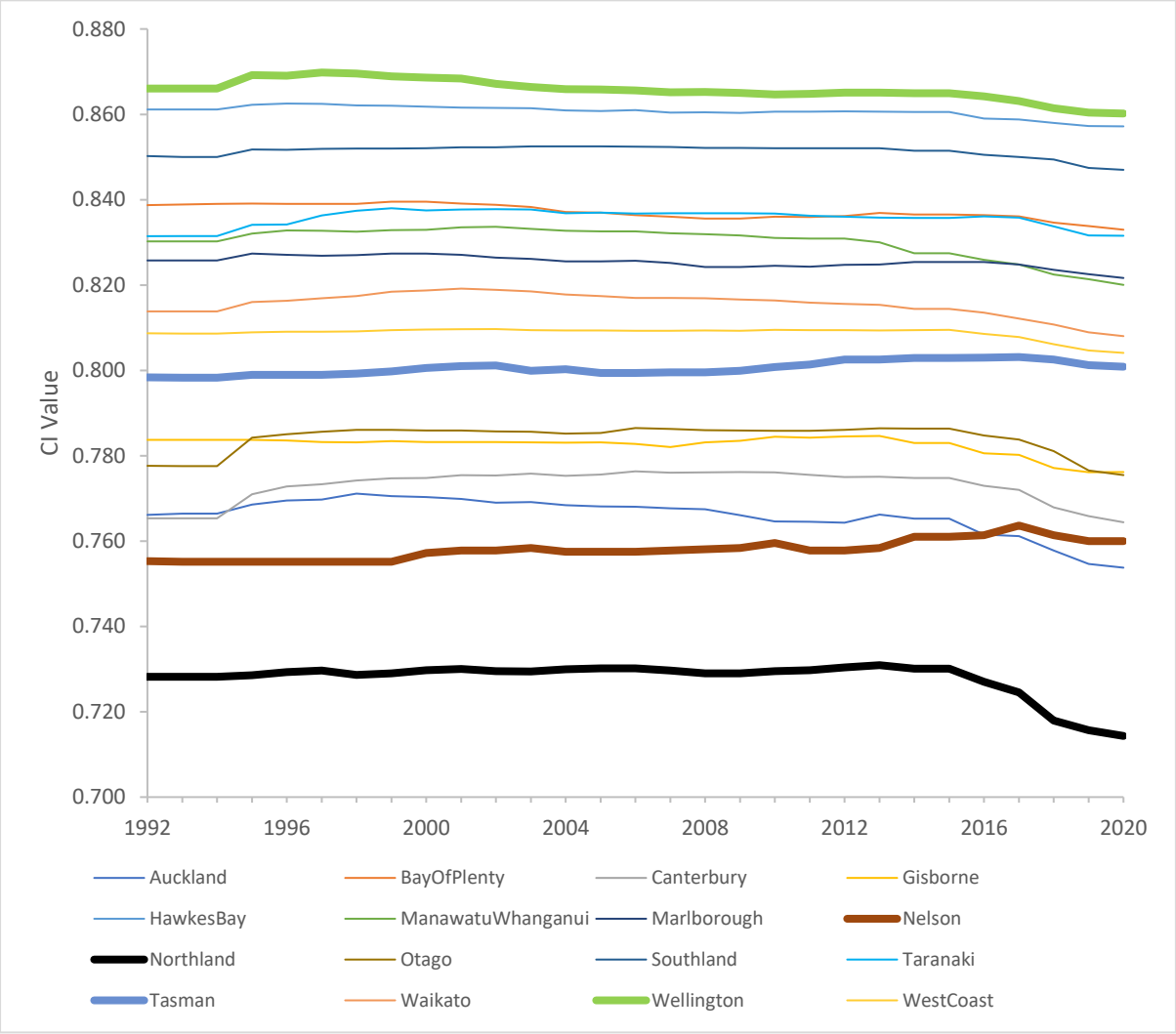

Figure 15. Clumpiness Index Results. *Note:* Clumpiness Index results show Wellington (bold green line) had the highest aggregation of indigenous forest and Northland (bold black line) the lowest. Nelson (bold blue line) and Tasman (bold brown line) were the only regions to record a net increase suggesting greater an improvement in connectivity of patches.

Hierarchical clustering results in Figure 16 display the three primary profile trends from the normalised CI data. The blue cluster contains 11 regions (Bay of Plenty, Marlborough, Hawke's Bay, Wellington, Waikato, Auckland, Manawatu-Whanganui, Gisborne, Southland, Northland, and West Coast) where normalised CI values were all above 0.5 in 1992, rising above 0.8 by 1998. In 2002, the first region in

the blue cluster, Wellington (bold blue line), fell below 0.8 while other regions, such as Northland (bold blue dashed line), Gisborne, West Coast, and Southland remained above 0.8 till 2015. Post- 2015 all regions in the blue cluster are in decline. The yellow clustered regions (Otago, Canterbury, and Taranaki) can be similarly characterised post-1998. However, from 1992-1994 all regions in the yellow cluster have a normalised CI value below 0.2. From 1994, the normalised CI value began to rise, with all regions in the yellow cluster rising above 0.8 by 1998. The remaining green cluster containing Nelson and Tasman both had normalised CI values below <0.2 from 1992-1998. From 1999-2017, both Nelson and Tasman's CI values rose, reaching their maximum observed values in 2017. Both regions then experienced a decline but remained above 0.5 by 2020.

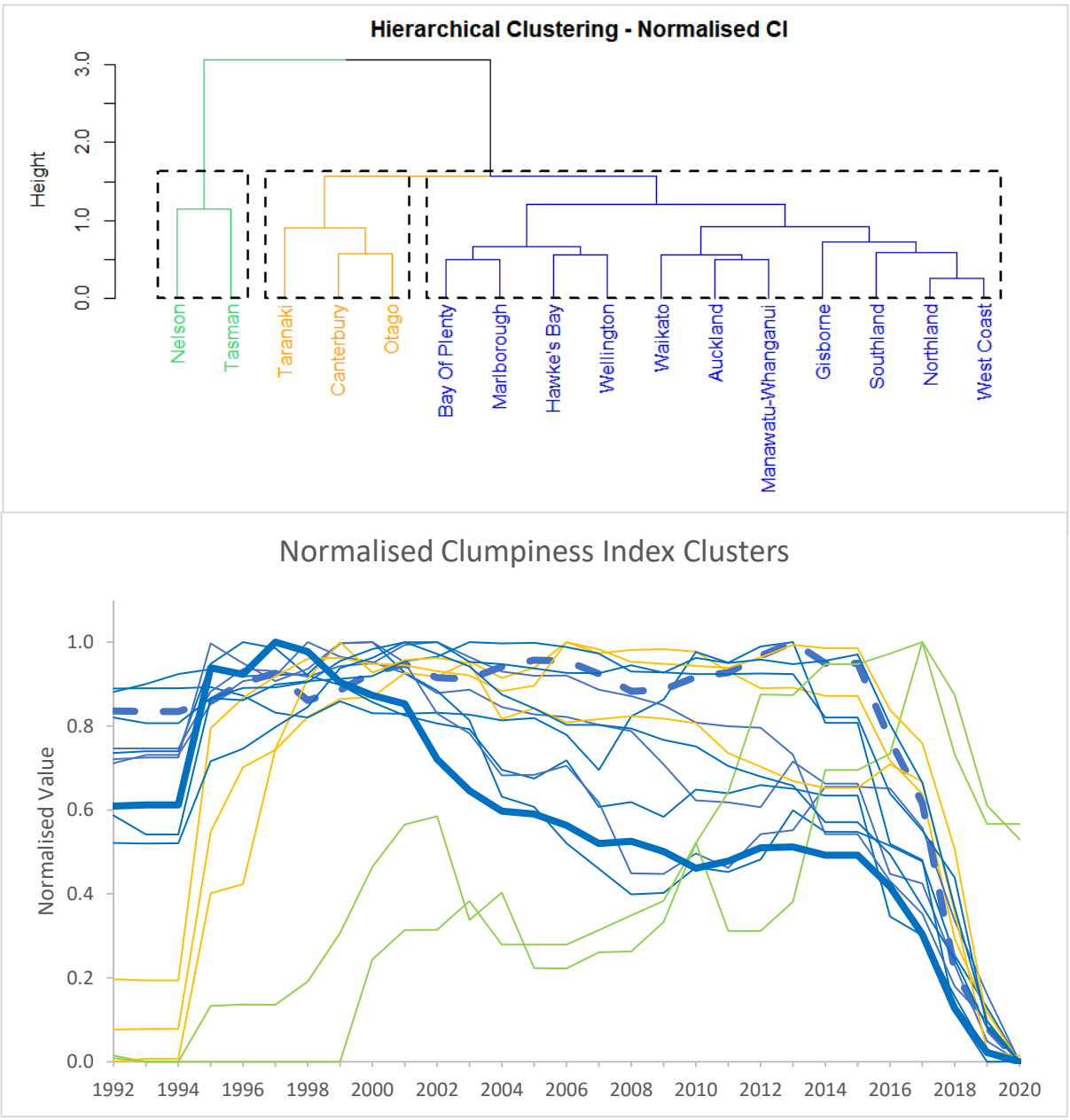

Figure 16. Clumpiness Index Results Hierarchically Clustered (top) and Normalised (Bottom). *Note:* Hierarchical clustering (top) from normalised regional CI results (bottom). The normalised CI results have been coloured by cluster for comparison.

3.6 Discussion

Landscape analysis of indigenous forest cover in regional New Zealand reveals spatial and temporal variability, supporting studies that suggest forest cover remains threatened and vulnerable to anthropogenic activities (McWethy et al., 2010; Ministry for the Environment & Stats NZ, 2022; Norton & Miller, 2000; Norton, 2002; Ohlemüller et al., 2006; Stevenson, 2004; Walker et al., 2021). The PLAND and CA statistics (Figures 7-8 and Table 3) extracted from the CCI-LC dataset show net increases

in indigenous forest occurred in 14 regions between 1992-2020 with only Nelson and Bay of Plenty recording net losses. However, maximum observed areal coverage varied over the study period with only three regions (Canterbury, Manawatu-Whanganui, and Taranaki) reaching peak coverage in 2020. In the remaining 13 regions, indigenous forest was in decline in 2020 with the greatest post-peak losses occurring in Bay of Plenty (9086 ha), Southland (6681 ha), and Tasman (5417 ha). As broad indicators of forest health, the CA/PLAND results validate the need for additional landscape configuration metrics to describe the effect forest loss and gain has on fragmentation, edge length, aggregation, and connectivity in regional New Zealand.

3.6.1 Edge-Perimeter Relationship

One aspect of forest health is the relationship between the forest edge and perimeter which can be examined by comparing the normalised CA and ED profiles. Assuming no restrictions, forest growth that expands steadily outwards from the core will increase in area faster than the increase in perimeter length (Midha & Mathur, 2010). Forest health in these areas is thought to be improving as the core expands and edge effects are reduced (Barbaro et al., 2012; Coops et al., 2004; Ewers & Didham, 2007; Trumbore et al., 2015). A side-by-side examination of the normalised CA and ED profiles in Appendix C, reveal area increased faster than perimeter length in regions like Northland (1994-2009), Manawatu-Whanganui (1994-2001), Gisborne (2000-2005), and Taranaki (1997-2003) and that this was more likely to occur in the first half of the study period.

This type of growth is limited by property and natural boundaries that prevent unrestricted forest expansion. However, within forest boundaries the opportunity for infilling to occur and simplify complex forest patch shapes also exists. Infilling can be observed from periods where CA increases, but ED remains quasi-stable. Examples of infilling can be seen in the West Coast (2000-2015), Southland (1995-2008), and Hawke's Bay (1992-1996).

Similarly, growth may occur in areas beyond the range of existing forest patches, creating patterns of fragmented growth. Fragmented growth may occur where ED increases at the same rate or faster than CA. This type of growth was observed in Auckland (2013-2020), Canterbury (2010-2020), Manawatu-Whanganui (2002-2020), Marlborough (2001-2004), Otago (1998-2005), Taranaki (2004-2020), Wellington (1997-2020), and West Coast (2015-2020). Interestingly, the indicators that fragmented growth was occurring were most often seen in the latter half of the study period.

The edge-perimeter relationship can also indicate forest loss, with evidence for both fragmented and managed deforestation over the study period. Midha and Mathur (2010) explain how managed forest loss can be described from forest patches where CA is declining, and ED falls at a lesser rate. This is the inverse to healthy forest growth and indicates a reduction in both area and shape complexity.

Evidence for managed forest loss is seen in Bay of Plenty (2008-2013), Tasman (2012-2017), Northland (2009-2013), and Nelson (2004-2011) along with other shorter periods of loss in several regions.

In contrast to managed forest loss, fragmented forest loss results in an increase in shape complexity associated with the growth of the forest edge and a decline in class area. In Northland (2018-2020), Bay of Plenty (2015-2020), Hawkes Bay (2015-2020), and Southland (2016-2020) the decline in CA and corresponding rise in ED suggest periods of fragmented forest loss occurred. Like fragmented forest growth, fragmented forest loss was more frequently observed near the end of the study period.

3.6.2 Spatial Configuration

As forest gains and losses affect patch shape, configuration, and distribution across the landscape, metrics that quantify such changes were employed to develop a more holistic picture of forest fragmentation. To measure changes in patch complexity the MFDI was calculated for each region. The MFDI, which has a scale range of 1-2, can be used to assess changes in patch shape from simple Euclidean geometry (1) to more complex patterns (2) which may indicate increasing fragmentation (Ewers & Didham, 2007; McGarigal & Marks, 1995). Figure 12 shows the rise in MFDI values prior to 2012-2015 in green clustered regions, indicating a rise in patch shape diversity and heterogeneity. In contrast, MFDI values in Nelson (yellow cluster) gradually declined over the same period which could be a product of greater shape homogenization and a simplification of existing patches.

The post-2015 decline seen in most regions seems to suggest a period of rapid shape simplification. However, LaGro (1991) explains how sharp declines in MFDI could still indicate rising fragmentation if a large proportion of small fragmented patches are reduced below the minimum mapping unit of the dataset. As the minimum mapping unit of the CCI-LC is 246 m^2, and the range of MFDI values from 1.031 in Nelson (2017) to 1.057 in Bay of Plenty (2013) were already close to Euclidean, the post-2015 decline may be related to data resolution. Support for this hypothesis may be found in the relationship between rising ED figures and low area growth during the same period which suggest shape fragmentation was occurring.

The CI can help detect spatial configuration changes indicative of a rise in forest fragmentation by assessing the degree of patch aggregation independently from shape and area (McGarigal & Marks, 1995; Neel et al., 2004). The CI ranges from -1 (highly disaggregated) to 1 (highly aggregated) with 0 indicating patch aggregation equal to a random distribution. The CI results in Figure 15 show patch aggregation ranged from a low of 0.71 in Northland (2020) to a high of 0.87 in Wellington (1997-1998), indicating indigenous forest patches in regional New Zealand have high aggregation. However, all regions, except Nelson and Tasman, recorded a net decline in CI over the study period. The net decline in CI, particularly towards the end of the study period, suggests indigenous forest patches are

becoming increasingly disaggregated, or fragmented, over time. In Nelson and Tasman, the net increase in CI signals an improvement in patch aggregation overall, but declining CI values in both regions from 2017-2020 indicates these regions also remain at risk.

Further support for increasing fragmentation can be found in the ENN results, a metric used to describe the spatial distribution of patches within a landscape. Landscapes with a low ENN distance have a higher number of patches and as fragmentation occurs the distance between patches declines (Lafortezza et al., 2010; McGarigal & Marks, 1995; Midha & Mathur, 2010; Taubenböck et al., 2019). The results in Figure 14 indicate most regions were experiencing increasing fragmentation over the 28-year period which accelerated from 2015-2020.

3.6.3 Identifying Hotspots

The results presented here point to growing fragmentation of indigenous forests across regional New Zealand but can be further utilized to identify hotspots of accelerated change. Auckland, for example, stands out as the second smallest region while having the second highest mean ENN distance between patches, the widest ENN range (169 m), and <10 % indigenous forest cover. The large distance between patches and the low percentage of land area covered in forest indicate the net growth in CA is creating a patchwork of small, isolated forests throughout the heavily urbanised environment which will be dominated by edge effects. The rise in ED coupled with declines in the CI, MFDI, and ENN distance also support increasingly fragmented growth, especially from 2015-2020.

Another example can be taken from Nelson which has a much higher proportion (>50 %) of indigenous forest than Auckland. In Nelson, ED and MFDI values trended downwards from 1992-2017 and CI rose, an indication that forest patches were being simplified and aggregated, due to broader-scale forest management as opposed to localised edge fragmentation. Post-2017, however, CA and CI declined while ED and MFDI began to rise. These results suggest localized edge fragmentation was occurring leading to an increase in the length of forest edge per hectare and a rise in patch complexity.

These examples demonstrate how landscape metrics can be used to identify periods of increased fragmentation and habitat degradation. They also highlight the complexity in monitoring regional forest fragmentation and the need for flexibility in the management approach. However, with this information, landscape managers can adopt strategies that target the underlying cause of forest degradation and look to improve the health and connectivity of existing forest fragments over the creation of new isolated plantings. In Auckland, for example, landscape managers may look to improve patch size and aggregation through alternative urban planning approaches that incorporate greenbelts or migration pathways, while in Nelson a policy change or public awareness campaign may be necessary to halt the rise of edge fragmentation (Ehlers Smith et al., 2019; Norton & Miller, 2000).

In doing so, management strategies can be more effectively targeted towards regional issues that are contributing towards a decline in forest health.

3.6.4 Data Limitations

Consideration should be given to the resolution of the CCI-LC dataset in assessing regional forest cover patterns. Staples, Ahmed, and Ewers (2012) explain how data resolution should match the scale of change to be monitored. Likewise, McGarigal and Marks (1995) describe how low-resolution raster's produce longer edge results due to the inherent matrix-like structure of raster data. With a pixel size of 246 m^2, the resolution of the CCI-LC dataset is well suited to global and national scale analyses with the benefit of easy accessibility, annual availability from 1992-2020, a high-quality classification methodology, and acceptance within the academic community (Bhatia & Cumming, 2020; Mousivand & Arsanjani, 2019). However, at regional level, the coarse resolution of the CCI-LC was found to limit the accuracy of results, making it best suited to preliminary investigations. Higher resolution (<10 m^2) multi- and hyperspectral datasets would improve accuracy and enable detection of small-scale changes, allowing landscape managers to pinpoint individual forest fragments and affected areas where gains and losses are occurring.

3.7 Conclusion

The landscape configuration metrics employed in this study indicate complex spatial configuration patterns and dynamics are present in mature indigenous forest patches across regional New Zealand. In line with other research, these results suggest indigenous forest management could benefit from the inclusion of additional landscape configuration metrics to support PLAND and CA as the primary indicators of forest health by providing further insight into the spatial dynamics of land cover change. In this regard, the resolution of the CCI-LC dataset used to generate landscape metrics proved to be sufficient for preliminary investigations but was limited by the low resolution of the raster dataset. Higher resolution multi- or hyperspectral data would improve the accuracy and precision of results, providing a more comprehensive dataset from which a greater understanding of forest patch dynamics, distribution, aggregation, and shape complexity can be derived. With this information, regional landscape managers will be able to effectively target management strategies towards localized hotspots of change and limit further degradation of indigenous forests.

4. Case Study 2: Improving Landscape Configuration Statistics at Farm-Scale with Classified, High-Resolution, Hyperspectral Imagery

4.1 Abstract

The results presented below demonstrate how high-resolution hyperspectral imaging, supervised classification, and landscape statistics can be used to classify and analyse land cover at farm-scale. This was achieved by collecting hyperspectral imagery above a rural property with the full-spectrum (380 nm – 1250 nm), high-resolution (1 m^2) AISA FENIX camera mounted in a Cessna 185. The imagery was radiometrically corrected in CaliGeoPRO, atmospherically corrected with a radiative transfer model, and georectified using ENVI software. A forest class and a non-forest class were then spectrally sampled from the georectified reflectance and used to train a 1D-CNN model. The classified output was analysed with the FRAGSTATS based *landscapemetrics* package in RStudio. The classified FENIX landscape statistics were compared to the low-resolution (246 m^2) CCI-LC and medium-resolution (100 m^2) LCDB classified datasets. Results reveal the FENIX had greater patch detection and precision in quantifying area and perimeter-based metrics than the multispectral derived LCDB and CCI-LC datasets. These findings present both financial and environmental opportunities to landowners and manages with large rural properties that incorporate diverse income streams from multiple land cover assemblages.

4.2 Introduction

Low resolution (>100 m) multispectral imagery has been successfully used to describe land cover at global and national scales but is not well-suited to regional scale analyses where high resolution imagery is required to detect small-scale change. High resolution (<2 m) multispectral imagery can provide greater detail at finer scales but is limited by the number of discrete spectral bands available for use in land cover classification models. High resolution hyperspectral imagery can satisfy the demand for both high resolution data and greater spectral ranges from which classification models can be improved, and additional land cover types can be detected. Utilising high resolution hyperspectral imagery to predict land cover can also improve the output of landscape configuration models at regional and local scales. This study aims to evaluate landscape metrics from spatial data of forested land at different spatial resolutions for the purpose of farm-scale management and planning.

4.2.1 Background

Forest inventories are important tools employed in forest health assessments to quantify changes in area, configuration, and distribution at various scales (Singh & Singh, 2013; Trumbore et al., 2015). At global and national scale, low resolution (>100 m^2) classified multispectral satellite imagery is

frequently used to quantify spatial change as it is well-suited to broad land cover assessments that require a good degree of accuracy while retaining the data handling capabilities associated with smaller image file size (Linyucheva & Kindlmann, 2021). For example, the European Space Agency (ESA) has developed the Climate Change Initiative - Land Cover (CCI-LC), a classified annual dataset available from 1992-2020 that has a spatial resolution of 246 m^2 and an image size of ~2.2 GB. The CCI-LC is derived from imagery acquired by several space-borne multispectral sensors and classified using a robust methodology that utilizes an *a-priori* classification system for general applicability over a range of scales (Herold & Di Gregorio, 2012; UCL-Geomatics, 2017). Several studies have demonstrated the applicability of the CCI-LC in a range of contexts and scales for describing forest cover change (Bhatia & Cumming, 2020; Guidigan et al., 2019; Linyucheva & Kindlmann, 2021; Mousivand & Arsanjani, 2019). However, Mousivand and Arsanjani (2019) note that while excellent for global analysis, the low spatial resolution can limit detection of smaller land cover features.

At national and regional scale, higher resolution multispectral imagery can be employed to improve spatial resolution and classification accuracy. In New Zealand, national and regional scale forest assessments are typically described from land cover statistics estimated from the Land Cover Database (LCDB V5.0) (e.g., Cieraad et al., 2015; Dymond et al., 2017; Golubiewski et al., 2020; Honnor et al., 2011; Pannell et al., 2021). The LCDB was developed by Landcare Research – Manaaki Whenua and may be defined as a medium-high resolution dataset with a nominal mapping unit of 1 ha (Manaaki Whenua - Landcare Research, 2020). It is available as a vector-based shapefile and covers five different dates: 1996/97, 2001/02, 2008/09, 2012/13, and 2018/19. Land cover classes have been classified from multispectral sensors onboard SPOT and LandSat satellites and manually enhanced through digitization and user feedback (Dymond et al., 2017). The length, resolution, and excellent classification methodology make the LCDB a valuable tool for regional and national scale forest health assessments.

Despite the high quality of the LCDB, it does have limitations as described by Dymond et al. (2017). The authors investigated five LCDB classes, including the indigenous forest and broadleaved indigenous hardwood classes, to determine the accuracy of change detection. They quantified class accuracy using over 30,000 samples from the 2001/02 and 2008/09 versions of the LCDB, finding smaller areal changes had a higher level of uncertainty at $\pm$30 % compared to $\pm$10 % for large area change. As a result, Dymond et al. (2017) suggest small-scale change in indigenous land covers have a significantly greater risk of being overlooked in forest threat assessments. They go on to describe how reducing uncertainty by improving small-scale change detection would require a higher resolution dataset than the present LCDB is constructed on.

High-resolution hyperspectral imagery has the potential to fulfill this need and contribute to improved forest health assessments by reducing uncertainty in classification accuracy at finer scales. For example, Pullanagari et al. (2017) explain how fine-scale hyperspectral imagery can be used to identify urban materials more accurately than multispectral data due to the greater range of spectral information available for feature identification during classification. In forested environments, Awad (2018) used supervised and unsupervised classification algorithms coupled with ground-truthing to compare the performance of two multispectral and two hyperspectral sensors in detecting stone pine (*Pinus pinea* L.). Awad (2018) found that supervised classification from the two hyperspectral sensors, Hyperion and CHRIS-Proba, had respective accuracies of 82 % and 92% compared to 52 % and 60 % for the multispectral ALI and Landsat8 sensors. Similarly, Halme et al. (2019) found hyperspectral imagery was better for species detection in forests than multispectral imagery due to the higher spectral resolution. Collectively, these studies illustrate how the increased spectral information in hyperspectral imagery can be utilized in a supervised classification algorithm to produce greater class accuracy than multispectral imagery with similar spatial resolution.

At national scale, the cost of acquisition and computational intensity required to process high-resolution hyperspectral data remains a limiting factor. However, at local-scale, aircraft equipped with a high-resolution hyperspectral camera can be deployed at relatively low cost to monitor hotspots of change, improve image resolution and classification along the forest edge, or provide species-specific information to property owners (Vali et al., 2020). This data could also be combined with larger-scale, low and medium resolution datasets, like the LCDB and CCI-LC, to provide additional information in forest health assessments. Furthermore, forest health assessments could benefit from the improved spatial and spectral resolution of hyperspectral imagery when quantifying forest configuration and connectivity of a particular species within a landscape.

4.3 Methods

4.3.1 Study Area

To demonstrate the benefits of high-resolution hyperspectral imagery at local-scale, imagery from a rural property in the Manawatu-Whanganui region was acquired on the 8-9 December 2018. The property covers around 5,680 ha of hill country and has an effective pasture area of 4,070 ha. Pastural land is used primarily for grazing sheep and cattle with areas of manuka (*Leptospermum scoparium*) and kanuka (Kunzea ericoides) employed in honey production. Large tracts of indigenous forest are also present on the property along with some plantations of exotic pines, poplar, and willow.

4.3.2 Survey Information

Imagery was collected with Specim's full spectrum AISA FENIX hyperspectral camera mounted in a Cessna 185. The survey was flown on a cloud-free day with sun altitude >35° to ensure optimal lighting conditions, avoid cloud shadowing, and minimize shadow length of surface objects. The survey was flown at 2,170 ft above ground level (AGL) to achieve a ground sampling distance of 1 m^2 per pixel at nadir. As the FENIX's push-broom sensor has a 384 m swath width, 45 flight lines (oriented north-south) were required to capture the 5680 ha property and maintain sufficient image overlap.

4.3.3 Image Processing

Following data capture, the hyperspectral images were radiometrically and atmospherically corrected to remove sensor bias, estimate atmospheric aerosols, and account for viewing and illumination geometry. Radiometric correction was applied first to the images using Specim's CaliGeoPRO software which converts the raw digital numbers stored in each pixel into radiance values. CaliGeoPRO was also used to extract navigational data collected by the aircraft's dGPS system and generate geographic look-up tables (GLTs) for georectification in post-processing.

Conversion to reflectance involved processing the navigational data and radiometrically corrected images using a radiative transfer model. Together, the radiative transfer model and navigational data were used to estimate water vapour above each pixel and determine the viewing illumination and geometry of a given pixel in relation to the sensor (Bhatia et al., 2018). A correction was then applied to each pixel value using the radiative transfer model, converting the images from radiance to reflectance. Upon completion, the atmospherically corrected images were georectified using the GLTs in preparation for classification.

4.3.4 Classification

A supervised classification methodology employing a one-dimensional convolutional neural network (1D-CNN) was selected to classify the atmospherically corrected images. Training data for the classification was collected for each strip using the georectified reflectance in ENVI 5.6 and a higher resolution (48 cm) RGB aerial orthophoto (acquired March 2018) to confirm spectral sample selection (see Figure 17). For the purposes of this work, the sampled pixels were classified as either forest or non-forest, with the forest class including exotic species, such as pines, willows, and poplars, along with native species. The non-forest class contained only pastural land, water courses and ponds, infrastructure, and exposed soil and gravel. Sample selection was performed in ENVI by collecting pixel

information for the given class in a range of topological regions spread across the property. Around 1700 pixels were sampled for each class and aggregated for model training.

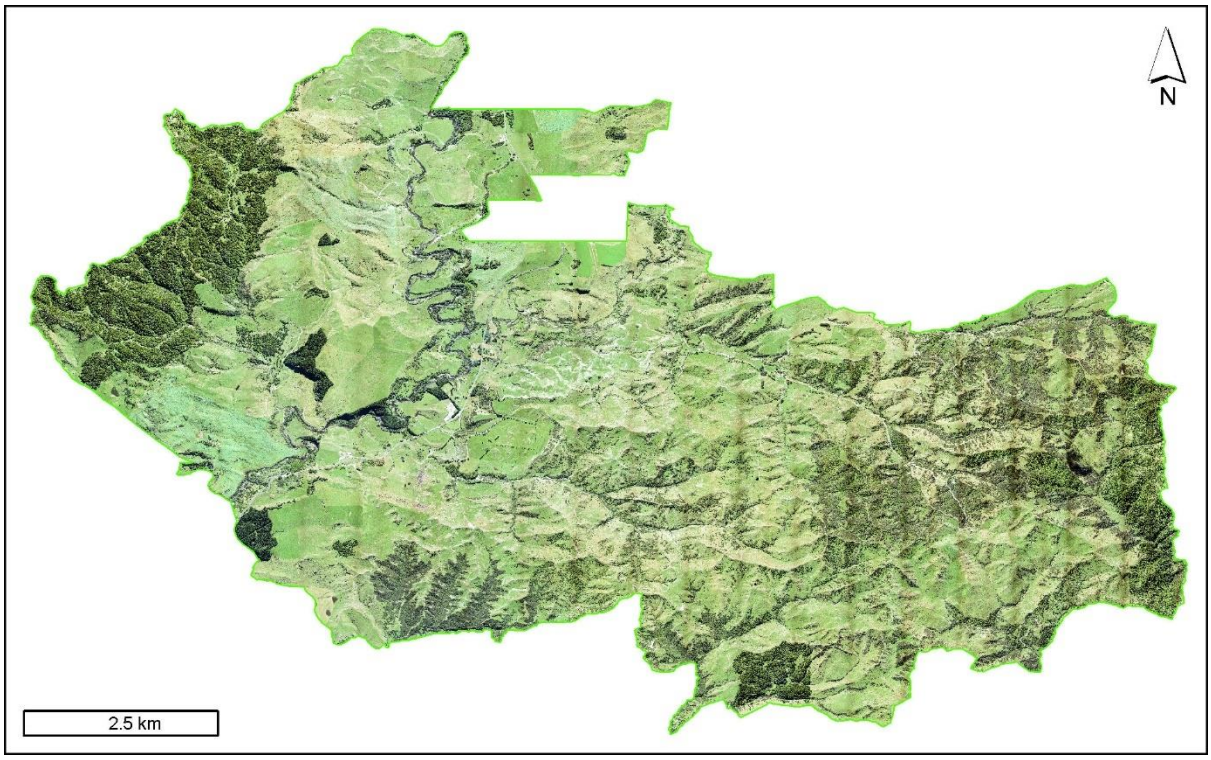

Figure 17. High Resolution RGB Orthophoto of the Rural Property Surveyed with the AISA FENIX.

To train the 1D-CNN, the sampled spectra were iteratively processed until a minimum model performance of 0.97 was achieved in both classes. Each iteration involved training the model, checking the classified outputs against the RGB orthophoto, and collecting additional spectral samples from poorly classified or noisy areas. Once model performance reached 0.97 in both classes, the 45 classified images were mosaicked together in ENVI and a 3x3 median filter was applied to remove remaining noise and visually improve the layer. The final mosaicked layer, shown in Figure 18, contains the classified forest class (blue areas) overlying the RGB orthophoto.

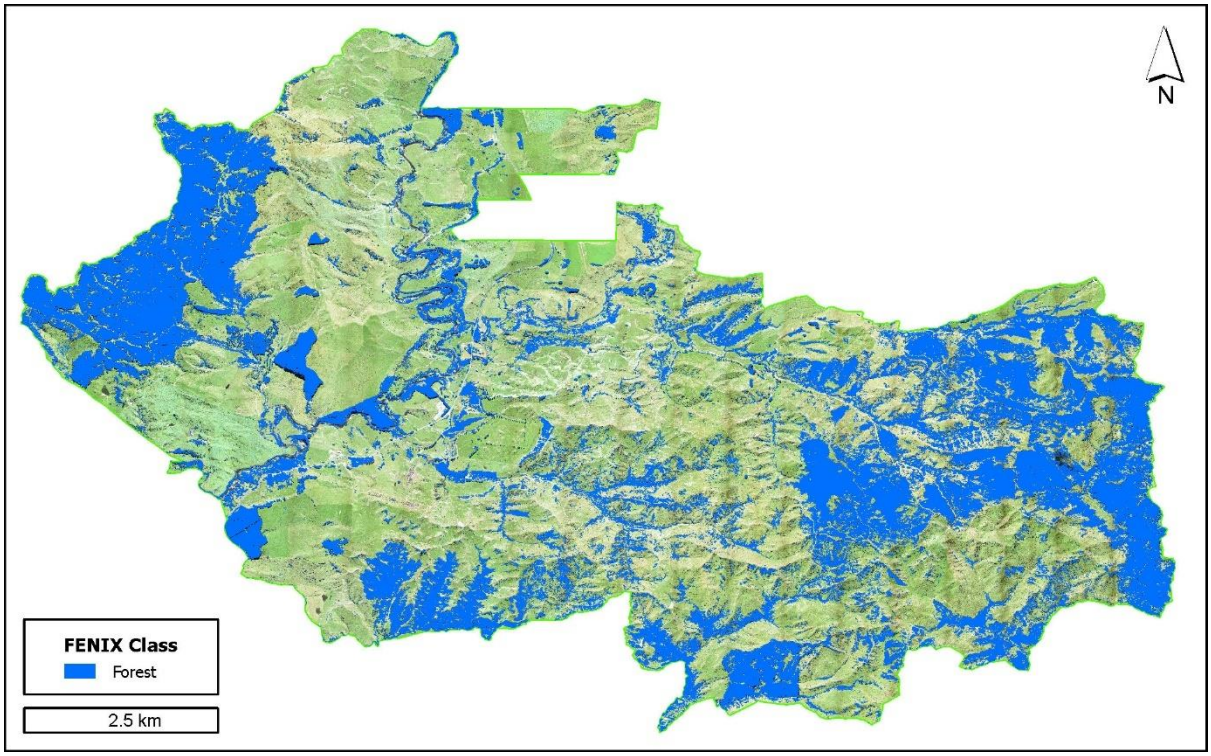

Figure 18. Classified Mixed Forest Class (Blue Areas) Derived from FENIX Imagery.

To compare the classified FENIX layer against the classified CCI-LC and LCDB layers, land cover classes correlating with forested and non-forested areas were identified within each dataset. This was achieved by clipping the 2018 LCDB and CCI-LC layers to the property boundary and extracting the classes shown in Table 4. Water and pastural classes were allocated as non-forest and the remaining classes were visually checked against the high resolution RGB orthophoto to ensure they were situated over native or mixed forest regions. Only two classes, the LCDB's harvested forest (Class 64) and the CCI-LC's mosaic cropland/natural vegetation (Class 30), were reallocated as non-forest during this stage of the process. The final allocation of each datasets classes as forest or non-forest is shown in Table 4, while Figure 19 displays the composition of forest classes over the high resolution RGB orthophoto.

Table 4. Allocation of Forest & Non-Forest Land Cover Classes from the LCDB and CCI-LC Datasets.

	LCDB		**CCI-LC**	
	Class Code	Description	Class Code	Description
FOREST	45	Herbaceous Freshwater Vegetation	40	Mosaic natural vegetation (tree, shrub, herbaceous cover) (>50%) / cropland (<50%)
	51	Gorse and/or Broom	50	Tree cover, broadleaved, evergreen, closed to open (>15%)
	52	Manuka and/or Kanuka	100	Mosaic tree and shrub (>50%) / herbaceous cover (<50%)
	54	Broadleaved Indigenous Hardwoods	110	Mosaic herbaceous cover (>50%) / tree and shrub (<50%)
	56	Mixed Exotic Shrubland	120	Shrubland
	68	Deciduous Hardwoods		
	69	Indigenous Forest		
	71	Exotic Forest		
NON-FOREST	21	River	30	Mosaic cropland (>50%) / natural vegetation (tree, shrub, herbaceous cover) (<50%)
	40	High Producing Exotic Grassland	130	Grassland
	41	Low Producing Grassland		
	64	Forest - Harvested		

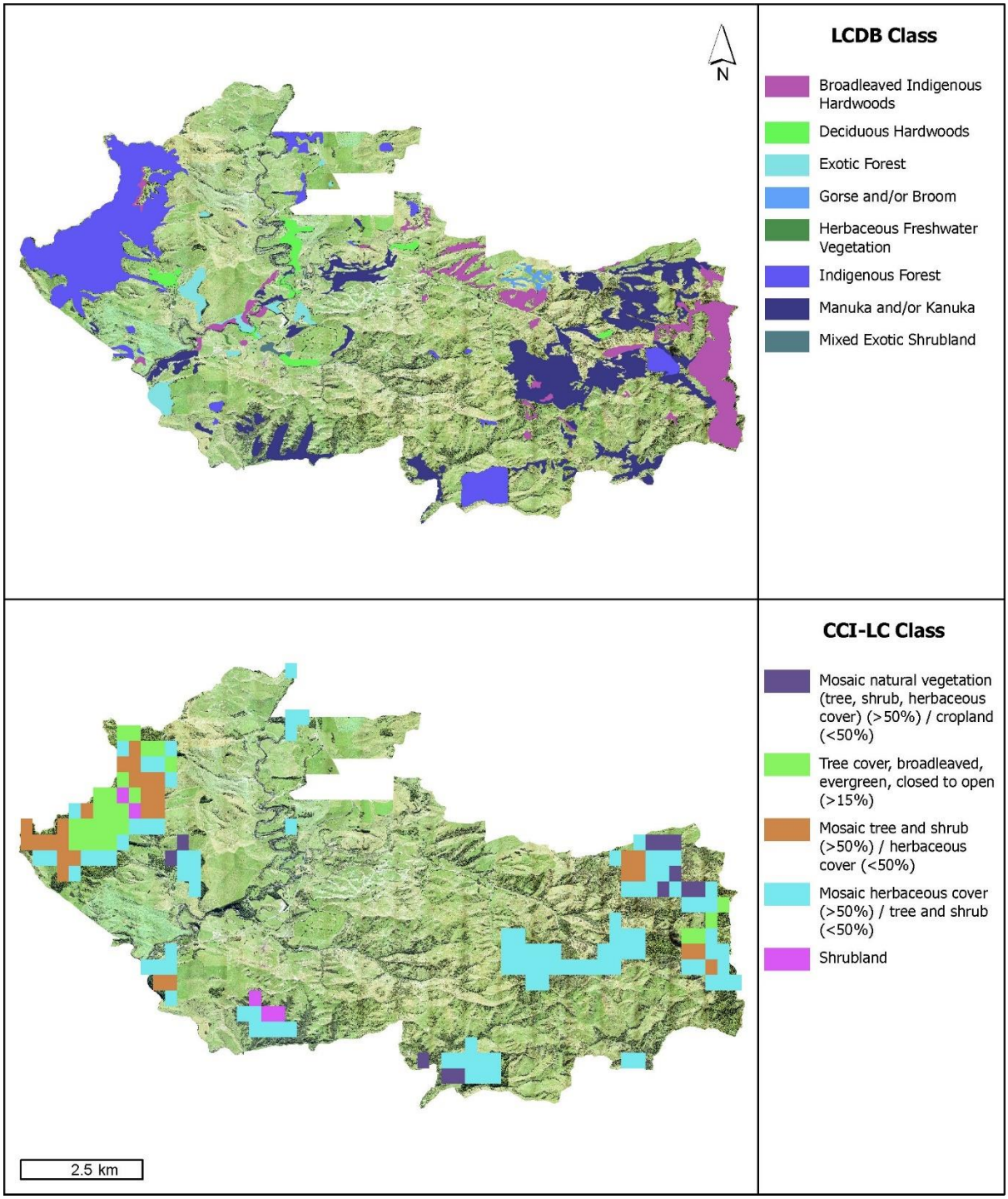

Figure 19. Land Cover Classes Merged to Create a Composite Forest Class for the LCDB and CCI-LC.

4.3.5 Landscape Analysis

Following completion of all three classified land cover layers, landscape configuration statistics were calculated in R-Studio with the FRAGSTATS derived *landscapemetrics* package (Hesselbarth et al., 2019). Each class level metric along with their respective units and a description are displayed in Table 5. Selected metrics describe various aspects of fragmentation, shape, and configuration within the

landscape and include class area, percentage landscape, total edge length, edge density, mean fractal dimension index, mean Euclidean nearest-neighbour distance, and clumpiness index.

Table 5. FRAGSTATS Landscape Metrics, Units, and Description.

Metric	Units	Description
Class Area (CA)	Hectares (ha)	Area encompassed by a class within a given landscape
Percentage of Landscape (PLAND)	Percent (%)	Percentage of landscape covered by a class
Total Edge (TE)	Metres (m)	Total length of class perimeter. Useful in monitoring changes in edge fragmentation
Edge Density (ED)	Metres per hectare (m ha^{-1})	A standardised value describing perimeter to area relationship of a class that can be employed across landscapes of varying size. Higher ED indicates a more fragmented forest margin
Mean Fractal Dimension Index (MFDI)	None	A measure of increasing shape complexity from simple Euclidean geometry. Ranging from 1-2, higher MFDI indicates greater shape complexity. A rise in MFDI may be an indicator that edge fragmentation is occurring
Mean Euclidean Nearest-Neighbour Distance (ENN)	Metres (m)	Mean Euclidean distance to nearest patch of same class. A measure of patch connectivity across a landscape
Number of Patches (NP)	None	Total number of patches within a class. Establishes a baseline for monitoring of patch fragmentation
Clumpiness Index (CI)	Percent (%)	A measure of patch aggregation. Range is from -1 (maximum disaggregation) to 1 (maximally clumped) with values above zero suggestive of greater patch aggregation or connectivity

4.4 Results

Figure 20 shows the difference in class area results between the datasets along with the proportion of forest and non-forest within the landscape. The total property area calculated by FRAGSTATS is shown above each column. This was quantified from the classified CCI-LC raster as 5605.9 ha, composed of 1032.5 ha of forest and 4573.4 ha of non-forest. The PLAND results, shown within the column, were 18.4 % forest and 81.6 % non-forest. The LCDB had a higher total class area of 5679.8

ha which was composed of 1372.3 ha of forest, covering 24.2 % of the landscape. Non-forested area was quantified as 4307.5 ha, equivalent to 75.8 % of the landscape. The property area quantified from the FENIX imagery was 5680.6 ha with 70.4 %, or 4001.0 ha, allocated as non-forest. Percentage of forest cover was highest in the FENIX imagery at 29.6 % of total land area (1679.6 ha).

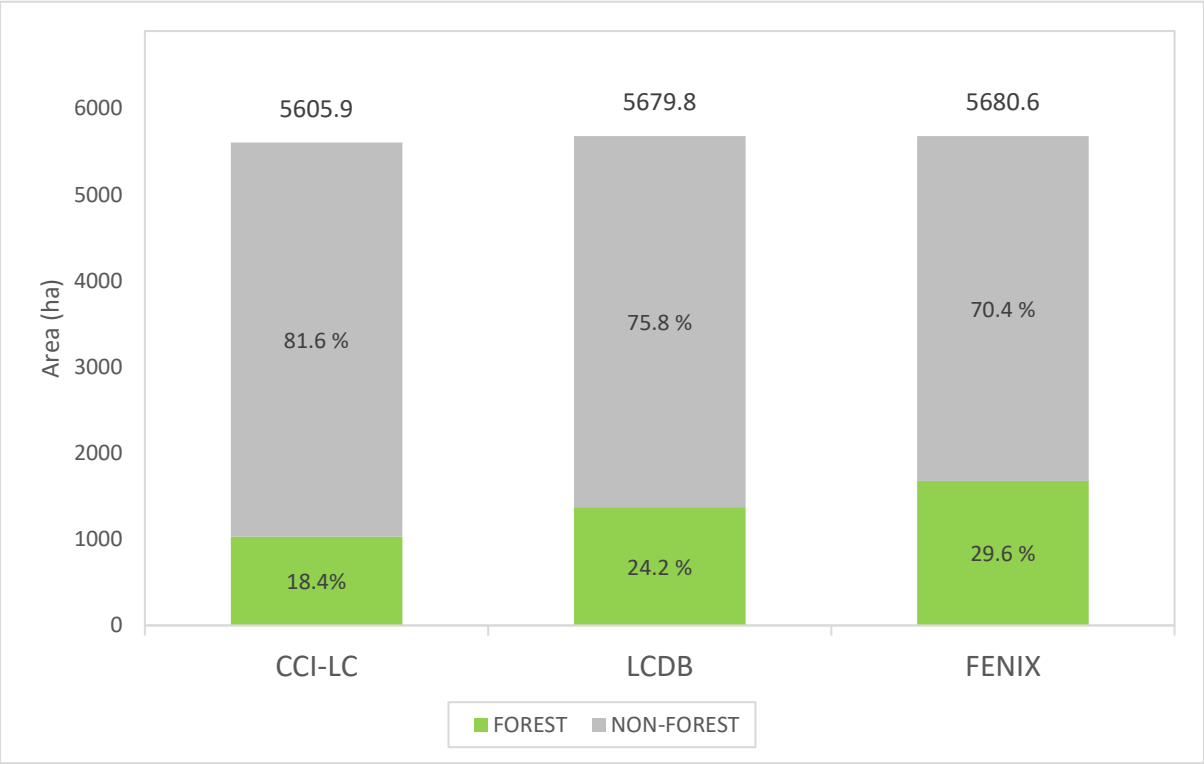

Figure 20. Forest and Non-Forest Class Area Quantified with FRAGSTATS. *Note:* The total area (forest and non-forest) is shown above each column. The figures within each column are the percentage of total land area occupied by forest (green) and non-forest (grey). Forested area was highest in the FENIX layer.

The metrics NP, TE, and ED were selected to further describe the area to perimeter relationship with results displayed in Table 6 for the forest class only. The NP result shows CA was calculated from 11 patches within the CCI-LC layer, 102 patches in the LCDB layer, and >40, 000 in the FENIX layer. The TE length of those patches (excluding property boundary) was computed as 37,460 m (CCI-LC), 271,097 m (LCDB), and 2,811,223 m (FENIX). These figures were converted to density per hectare in FRAGSTATS with 6.7 m ha^{-1} for the CCI-LC, 47.7 m ha^{-1} for the LCBD, and 494.9 m ha^{-1} for the FENIX.

Table 6. The Quantified Landscape Metric Results for Each Dataset.

Metric	CCI-LC	LCDB	FENIX
Total Property Area (ha)	5605.9	5679.8	5680.6
CA (ha)	1032.5	1372.3	1679.6
PLAND (%)	18.4	24.2	29.6
NP	11	102	40277
TE (m)	37460	271097	2811223
ED (m ha^{-1})	6.7	47.7	494.9
ENN (m)	1068	95	6
MFDI	1.03	1.15	1.16
CI (%)	0.79	0.99	0.94

Patch shape complexity and configuration was quantified by the ENN distance, MFDI, and CI metrics which are displayed at the bottom of Table 6. These results show that the CCI-LC had an ENN distance of 1068 m, the LCDB was recorded as 95 m, and the high-resolution FENIX had an average patch-to-patch distance of 6 m. Average shape complexity was quantified with the MFDI as 1.03 in the CCI-LC, 1.15 in the LCDB, and 1.16 in the FENIX layer. Forest configuration across the landscape was quantified using the CI which describes the likelihood of patch aggregation in a random distribution. The LCDB had a CI value of 0.79, the LCDB had the highest value at 0.99, and the FENIX had a CI value of 0.94.

4.5 Discussion

In this study, corresponding landscape configuration statistics were derived from low, medium, and high-resolution classified imagery of a rural property located in the Manawatu-Whanganui hill country. The low-resolution CCI-LC dataset, designed for global and national scale analyses, was found to be too coarse for utilization in farm-scale land cover classification, despite correlating well with large tracts of forest across the 5680 ha property (See Figure 21). The limiting factor is primarily the 246 m^2 pixel size which resulted in only 11 classified forest patches compared to 102 in the LCDB layer and >40,000 in the FENIX layer. The CCI-LC's larger pixel size inevitably incorporates non-forest areas within areas classified as forest, reducing accuracy across all derived landscape statistics. An example can be seen in Figure 5 where both forest and non-forest classes are contained within the yellow hatched area indicating the extent of the forest class. Beyond the yellow hatched area, forest can also be seen mis-classified as non-forest.

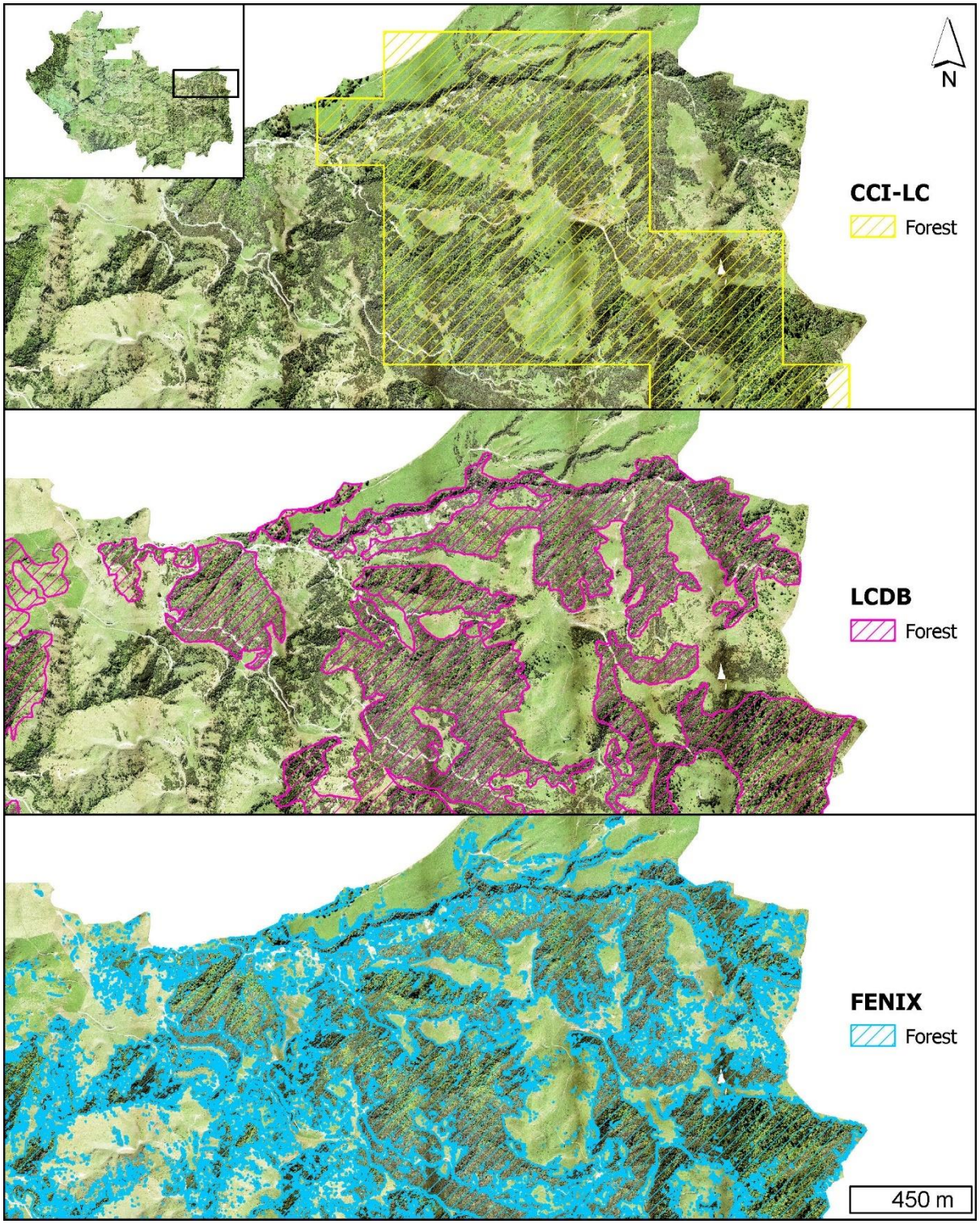

Figure 21. Comparison of Classification Accuracy Between Layers. *Note:* The low-resolution CCI-LC layer (top) misclassifies large areas of forest (yellow hatched area) as non-forest. The LCDB layer (middle) has greater accuracy, but large forested areas (likely recolonised between updates of the database) have been misclassified. The FENIX (bottom) has the highest classification accuracy which is vital to detecting fragmentation at local scale.

Another issue with using the CCI-LC at farm-scale is that the classifier was designed with broad land cover categories intended for general applicability across globally diverse environments. The multispectral derived LCDB attempts to resolve this issue with a classification specifically created for New Zealand land cover. With its 1 ha nominal accuracy and wide range of land cover categories, the LCDB is the most comprehensive land cover database available in New Zealand for national and regional analyses.

There are, however, two significant limitations to the LCDB that restrict its capabilities for use in managing land cover change at local-scale. The first limitation is that due to the size and level of detail required in maintaining a national dataset, updated versions of the LCDB are only released every 4-7 years. In between releases, land cover can change dramatically, particularly in areas where colonizing species, such as manuka, kanuka, gorse, or broom are allowed to take hold. For example, in Figure 21, manuka, kanuka, and smaller patches of regenerating native forest are visible beyond the classified LCDB forest polygons (pink hatched area). This could become an issue when up to date classified imagery is required for economic purposes like managing manuka honey production, calculating carbon credits, assessing storm damage, quantifying effective pasture area, and monitoring invasive weed species.

The second limitation of the LCDB is that the classified polygons that comprise the database lack definition along class boundaries. As can be seen in Figure 22, the higher resolution FENIX polygons (blue) correspond better with the forest boundary than the LCDB polygons (pink). This is reflected in the TE results in Table 6 which shows the combined boundary length of LCDB forest patches measured 271,097 m - a significant improvement over the low-resolution CCI-LC's 37,460 m TE result. However, the high-resolution FENIX boundary measured over ten times higher than the LCDB with a total length of 2,811,223 m. The derived ED result, which is a product of TE and landscape area, also improved with resolution, rising from 47.7 m ha^{-1} (LCDB) to 494.9 m ha^{-1} (FENIX) (McGarigal & Marks, 1995).

In utilizing high-resolution hyperspectral imagery for classification of class area and perimeter metrics, shape configuration and aggregation metrics were improved as well. In Table 6, the ENN distance, for example, dropped from 95 m in the LCDB classification to 6 m in the FENIX. The FENIX's 6 m mean patch-to-patch distance implies the distribution of forest patches is more fragmented than the LCDB result. The CI result supports higher fragmentation with a 5 % decline in patch aggregation between the LCDB (99 %) and FENIX (94%) layers. Additionally, a slight rise in the MFDI from 1.15 (LCBD) to 1.16 (FENIX) suggests mean shape complexity was more convoluted in the FENIX classification – an indicator of greater edge fragmentation.

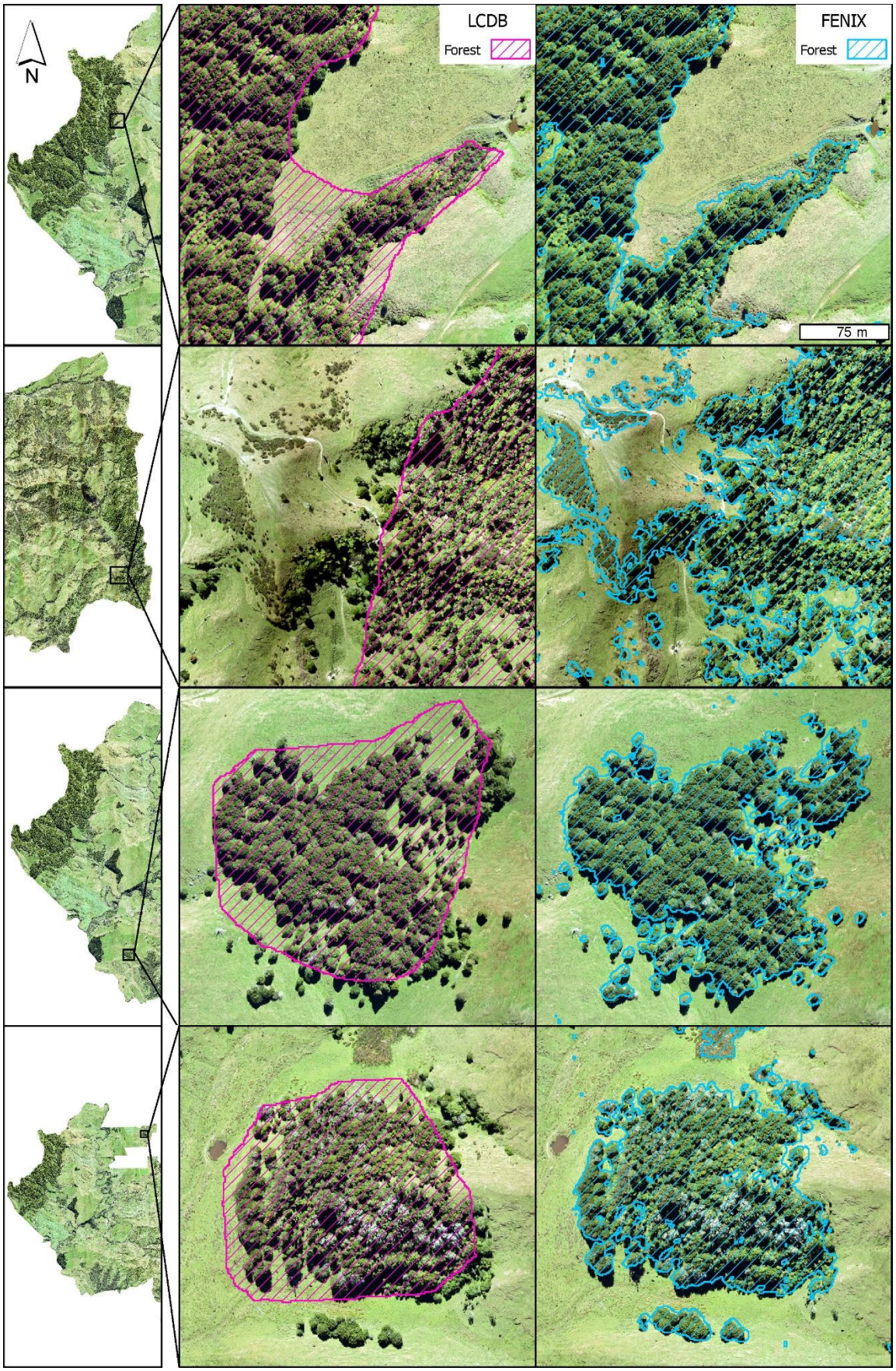

Figure 22. Comparison of the Difference in Edge Detail Between the LCDB and FENIX layers.

Combined, the landscape statistics derived from the high-resolution hyperspectral imagery provide a more detailed summation of forest patch area, configuration, and fragmentation at farm-scale than the LCDB or CCI-LC. Although these results are not surprising given the resolution of the LCDB and CCI-LC, high-resolution imagery in conjunction with medium and low resolution datasets can provide both financial and environmental benefits to landowners and land managers. For example, the 300 ha of additional forest area calculated from the FENIX imagery (compared to the LCDB) reduces the effective pasture area used to manage stocking rates yet it increases carbon sequestration capacity. Landowners could utilise this information by reducing stock units and applying for carbon credits to compensate for the additional forest area.

In broader scale land management, hotspots, or areas of rapid change, could be identified from lower resolution LCDB or CCI-LC data and then resurveyed at high-resolution in order to improve the classification of land cover and the quantification of forest fragmentation statistics. The improved classification accuracy achievable with higher resolution spectral data enables the development of more effective monitoring and management strategies that allocate resources towards rapidly degrading patches across the regional landscape. This type of hierarchical, multi-resolution monitoring approach would ensure data acquisition was cost effective and limited to the most at risk areas. It could also be undertaken in between releases of the LCDB to provide greater temporal resolution and prevent or minimise further degradation and fragmentation of forest remnants through closer monitoring.

High-resolution multispectral imagery could also be employed, potentially at lower cost, to achieve similar outcomes. However, there are two main advantages in using classified hyperspectral data for forest fragmentation assessments. The first is that higher classification accuracy is achievable with hyperspectral data which reduces misclassification and enhances the potential efficacy of classification-facilitated control measures. Secondly, the contiguous bands of full spectrum hyperspectral sensors offer more flexibility when it comes to classifying spectral data from new threats than the discrete bands of multispectral sensors. This offers greater opportunity to successfully classify new threats and add the class to the existing spectral library of invasive species.

4.6 Conclusion

These findings demonstrate how land cover statistics can be improved with classified, high-resolution, hyperspectral imagery and applied at farm-scale. Using a supervised classification methodology, atmospherically corrected hyperspectral images were analysed with FRAGSTATS to obtain common landscape metrics. Two multispectral-derived datasets, the low-resolution CCI-LC and medium-resolution LCDB dataset, were also analysed for comparison. Results from the landscape analyses

show the number of patches detected in the hyperspectral imagery was much higher than in both multispectral-derived datasets. This improved the calculation of class area, perimeter length, shape configuration, and aggregation metrics that are commonly employed in forest health and fragmentation assessments.

These results are to be expected with higher resolution data but offer the potential to contribute to forest health assessments through a multi-scaled forest health framework. This would utilise lower resolution datasets, like the LCDB and CCI-LC, with greater spatial coverage to derive national level fragmentation statistics while employing high-resolution hyperspectral data to capture additional data in rapidly fragmenting hotspot areas at farm-scale. Utilising an integrated, hierarchical approach would allow for the derivation of national-level fragmentation statistics while ensuring the capture of fine-grained details in specific regions. Leveraging the rich spectral information provided by hyperspectral data, decision-makers and land managers in affected areas could then make informed choices regarding resource allocation, conservation efforts, or mitigation strategies, leading to more effective land management decisions.

5. Synthesis

As demonstrated in both case studies, the utilisation of landscape metrics to quantify the spatial arrangement of indigenous forest shows considerable promise in improving forest health assessments over a range of scales. Key to this approach, is the inclusion of metrics that relate to a broad range of ecological processes associated with declining forest health. This includes both fragmentation and edge effects, an overarching term describing the change in various functional and structural processes within a defined edge zone around the forest interior. Fragmentation and edge effects are two of the greatest threats facing indigenous forest remnants in New Zealand, particularly in the highly fragmented lowlands, however, state of the environment reports frequently fail to include them in fragmentation analyses.

Part of the issue in reporting fragmentation is a lack of available data on land fragmentation statistics. The national scale case study presented above attempts to provide a methodology by which this issue can be rectified. This was achieved by analysing a publicly available land cover dataset (CCI-LC) with landscape analysis software. The online accessibility of both dataset and software made this methodology straight forward and easy to implement. Furthermore, the annual coverage of the dataset over a 28-year period allowed for a time-series analysis of forest cover change over an extended period.

One of the main drawbacks of this approach was that the resolution of the CCI-LC made extraction of forest fragmentation statistics at regional level less meaningful. The CCI-LC's 246 x 246 m pixel size is sufficient for its primary purpose of providing global-scale land cover data but at national level, particularly for a small country like New Zealand, the 246 m^2 pixel size was best suited to quantifying larger forested patches. As the largest indigenous forest areas are publicly owned and protected from deforestation by legislation, they are far less likely to experience degradation than the small (<246 m^2), fragmented, remnants on privately-owned land. The CCI-LC dataset is therefore best suited to broad generalisations of land cover pattern but detection of localized fragmentation a finer resolution dataset is desirable.

Another drawback inherent in the CCI-LC dataset was its global land cover classification system. Correlating a CCI-LC forest class to New Zealand's mature indigenous forest class found in the higher resolution LCDB was achieved with around 80 % accuracy. Furthermore, only a single CCI-LC class was selected to represent mature indigenous forest. Considering the low resolution of the CCI-LC, it may have been worthwhile incorporating all indigenous vegetation commonly found in forested areas. This would have included adjacent transitional and successional species, such as manuka, kanuka, and tree

fern dominated areas, for a broader overview of spatial fragmentation patterns more appropriate to the resolution of the classification.

An alternative methodology would be to analyse regional forest configuration patterns using data from the LCDB. This would effectively solve both the resolution issue and class selection issues as the LCDB has a 1 ha nominal mapping unit and a classification system designed specifically for New Zealand land cover classes. The LCDB's bespoke classification system also has the advantage of application across other native land cover types such that fragmentation of grasslands, wetlands, or fernlands could also be analysed and included in state of the environment reporting.

At local scale, however, there are two key issues with using the LCDB in spatial configuration analysis. Firstly, the 1 ha mapping unit can be a limiting factor in terms of edge detection. The second case study demonstrated this point with a farm-scale analysis that revealed the lack of detail in the LCDB classification along the forest edge when compared to the 1 m^2 pixel resolution of the FENIX imagery. As fragmentation along the forest boundary is a primary contributor to the increased penetration of edge effects, the additional detail available with the FENIX is far better suited to small, localized forest monitoring programs than the LCDB.

The second issue with employing the LCDB for local scale landscape analysis is that the database is only updated every 4-7 years. The infrequency at which updates occur presents a potential barrier for monitoring local fragmentation as it may be too infrequent to prevention forest degradation in rapidly fragmenting areas. Evidence of this was observed in the farm-scale analyses whereby areas of forest growth were captured by the FENIX but missing from the LCDB polygons. While classification error is inherent in all land cover datasets, the misclassification of the forest edge and infrequency in which it is updated make it less reliable for local landscape analysis and hotspot monitoring than sensors like the readily deployable, high-resolution FENIX. However, there are scale limitations with airborne sensors, restricting their usage to localised hotspot monitoring rather than regional scale database creation. Therefore, a multi-scaled, hierarchical approach is recommended that incorporates lower resolution multispectral derived datasets (like the CCI-LC and LCDB) for broad scale fragmentation analysis, followed with higher resolution multi- or hyperspectral data in hotspot areas.

5.1 Future Research

The implications of these findings are in line with other research that fragmentation indices beyond quantification of area would be of significant benefit in monitoring and reporting of forest health. New Zealand's indigenous forest remnants, particularly on private land, are highly vulnerable to degradation but spatial configuration analyses could be of benefit in reducing fragmentation and improving connectivity between isolated patches. A multi-scaled approach would assist in improving

a range of ecological processes associated with forest health, including both functional and structural components. It could also create greater public awareness of the extent and rate of forest fragmentation, helping assist in better decision making and protection of isolated remnants with legislation created to regulate the issue in rapidly fragmenting hotspot areas. Finally, landscape metrics that quantify various aspects of forest health could be useful in future research for monitoring or identification of changes in external drivers of forest degradation associated with changing landuse patterns.

5.2 Conclusion

This research sought to quantify and describe changes in indigenous forest fragmentation in New Zealand over a 28-year period. This was achieved through landscape configuration analysis of the low-resolution, classified CCI-LC dataset. It was argued that state of the environment reports produced at all levels of government often employ landscape metrics that only quantify area or percentage of landscape change. The lack of configuration-based metrics more appropriately suited to quantifying landscape pattern and connectivity was demonstrated and used to justify their application in a national scale fragmentation assessment. The results from the national scale assessment revealed the utility in applying landscape fragmentation indices in forest health reporting, especially with regards to identification of at risk or rapidly fragmenting areas. These findings highlighted the importance of image resolution when quantifying landscape fragmentation and the need for higher-resolution imagery in the monitoring of local hotspot areas to improve metric accuracy.

The value of high-resolution imagery in local-scale fragmentation assessments was then demonstrated on a rural property. The property was surveyed with the high-resolution AISA FENIX hyperspectral camera and land cover was classified with a 1D-CNN. The resulting classified layer was analysed with FRAGSTATS and compared to the medium-resolution LCDB, and the low-resolution CCI-LC classified imagery. The high-resolution imagery was found to be capable of far greater detail along the forest boundary than the medium and low resolution imagery. As changes in forest boundary length are associated with fragmentation, connectivity, and the penetration of edge effects, these findings support the need for high-resolution classified imagery and landscape configuration metrics in assessing forest health. However, the acquisition of high-resolution, classified imagery at regional and national scale is financially prohibitive at present and best suited to local-scale monitoring as part of a multi-scaled approach to forest health management that utilises other classified datasets like the CCI-LC and LCDB.

The two case studies presented here indicate landscape configuration indices have the potential to improve forest health monitoring and reporting in New Zealand. While high-resolution imagery for

regional and national scale analyses are dependent on future reductions in the cost of data acquisition, landscape configuration indices could be immediately applied to the current medium-resolution LCDB dataset. This would provide baseline statistics of fragmentation and connectivity in indigenous forest patches as well as other threatened native vegetation types. Vulnerable, highly fragmented areas could then be closely monitored using high-resolution airborne or satellite imagery if desired, targeting data collection to the most at risk areas.

6. References

Ahmad, A., & Quegan, S. (2013). Comparative analysis of supervised and unsupervised classification on multispectral data. *Applied Mathematical Sciences*, *7*(74), 3681-3694.

Allen, R. B., Bellingham, P. J., Holdaway, R. J., & Wiser, S. K. (2013). New Zealand's indigenous forests and shrublands. *Ecosystem services in New Zealand—condition and trends. Manaaki Whenua Press, Lincoln*, 34-48.

Andren, H. (1994). Effects of habitat fragmentation on birds and mammals in landscapes with different proportions of suitable habitat: a review. *Oikos*, 355-366.

Ausseil, A.-G. E., Dymond, J. R., & Weeks, E. S. (2011). Provision of natural habitat for biodiversity: quantifying recent trends in New Zealand. *Biodiversity loss in a changing planet*, 201-220.

Awad, M. M. (2018). Forest mapping: a comparison between hyperspectral and multispectral images and technologies. *Journal of Forestry Research*, *29*(5), 1395-1405.

Bahadur KC, K. (2009). Improving Landsat and IRS image classification: evaluation of unsupervised and supervised classification through band ratios and DEM in a mountainous landscape in Nepal. *Remote Sensing*, *1*(4), 1257-1272.

Barbaro, L., Brockerhoff, E. G., Giffard, B., & van Halder, I. (2012). Edge and area effects on avian assemblages and insectivory in fragmented native forests. *Landscape Ecology*, *27*(10), 1451-1463. https://doi.org/10.1007/s10980-012-9800-x

Bhatia, N., & Cumming, G. S. (2020). Deforestation and economic growth trends on oceanic islands highlight the need for meso-scale analysis and improved mid-range theory in conservation. *Ecology and Society*, *25*(3). https://doi.org/10.5751/es-11713-250310

Bhatia, N., Iordache, M.-D., Stein, A., Reusen, I., & Tolpekin, V. A. (2018). Propagation of uncertainty in atmospheric parameters to hyperspectral unmixing. *Remote Sensing of Environment*, *204*, 472-484. https://doi.org/https://doi.org/10.1016/j.rse.2017.10.008

Boori, M., Paringer, R., Choudhary, K., & Kupriyanov, A. (2018). *Supervised and unsupervised classification for obtaining land use/cover classes from hyperspectral and multi-spectral imagery* (Vol. 10773). SPIE. https://doi.org/10.1117/12.2322624

Bourgoin, C., Betbeder, J., Le Roux, R., Gond, V., Oszwald, J., Arvor, D., Baudry, J., Boussard, H., Le Clech, S., & Mazzei, L. (2021). Looking beyond forest cover: an analysis of landscape-scale predictors of forest degradation in the Brazilian Amazon. *Environmental Research Letters*, *16*(11), 114045.

Brockerhoff, E., Burns, B., Shaw, W., Deconchat, M., & Hock, B. (2006). *Forest biodiversity: Identifying the issues and opportunities for management*.

Cieraad, E., Walker, S., Price, R., & Barringer, J. (2015). An updated assessment of indigenous cover remaining and legal protection in New Zealand's land environments. *New Zealand Journal of Ecology*, *39*(2), 309-315.

Cocklin, C., & Doorman, P. (1994). Ecosystem protection and management in New Zealand: a private land perspective. *Applied Geography*, *14*(3), 264-281. https://doi.org/https://doi.org/10.1016/0143-6228(94)90042-6

Coops, N. C., White, J. D., & Scott, N. A. (2004). Estimating fragmentation effects on simulated forest net primary productivity derived from satellite imagery. *International Journal of Remote Sensing*, *25*(4), 819-838. https://doi.org/10.1080/0143116031000115094

Crist, M. R., Wilmer, B., & Aplet, G. H. (2005). Assessing the value of roadless areas in a conservation reserve strategy: biodiversity and landscape connectivity in the northern Rockies. *Journal of Applied Ecology*, *42*(1), 181-191.

Curran-Cournane, F., Carrick, S., Barnes, M. G., Ausseil, A.-G., Drewry, J. J., Bain, I. A., Golubiewski, N. E., Jones, H. S., Barringer, J., & Morell, L. (2023). Cumulative effects of fragmentation and development on highly productive land in New Zealand. *New Zealand Journal of Agricultural Research*, *66*(1), 1-24. https://doi.org/10.1080/00288233.2021.1918185

Davis, M. R., Allen, R. B., & Clinton, P. W. (2003). Carbon storage along a stand development sequence in a New Zealand Nothofagus forest. *Forest Ecology and Management*, *177*(1), 313-321. https://doi.org/https://doi.org/10.1016/S0378-1127(02)00333-X

Department of Conservation. (n.d.). *Bush layers*. Department of Conservation. https://www.doc.govt.nz/get-involved/run-a-project/restoration-advice/bush-restoration/understand-the-bush/bush-layers/

Didham, R. K., & Ewers, R. M. (2012). Predicting the impacts of edge effects in fragmented habitats: Laurance and Yensen's core area model revisited. *Biological Conservation*, *155*, 104-110. https://doi.org/https://doi.org/10.1016/j.biocon.2012.06.019

Dodd, M., Barker, G., Burns, B., Didham, R., Innes, J., King, C., Smale, M., & Watts, C. (2011). Resilience of New Zealand indigenous forest fragments to impacts of livestock and pest mammals. *New Zealand Journal of Ecology*, 83-95.

Dowding, J. E., & Murphy, E. C. (2001). The impact of predation by introduced mammals on endemic shorebirds in New Zealand: a conservation perspective. *Biological Conservation*, *99*(1), 47-64. https://doi.org/https://doi.org/10.1016/S0006-3207(00)00187-7

Duda, T., & Canty, M. (2002). Unsupervised classification of satellite imagery: choosing a good algorithm. *International Journal of Remote Sensing*, *23*(11), 2193-2212.

Dymond, J., Ausseil, A.-G., Kirschbaum, M., Carswell, F., & Mason, N. (2013). Opportunities for restoring indigenous forest in New Zealand. *Journal of the Royal Society of New Zealand*, *43*(3), 141-153.

Dymond, J. R., Shepherd, J. D., Newsome, P. F., & Belliss, S. (2017). Estimating change in areas of indigenous vegetation cover in New Zealand from the New Zealand land cover database (LCDB). *New Zealand Journal of Ecology*, *41*(1), 56-64. https://doi.org/10.20417/nzjecol.41.5

Ehlers Smith, D. A., Ehlers Smith, Y. C., & Downs, C. T. (2019). Promoting functional connectivity of anthropogenically-fragmented forest patches for multiple taxa across a critically endangered biome. *Landscape and Urban Planning*, *190*, 103579. https://doi.org/https://doi.org/10.1016/j.landurbplan.2019.05.010

Eikaas, H. S. (2004). The effect of habitat fragmentation on New Zealand native fish: a GIS approach.

El Abbassi, M., Overbeck, J., Braun, O., Calame, M., van der Zant, H. S., & Perrin, M. L. (2021). Benchmark and application of unsupervised classification approaches for univariate data. *Communications Physics*, *4*(1), 50.

Enderle, D. I., & Weih Jr, R. C. (2005). Integrating supervised and unsupervised classification methods to develop a more accurate land cover classification. *Journal of the Arkansas Academy of Science*, *59*(1), 65-73.

ESA Climate Change Initiative - Land Cover. (n.d.). *Land cover classification gridded maps from 1992 to present derived from satellite observations*. https://doi.org/10.24381/cds.006f2c9a

Ewers, R. M., & Didham, R. K. (2007). The Effect of Fragment Shape and Species' Sensitivity to Habitat Edges on Animal Population Size. *Conservation Biology*, *21*(4), 926-936. https://doi.org/10.1111/j.1523-1739.2007.00720.x

Ewers, R. M., Kliskey, A. D., Walker, S., Rutledge, D., Harding, J. S., & Didham, R. K. (2006). Past and future trajectories of forest loss in New Zealand. *Biological Conservation*, *133*(3), 312-325. https://doi.org/10.1016/j.biocon.2006.06.018

Forbes, A. S., Wallace, K. J., Buckley, H. L., Case, B. S., Clarkson, B. D., & Norton, D. A. (2020). Restoring mature-phase forest tree species through enrichment planting in New Zealand's lowland landscapes. *New Zealand Journal of Ecology*, *44*(1), 1-9.

Fynn, I. E., & Campbell, J. (2018). Forest fragmentation and connectivity in Virginia between 2001 and 2011. *Journal of Landscape Ecology*, *11*(3), 98-119.

Galicia, L., Zarco‐Arista, A. E., Mendoza‐Robles, K. I., Palacio‐Prieto, J. L., & García‐Romero, A. (2008). Land use/cover, landforms and fragmentation patterns in a tropical dry forest in the southern Pacific region of Mexico. *Singapore Journal of Tropical Geography*, *29*(2), 137-154.

Giannoni, L., Lange, F., & Tachtsidis, I. (2018). Hyperspectral imaging solutions for brain tissue metabolic and hemodynamic monitoring: past, current and future developments. *J Opt*, *20*(4), 044009. https://doi.org/10.1088/2040-8986/aab3a6

Gillman, L. N. (2008). Assessment of sustainable forest management in New Zealand indigenous forest. *New Zealand Geographer*, *64*(1), 57-67.

Golubiewski, N., Lawrence, G., Zhao, J., & Bishop, C. (2020). *Auckland's urban forest canopy cover: state and change (2013-2016/2018)*. Auckland Council Research and Evaluation Unit, RIMU Auckland, New Zealand.

Govender, M., Chetty, K., Naiken, V., & Bulcock, H. (2008). A comparison of satellite hyperspectral and multispectral remote sensing imagery for improved classification and mapping of vegetation. *Water sa*, *34*(2), 147-154.

Guidigan, M. L. G., Sanou, C. L., Ragatoa, D. S., Fafa, C. O., & Mishra, V. N. (2019). Assessing Land Use/Land Cover Dynamic and Its Impact in Benin Republic Using Land Change Model and CCI-LC Products. *Earth Systems and Environment*, *3*(1), 127-137. https://doi.org/10.1007/s41748-018-0083-5

Hall, R. K., Watkins, R. L., Heggem, D. T., Jones, K. B., Kaufmann, P. R., Moore, S. B., & Gregory, S. J. (2009). Quantifying structural physical habitat attributes using LIDAR and hyperspectral imagery. *Environ Monit Assess*, *159*(1-4), 63-83. https://doi.org/10.1007/s10661-008-0613-y

Halme, E., Pellikka, P., & Mottus, M. (2019). Utility of hyperspectral compared to multispectral remote sensing data in estimating forest biomass and structure variables in Finnish boreal forest. *International Journal of Applied Earth Observation and Geoinformation*, *83*, 101942.

Harris, R. J., & Burns, B. R. (2000). Beetle assemblages of kahikatea forest fragments in a pasture-dominated landscape. *New Zealand Journal of Ecology*, 57-67.

Hasmadi, M., Pakhriazad, H., & Shahrin, M. (2009). Evaluating supervised and unsupervised techniques for land cover mapping using remote sensing data. *Geografia: Malaysian Journal of Society and Space*, *5*(1), 1-10.

Hawes, P., & Memon, P. A. (1998). Prospects for sustainable management of indigenous forests on private land in New Zealand. *Journal of Environmental Management*, *52*(2), 113-130.

Herold, M., & Di Gregorio, A. (2012). Evaluating land-cover legends using the UN land-cover classification system. In *Remote Sensing of Land Use and Land Cover: Principles and Applications* (pp. 65-90). CRC Press.

Hesselbarth, M. H., Sciaini, M., With, K. A., Wiegand, K., & Nowosad, J. (2019). landscapemetrics: An open‐source R tool to calculate landscape metrics. *Ecography*, *42*(10), 1648-1657.

Honnor, L., Batelaan, E., & Zucchetto, D. (2011). *State of the Environment Report on Biodiversity 2011*. https://ref.coastalrestorationtrust.org.nz/site/assets/files/5385/state-of-the-environment-report-biodiversity-2011.pdf

Hutchison, M. A. S. (2009). Interactions between habitat fragmentation and invasions: factors driving exotic plant invasions in native forest remnants, West Coast, New Zealand.

Imre, A., & Bogaert, J. (2004). The fractal dimension as a measure of the quality of habitats. *Acta Biotheoretica*, *52*, 41-56.

Jedraszak, A., Dalke-Swiderska, M., Kazmierczak, K., Skrzypek, K., & Miotke, M. SUSTAINABLE MANAGEMENT OF INDIGENOUS FORESTS IN NEW ZEALAND.

Keyghobadi, N. (2007). The genetic implications of habitat fragmentation for animals. *Canadian Journal of Zoology*, *85*(10), 1049-1064.

Kozak, J., Ziółkowska, E., Vogt, P., Dobosz, M., Kaim, D., Kolecka, N., & Ostafin, K. (2018). Forest-cover increase does not trigger forest-fragmentation decrease: Case Study from the Polish Carpathians. *Sustainability*, *10*(5), 1472.

Lafortezza, R., Coomes, D. A., Kapos, V., & Ewers, R. M. (2010). Assessing the impacts of fragmentation on plant communities in New Zealand: scaling from survey plots to landscapes. *Global Ecology and Biogeography*, *19*(5), 741-754.

LaGro, J. J. (1991). Assessing patch shape in landscape mosaics. *Photogrammetric Engineering & Remote Sensing*, *57*, 285-293.
Land Information New Zealand. (2022). *LINZ Data Service*. https://data.linz.govt.nz
Laurance, W. F. (2000). Do edge effects occur over large spatial scales? *Trends in ecology & evolution*, *15*(4), 134-135.
Laurance, W. F., & Yensen, E. (1991). Predicting the impacts of edge effects in fragmented habitats. *Biological Conservation*, *55*(1), 77-92.
Liang, S., & Wang, J. (2020). *Advanced remote sensing : terrestrial information extraction and applications* (2nd ed.) [Bibliographies Online Non-fiction Electronic document]. Academic Press. https://ezproxy.massey.ac.nz/login?url=https://www.sciencedirect.com/science/book/9780128158265
Linyucheva, A., & Kindlmann, P. (2021). A review of global land cover maps in terms of their potential use for habitat suitability modelling. *European Journal of Environmental Sciences*, *11*(1), 46-61.
Liu, X. (2005). Supervised classification and unsupervised classification.
Liu, X. X., Yu, L., Li, W., Peng, D. L., Zhong, L. H., Li, L., Xin, Q. C., Lu, H., Yu, C. Q., & Gong, P. (2018). Comparison of country-level cropland areas between ESA-CCI land cover maps and FAOSTAT data [Article]. *International Journal of Remote Sensing*, *39*(20), 6631-6645. https://doi.org/10.1080/01431161.2018.1465613
Lövei, G. L., & Cartellieri, M. (2000). Ground beetles (Coleoptera, Carabidae) in forest fragments of the Manawatu, New Zealand: collapsed assemblages? *Journal of Insect Conservation*, *4*, 239-244.
Manaaki Whenua - Landcare Research. (2019). *LCDB v5. 0—Land Cover Database version 5.0, Mainland New Zealand*. https://doi.org/10.26060/W5B4-WK93
Manaaki Whenua - Landcare Research. (2020). *Land fragmentation environmental reporting indicator – technical methods for analysis from 2002 to 2019* [Contract report](LC3846). https://environment.govt.nz/assets/Publications/land-fragmentation-report.pdf
McGarigal, K., & Marks, B. (1995). FRAGSTATS—Spatial Pattern Analysis Program for Quantifying Landscape Structure. *U. S. Forest Service General Technical Report*. https://doi.org/10.2737/PNW-GTR-351
McGarigal, K. S., Cushman, S., Neel, M., & Ene, E. (2002). FRAGSTATS: Spatial pattern analysis program for categorical maps.
McGlone, M. (1985). Plant biogeography and the late Cenozoic history of New Zealand. *New Zealand journal of botany*, *23*(4), 723-749.
McWethy, D. B., Whitlock, C., Wilmshurst, J. M., McGlone, M. S., Fromont, M., Li, X., Dieffenbacher-Krall, A., Hobbs, W. O., Fritz, S. C., & Cook, E. R. (2010). Rapid landscape transformation in South Island, New Zealand, following initial Polynesian settlement [Article]. *Proceedings of the National Academy of Sciences of the United States of America*, *107*(50), 21343-21348. https://doi.org/10.1073/pnas.1011801107
Midha, N., & Mathur, P. K. (2010). Assessment of Forest Fragmentation in the Conservation Priority Dudhwa Landscape, India using FRAGSTATS Computed Class Level Metrics. *Journal of the Indian Society of Remote Sensing*, *38*(3), 487-500. https://doi.org/10.1007/s12524-010-0034-6
Ministry for the Environment & Stats NZ. (2022). *New Zealand's Environmental Reporting Series: Environment Aotearoa 2022* (ME 1634). M. f. t. E. a. S. NZ. www.environment.govt.nz
Monks, A., Hayman, E., & Walker, S. (2019). Attrition of recommended areas for protection. *New Zealand Journal of Ecology*, *43*(2), 1-11.
Mousivand, A., & Arsanjani, J. J. (2019). Insights on the historical and emerging global land cover changes: The case of ESA-CCI-LC datasets. *Applied Geography*, *106*, 82-92. https://doi.org/https://doi.org/10.1016/j.apgeog.2019.03.010

Neel, M. C., McGarigal, K., & Cushman, S. A. (2004). Behavior of class-level landscape metrics across gradients of class aggregation and area. *Landscape Ecology*, *19*(4), 435-455.
Norton, B. D. A., & Miller, C. J. (2000). Some issues and options for the conservation of native biodiversity in rural New Zealand. *Ecological Management & Restoration*, *1*(1), 26-34.
Norton, D. A. (2002). Edge effects in a lowland temperate New Zealand rainforest. *DOC Science Internal Series*(27), 33 pp.-33 pp. https://www.doc.govt.nz/Documents/science-and-technical/DSIS27.pdf
Noss, R. F. (1999). Assessing and monitoring forest biodiversity: A suggested framework and indicators. *Forest Ecology and Management*, *115*(2), 135-146. https://doi.org/https://doi.org/10.1016/S0378-1127(98)00394-6
Ogden, J. (1995). The long-term conservation of forest diversity in New Zealand. *Pacific Conservation Biology*, *2*(1), 77-90.
Ohlemüller, R., Walker, S., & Bastow Wilson, J. (2006). Local vs regional factors as determinants of the invasibility of indigenous forest fragments by alien plant species. *Oikos*, *112*(3), 493-501.
Olaode, A., Naghdy, G., & Todd, C. (2014). Unsupervised Classification of Images: A Review. *International Journal of Image Processing*, *8*, 2014-2325.
Pan, Y., Birdsey, R. A., Phillips, O. L., & Jackson, R. B. (2013). The structure, distribution, and biomass of the world's forests. *Annual Review of Ecology, Evolution, and Systematics*, *44*, 593-622.
Pannell, J. L., Buckley, H. L., Case, B. S., & Norton, D. A. (2021). The significance of sheep and beef farms to conservation of native vegetation in New Zealand. *New Zealand Journal of Ecology*, *45*(1), 1-11.
Pullanagari, R., Kereszturi, G., Yule, I. J., & Ghamisi, P. (2017). Assessing the performance of multiple spectral–spatial features of a hyperspectral image for classification of urban land cover classes using support vector machines and artificial neural network. *Journal of Applied Remote Sensing*, *11*(2), 026009-026009.
Richard, Y., & Armstrong, D. P. (2010). The importance of integrating landscape ecology in habitat models: isolation-driven occurrence of north island robins in a fragmented landscape. *Landscape Ecology*, *25*, 1363-1374.
Richards, J. A., & Richards, J. A. (2022). Supervised classification techniques. *Remote sensing digital image analysis*, 263-367.
Riitters, K., Wickham, J., O'Neill, R., Jones, B., & Smith, E. (2000). Global-scale patterns of forest fragmentation. *Conservation Ecology*, *4*(2), Article 3. <Go to ISI>://WOS:000167492900005
Riitters, K. H., Wickham, J. D., O'neill, R. V., Jones, K. B., Smith, E. R., Coulston, J. W., Wade, T. G., & Smith, J. H. (2002). Fragmentation of continental United States forests. *Ecosystems*, *5*, 0815-0822.
Riutta, T., Slade, E. M., Morecroft, M. D., Bebber, D. P., & Malhi, Y. (2014). Living on the edge: quantifying the structure of a fragmented forest landscape in England. *Landscape Ecology*, *29*, 949-961.
Roche, M. (2017). Forest governance and sustainability pathways in the absence of a comprehensive national forest policy — The case of New Zealand. *Forest Policy and Economics*, *77*, 33-43. https://doi.org/https://doi.org/10.1016/j.forpol.2015.12.007
Roughgarden, J., Running, S. W., & Matson, P. A. (1991). What does remote sensing do for ecology? *Ecology*, *72*(6), 1918-1922.
Rutledge, D. T. (2003). Landscape indices as measures of the effects of fragmentation: can pattern reflect process?
Scarsbrook, M. R., & Halliday, J. (1999). Transition from pasture to native forest land-use along stream continua: effects on stream ecosystems and implications for restoration. *New Zealand Journal of Marine and Freshwater Research*, *33*(2), 293-310. https://doi.org/10.1080/00288330.1999.9516878

Schindler, J., Dymond, J. R., Wiser, S. K., & Shepherd, J. D. (2021). Method for national mapping spatial extent of southern beech forest using temporal spectral signatures. *International Journal of Applied Earth Observation and Geoinformation*, *102*, 102408.

Singh, K. D., & Singh, K. D. (2013). Global forest resources assessments. *Capacity Building for the Planning, Assessment and Systematic Observations of Forests: With Special Reference to Tropical Countries*, 203-211.

Smale, M. C., Ross, C. W., & Arnold, G. C. (2005). Vegetation recovery in rural kahikatea (Dacrycarpus dacrydioides) forest fragments in the Waikato region, New Zealand, following retirement from grazing. *New Zealand Journal of Ecology*, *29*(2), 261-269. <Go to ISI>://WOS:000234235300010

Staples, C., Ahmed, S., & Ewers, R. M. (2012). Sensitivity of GIS patterns to data resolution: a case study of forest fragmentation in New Zealand. *New Zealand Journal of Ecology*, 203-209.

Stevenson, B. (2004). Changes in phosphorus availability and nutrient status of indigenous forest fragments in pastoral New Zealand hill country. *Plant and Soil*, *262*, 317-325.

Taubenböck, H., Wurm, M., Geiß, C., Dech, S., & Siedentop, S. (2019). Urbanization between compactness and dispersion: Designing a spatial model for measuring 2D binary settlement landscape configurations. *International Journal of Digital Earth*, *12*(6), 679-698.

Taylor-Smith, B., Morgan-Richards, M., & Trewick, S. A. (2020). Patterns of regional endemism among New Zealand invertebrates. *New Zealand Journal of Zoology*, *47*(1), 1-19.

Tilling, A. (1992). Indigenous forest management in New Zealand: from interventionist to monetarist policies and the special case of the South Island's West Coast. *New Zealand Forestry*, *37*(4), 8-13.

Toth, C., & Jóźków, G. (2016). Remote sensing platforms and sensors: A survey. *ISPRS Journal of Photogrammetry and Remote Sensing*, *115*, 22-36. https://doi.org/https://doi.org/10.1016/j.isprsjprs.2015.10.004

Trumbore, S., Brando, P., & Hartmann, H. (2015). Forest health and global change. *Science*, *349*(6250), 814-818.

UCL-Geomatics. (2017). Land Cover CCI. Product User Guide Version 2.0 [pdf] [1.1]. https://climate.esa.int/media/documents/ESACCI-LC-Ph2-PUGv3_1.1.pdf

Vali, A., Comai, S., & Matteucci, M. (2020). Deep learning for land use and land cover classification based on hyperspectral and multispectral earth observation data: A review. *Remote Sensing*, *12*(15), 2495.

van den Belt, M., & Blake, D. (2014). Ecosystem services in new Zealand agro-ecosystems: A literature review. *Ecosystem Services*, *9*, 115-132. https://doi.org/https://doi.org/10.1016/j.ecoser.2014.05.005

Walker, S., Bellingham, P. J., Kaine, G., Richardson, S., Greenhalgh, S., Simcock, R., Brown, M. A., Stephens, T., & Lee, W. G. (2021). What effects must be avoided, remediated or mitigated to maintain indigenous biodiversity? *New Zealand Journal of Ecology*, *45*(2), 1-12. https://www-jstor-org.ezproxy.massey.ac.nz/stable/48621893

Wang, H., Wen, X. J., Wang, Y. J., Cai, L. P., Peng, D., & Liu, Y. X. (2021). China's Land Cover Fraction Change during 2001-2015 Based on Remote Sensed Data Fusion between MCD12 and CCI-LC [Article]. *Remote Sensing*, *13*(3), 17, Article 341. https://doi.org/10.3390/rs13030341

Young, A., & Mitchell, N. (1994). Microclimate and vegetation edge effects in a fragmented podocarp-broadleaf forest in New Zealand. *Biological Conservation*, *67*(1), 63-72. https://doi.org/10.1016/0006-3207(94)90010-8

Zeide, B. (1991). Fractal geometry in forestry applications. *Forest Ecology and Management*, *46*(3-4), 179-188.

Zhang, Y., Lee, K., & Lee, H. (2016). Augmenting supervised neural networks with unsupervised objectives for large-scale image classification. International conference on machine learning,

Ziter, C., Bennett, E. M., & Gonzalez, A. (2013). Functional diversity and management mediate aboveground carbon stocks in small forest fragments. *Ecosphere*, *4*(7), 1-21.

Appendix A

Climate Change Initiative – Land Cover Classes

Class Code	Label
0	No Data
10	Cropland, rainfed
20	Cropland, irrigated or post-flooding
30	Mosaic cropland (>50%) / natural vegetation (tree, shrub, herbaceous cover) (<50%)
40	Mosaic cropland (>50%) / natural vegetation (tree, shrub, herbaceous cover) (>50%) / cropland (<50%)
50	Tree cover, broadleaved, evergreen, closed to open (>15%)
60	Tree cover, broadleaved, deciduous, closed to open (>15%)
70	Tree cover, needleleaved, evergreen, closed to open (>15%)
80	Tree cover, needleleaved, deciduous, closed to open (15%)
90	Tree cover, mixed leaf type (broadleaved and needleleaved)
100	Mosaic tree and shrub (>50%) / herbaceous cover (<50%)
110	Mosaic herbaceous cover (>50%) / tree and shrub (<50%)
120	Shrubland
130	Grassland
140	Lichens and mosses
150	Sparse vegetation (tree, shrub, herbaceous cover) (<15%)
160	Tree cover, flooded, fresh, or brackish water
170	Tree cover, flooded, saline water
180	Shrub or herbaceous cover, flooded, fresh/saline/brackish water
190	Urban areas
200	Bare areas
210	Water bodies
220	Permanent snow and ice

Appendix B

CCI-LC PRE-PROCESSING WORKFLOW

When accessed, the Climate Data Store contained two land cover dataset versions, v2.0.7cds (1992-2015) and v2.1.1 (2016-2020). Both versions were retrieved in the available NetCDF format resulting in 28 files in NetCDF format, each exceeding 2GB in size. Data preparation was performed to reduce file size, improve data handling, and decrease computational processing time during landscape analysis. This was achieved by converting the NetCDF image to GeoTIFF with the 'Make NetCDF Raster Layer' tool in ArcGIS Pro. A square bounding box was used to extract the New Zealand landmass from the global land cover dataset before applying lossless LZW compression - an ArcGIS file compression type that retains all raster cell values. Next the ocean class within the square bounding box was clipped along only the NZ coastline using the 'Extract by Mask' tool. The tool requires a feature mask from within which the raster cell values of the land cover layer may be extracted. To ensure a high degree of accuracy and correlation with other national datasets, the *NZ Coastlines and Islands Polygons (Topo 1:500k)* shapefile was retrieved from NZ's leading government agency for location data, Land Information New Zealand (https://data.linz.govt.nz/), and employed as the feature mask. The extracted land cover image was now bound to the NZ coastline in GeoTIFF format with a file size <5Mb. This process of converting from NetCDF to GeoTIFF, bounding box extraction, LZW compression, and NZ coastline extraction was repeated for each file, resulting in a national dataset containing 28 classified land cover images from 1992-2020.

To obtain smaller regional datasets for further analysis, the national land cover dataset was divided along NZ's regional council boundaries. Extraction of the regional datasets followed a similar process to that outlined above with the 'Extract by Mask' tool. In this case, however, the feature mask employed was the *Regional Council 2020 (Generalised)* shapefile retrieved from Stats NZ (https://datafinder.stats.govt.nz/), the organization responsible for maintaining the regional council boundaries dataset for NZ. Each region within the shapefile was used as a feature mask in the 'Extract by Mask' tool. The regional output land cover data was used to create 16 regional land cover datasets, each containing 28 images for the 1992-2020 period.

Appendix C

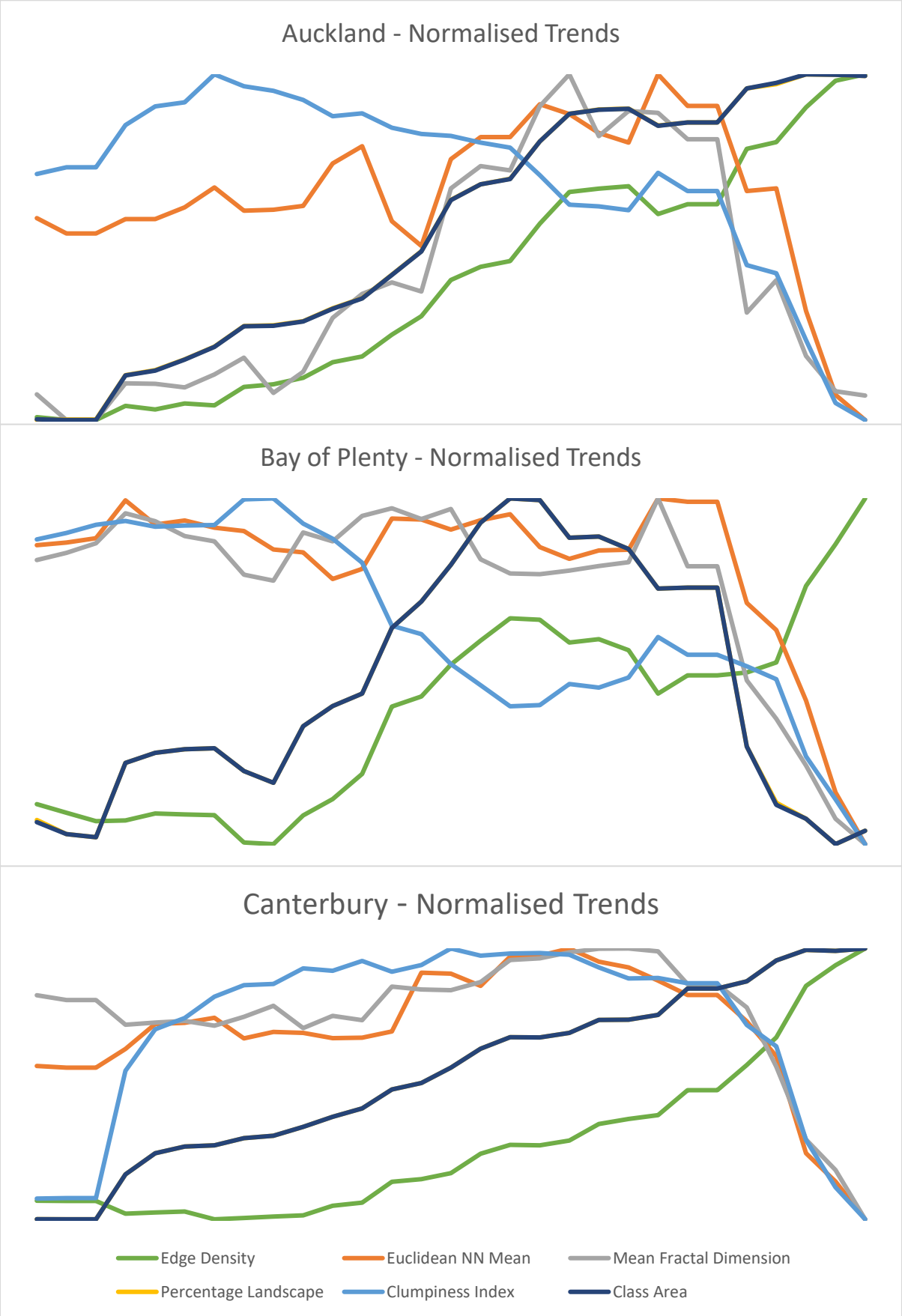
Auckland - Normalised Trends
Bay of Plenty - Normalised Trends
Canterbury - Normalised Trends
Edge Density
Euclidean NN Mean
Mean Fractal Dimension
Percentage Landscape
Clumpiness Index
Class Area

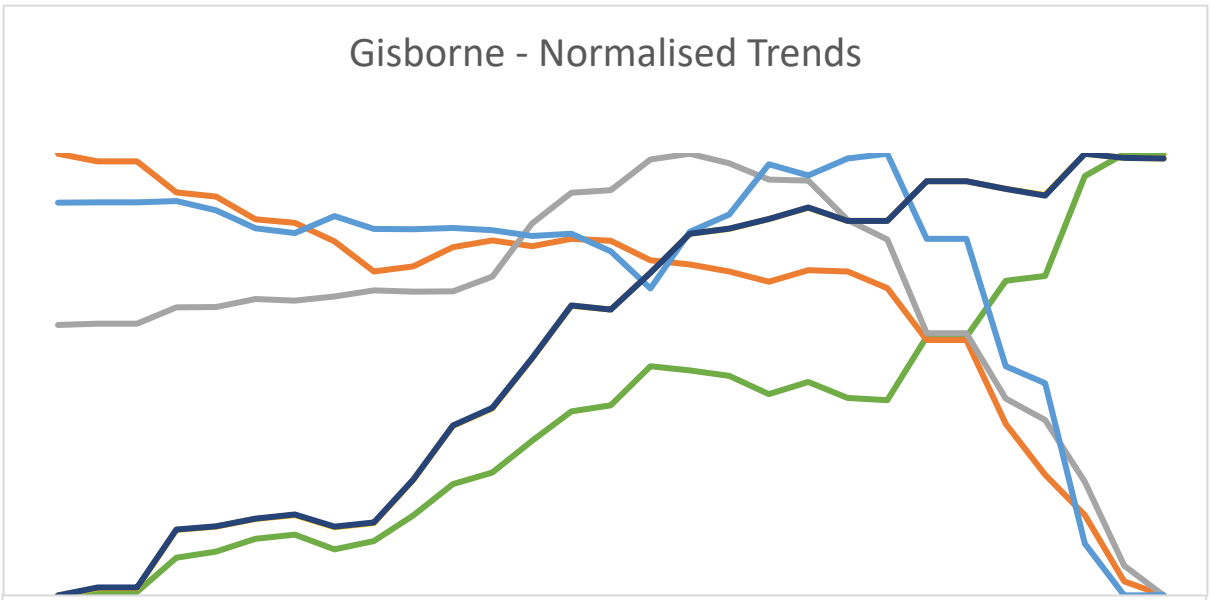
Gisborne - Normalised Trends

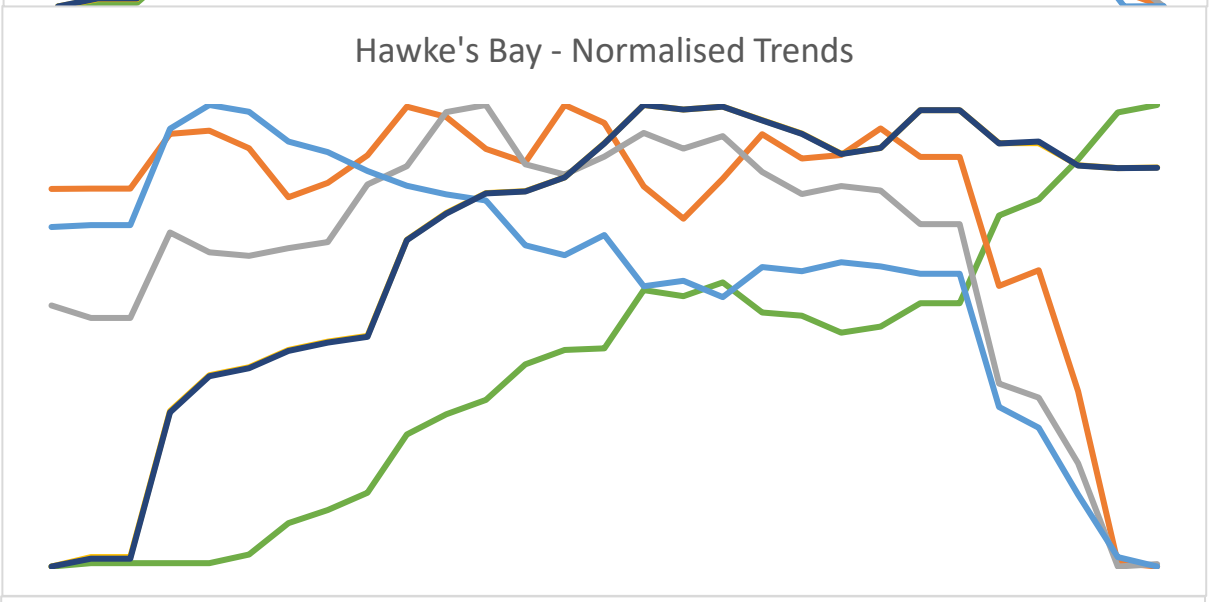
Hawke's Bay - Normalised Trends

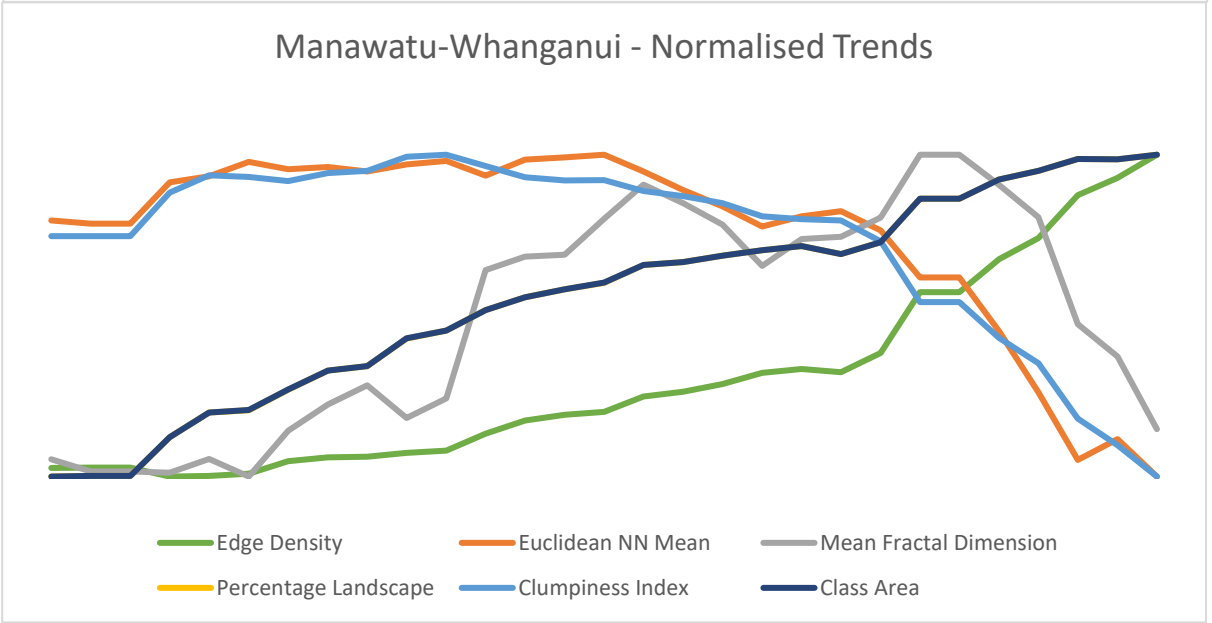
Manawatu-Whanganui - Normalised Trends
Edge Density
Euclidean NN Mean
Mean Fractal Dimension
Percentage Landscape
Clumpiness Index
Class Area

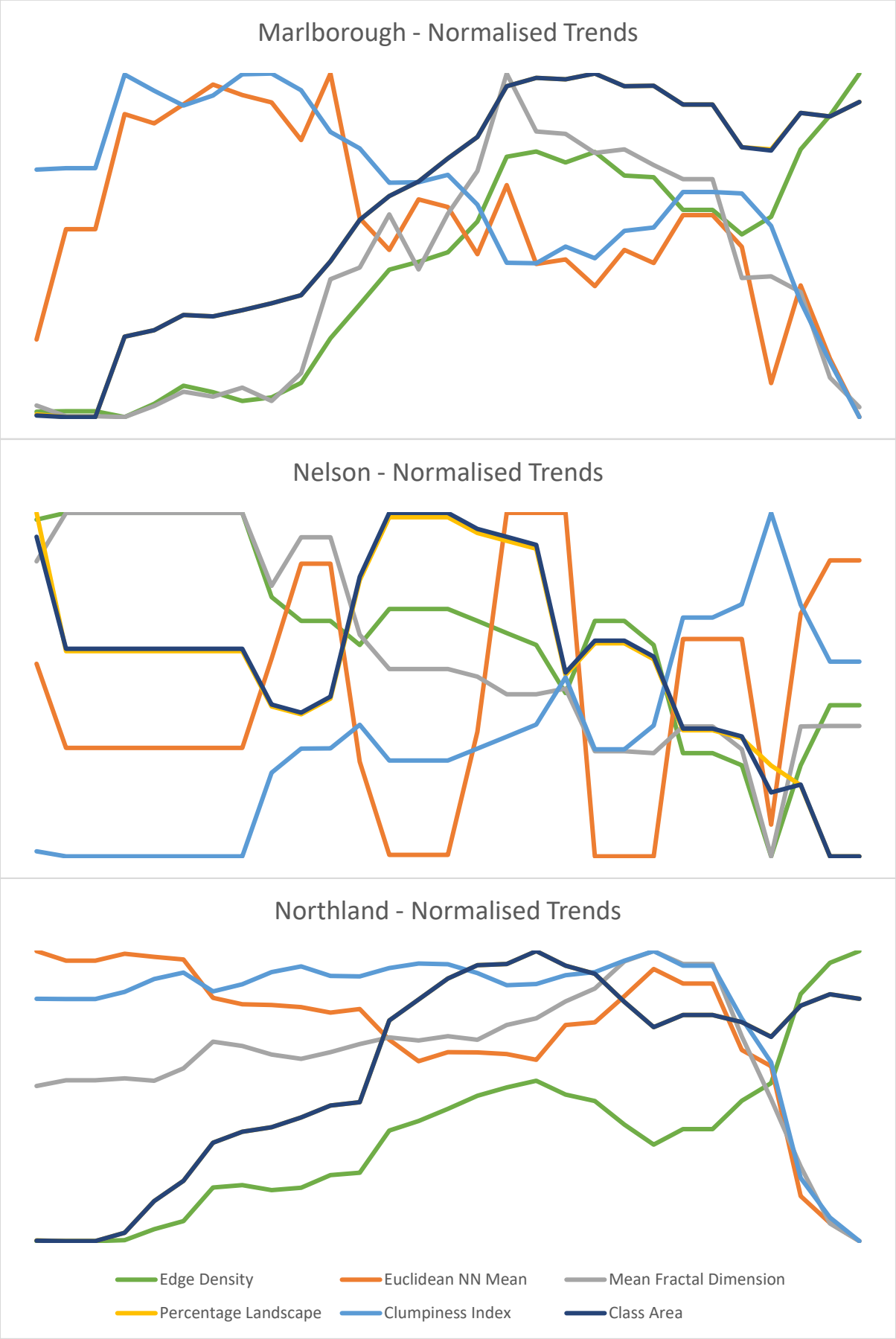
Marlborough - Normalised Trends
Nelson - Normalised Trends
Northland - Normalised Trends
Edge Density
Euclidean NN Mean
Mean Fractal Dimension
Percentage Landscape
Clumpiness Index
Class Area

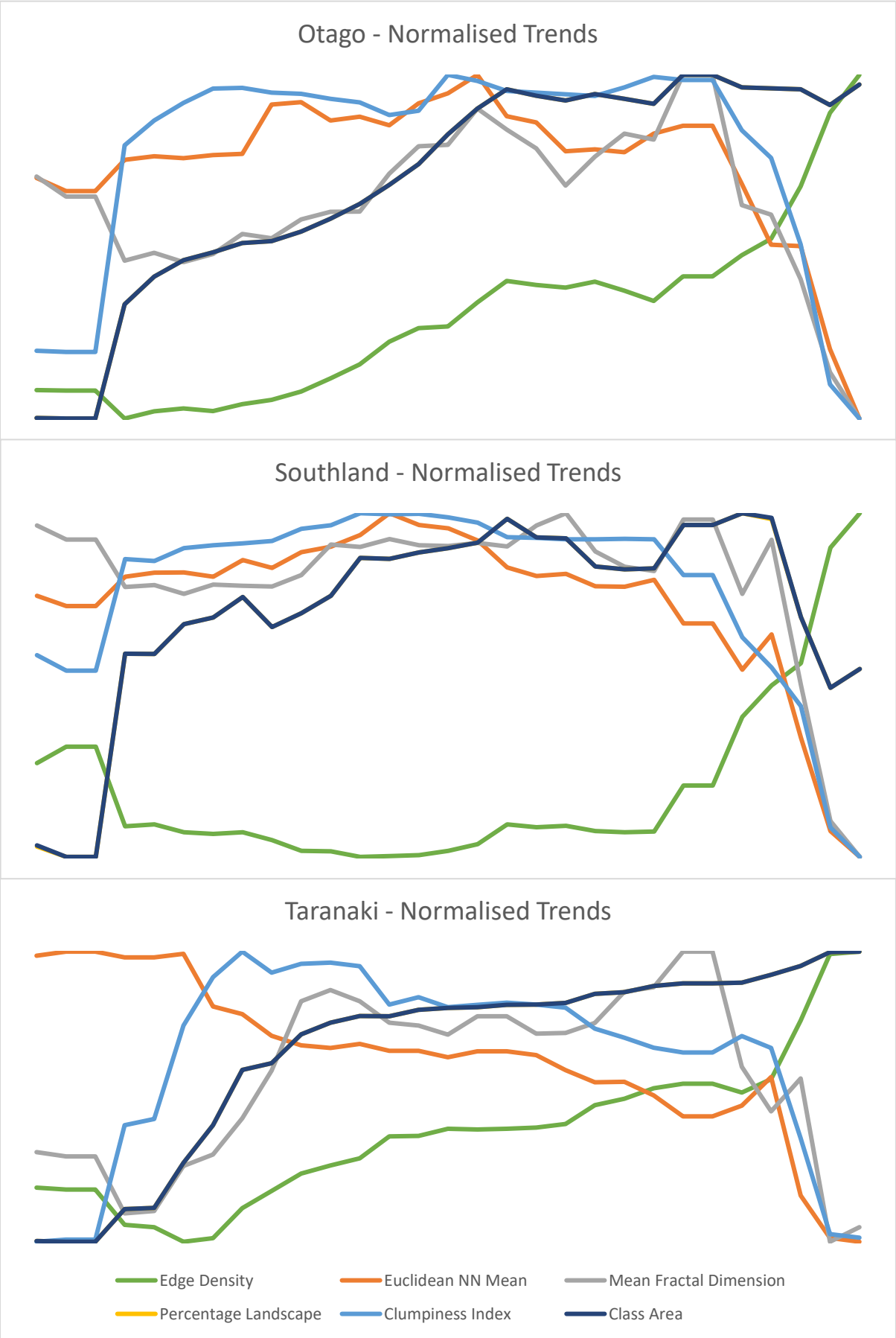
Otago - Normalised Trends
Southland - Normalised Trends
Taranaki - Normalised Trends
Edge Density
Euclidean NN Mean
Mean Fractal Dimension
Percentage Landscape
Clumpiness Index
Class Area

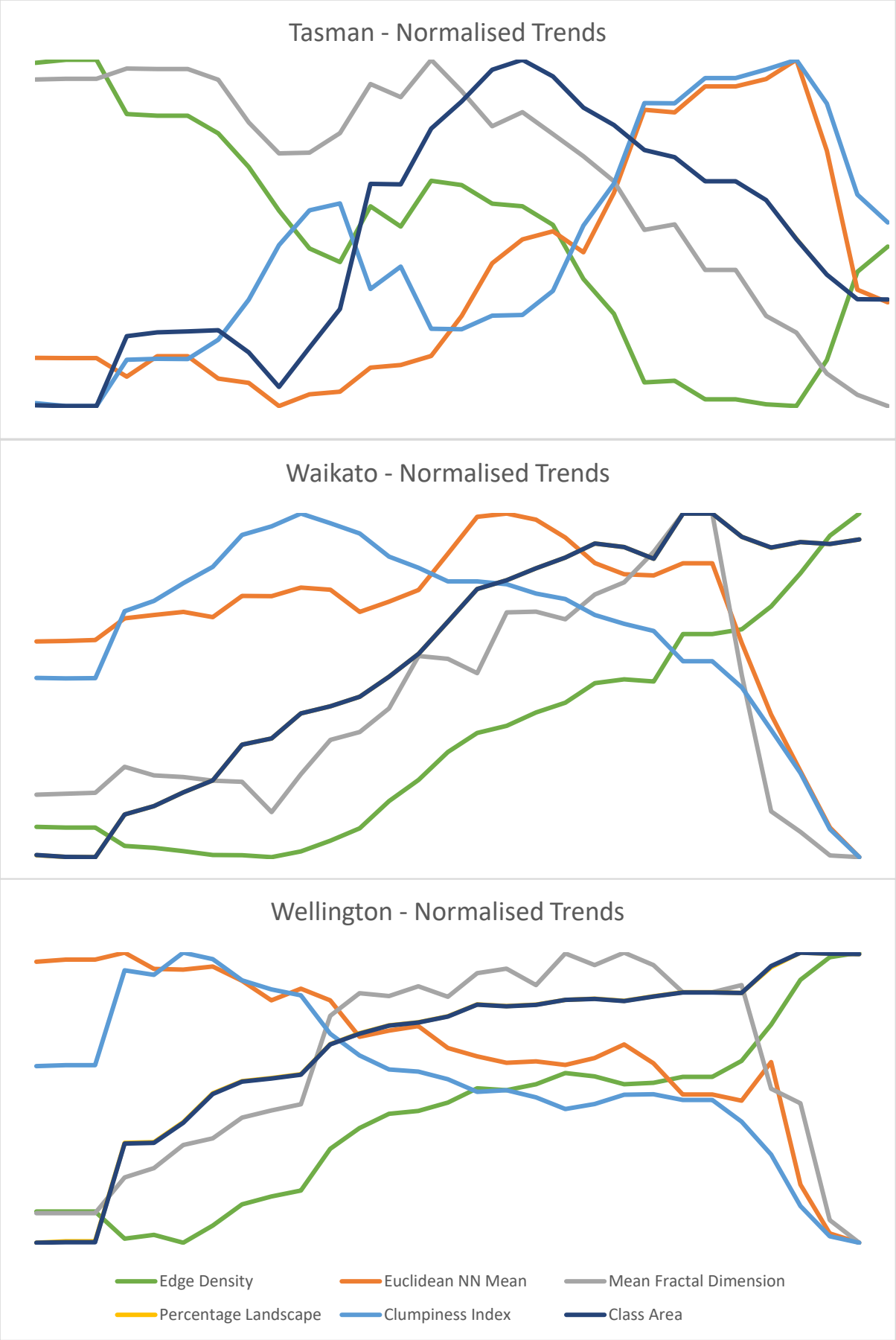
Tasman - Normalised Trends
Waikato - Normalised Trends
Wellington - Normalised Trends
Edge Density
Euclidean NN Mean
Mean Fractal Dimension
Percentage Landscape
Clumpiness Index
Class Area

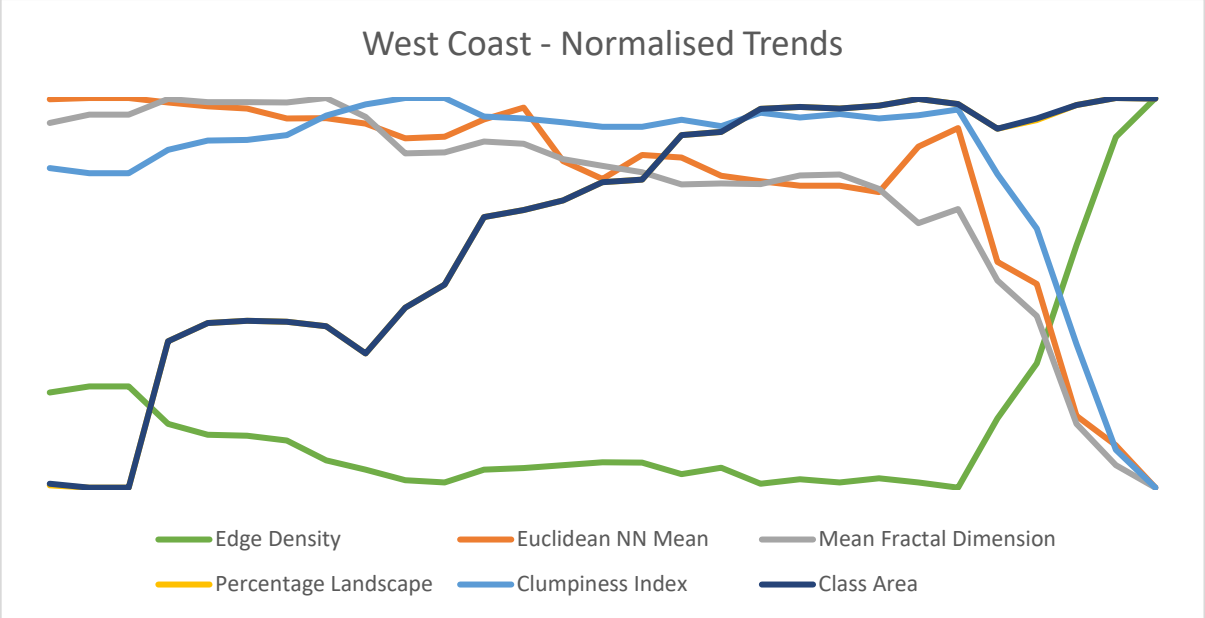
West Coast - Normalised Trends
Edge Density
Euclidean NN Mean
Mean Fractal Dimension
Percentage Landscape
Clumpiness Index
Class Area